Research on key techniques in passive optical networks and optical grid applications

Min Zhu

THESE DE DOCTORANT
DE L'ECOLE NORMALE SUPERIEURE DE CACHAN

Présenteé par
Monsieur Min ZHU

pour obtenir le grade de
DOCEURE DE L'ECOLE NORMALE SUPERIEURE DE CACHAN

Domain :
ELECTRONIQUE-ELECTROTECHNIQUE-AUTOMATIQUE

Sujet de la thèse :
Research on Key Techniques in Passive Optical Networks and Optical Grid Applications

Thèse présenteé et soutenue à Shanghai le 14 avril 2012 devant le jury composé de :

Weisheng HU	Professor of SJTU	Presidente
Yaohui JIN	Professor of SJTU	Rapporteur
Wei GUO	Professor of SJTU	Rapporteur
Yi DONG	Professor of SJTU	Rapporteur
Anne WEI	Professor of CNAM Paris	Examinatrice
Shilin Xiao	Professor of SJTU	Directrice de these
Benoit GELLER	Professor of ENS Cachan	Directrice de these

Laboratoir SATIE
61, avenue du President Wilson, 94235 CACHAN CEDEX (France)

Abstract

The bandwidth-intensive applications, such as interactive video and multimedia services, have further increased the demand of bandwidth. Thus wavelength division multiplexing passive optical network (WDM-PON) is viewed as a promising candidate to realize the next generation optical access networks due to its dedicated bandwidth for each subscriber and more flexible bandwidth management. The first half of this thesis will cover three technologies in a WDM-PON, including multicast overlay scheme, automatic protection switching scheme and tunable Fabry-Perot laser diode (FP-LD) self-seeding scheme. In the second half of the thesis, WDM optical network is utilized as a virtual computing environment, which connects widely distributed computing resources to support large-scale scientific, engineering or commercial computing applications. It is so called “optical Grid” systems. Grid applications may range from the simple transfer of a large data set to the complex execution of a collection of interdependent tasks. Especially, we for the first time introduce the Grid applications into WDM optical access networks to realize massive data aggregations. However, for such a system involving many heterogeneous computing and network resources, faults seem to be inevitable. This thesis will also address the issue of maximizing grid application availability in real-time optical Grid systems through resource-fault-tolerant scheduling techniques.

We will briefly discuss our works in the following sub-topics.

1. Multicast Overlay Scheme in WDM-PONs

Multicast overlay scheme in a WDM-PON can be realized by establishing one-to-many light paths on the optical layer, and thus reduces the loading of the electronic network processors or routers on the network layer and achieves much higher processing speed. In this thesis, we have proposed two feasible schemes to overlay multicast transmission onto the existing point-to-point traffic in a WDM-PON.

1) In the first approach, by using a dynamic wavelength reflector in each WDM channel, OLT selectively enable the multicast data imposed on the corresponding downstream unicast carrier. Several different configurations of the dynamic wavelength reflector are presented, which consist of mature and simple devices. The reconfigurable multicast control is centralized in the OLT and is transparent to all ONUs. No light source is needed in the ONUs by employing re-modulation technique.
2) The second approach uses a dual-parallel MZM (DPMZM) in each wavelength channel to generate the optical sidebands for multicast DPSK data modulation. The downstream unicast NRZ data is carried on the optical baseband carrier, which will be re-modulated with the upstream NRZ data at the respective ONU. By simply switching the RF control signal on or off, the centralized multicast function can be reconfigured quickly and dynamically. As the downstream unicast signal and the upstream signal are carried on different fiber paths, while the upstream signal and the multicast signal are carried on different subcarriers, though on the same fiber path, the possible Rayleigh backscattering effect is much alleviated.

2. Protection Switching Schemes in WDM-PONs

A survivable WDM-PON architecture which provides automatic protection switching (APS) capability can avoid enormous loss in data and business due to fiber cuts. We will propose and demonstrate two novel survivable WDM-PON architectures:

1) Centrally-controlled intelligent protection scheme in a single WDM-PON: By monitoring the optical power of each channel on both the working and protection paths, the proposed scheme can perform an effective protection switching with the aid of the proposed logic decision unit in more practical operation scenarios. The scheme can deal with both the feeder fiber and the distribution fiber failures.
2) Cross-protection dual-PON-based architecture with colorless ONUs: It can provide 1+1 protection for downstream traffic and 1:1 protection for upstream data against both feeder fiber and distribution fiber failures by using the fiber links and AWGs of the neighboring WDM-PON. It has the minimum number of extra protection fibers, the much improved wavelength utilization and the better transmission performance compared with the other existing protection schemes.

3. Upstream Multi-Wavelength Shared PON

Providing cost-effective, smooth capacity upgrades while maintaining compatibility with existing PON standards will be of great concern for network operators. A novel UMWS-PON will be presented and demonstrated based on the proposed three possible configurations of the tunable FP-LD self-seeding module at ONU. The PON not only upgrades easily upstream bandwidth capacity by introducing multiple wavelengths, but

also improves significantly bandwidth utilization by sharing wavelength resources. We also for the first time study the impact of channel SL on the network performance.

4. DAG Applications in Optical Grids

Because optical grid systems generally involve many heterogeneous computing and network resources, network or Grid resource faults seem to be inevitable. We have proposed two resource-fault-tolerant scheduling schemes for optical Grid applications:

1) The first scheme focus only on optical link failures, the proposed Availability-Driven Scheduling (ADS) scheme improves the availability iteratively under the application deadline requirements. Its performance advantages will be stated clearly in the comparison with two other DAG scheduling schemes in different network scenarios.
2) The second one addresses the case of grid resource failures in optical Grids by using a primary-backup approach. It allocates simultaneously two copies of each computation task to two different Grid resources. Through simulation results, we can see that it improves greatly application availability and induces less the overhead in scheduling length when the more network resources are available.

In the end, a brief summary of all discussed topics in this thesis is given. The main contributions of this thesis and several further studies or worth studies are pointed out at this part.

Keywords: WDM-PON, multicast overlay, automatic protection switching, self-seeding FP-LD, optical Gird, fault-tolerant scheduling

Acknowledgements

First and foremost, I would like to express my sincere gratitude to my advisor of China, Prof. Shilin XIAO, who is an endless source of enthusiasm, ideas, and patience. It was him who led me into this exciting research area of optical communications, and has offered me constant encouragement and advice throughout the last five years. I hope I have learned from him not just his broad knowledge, but his insights, inspiration and his way of conducting research.

Also, I would like to express my sincere gratitude and appreciation to my advisor of France, Prof. Benoit GELLER, for his scientific support, patience, and encouragement throughput my studies. I am extremely proud and honored to have the opportunity to associate my name with him. If Ph.D. is a learning experience, I have learned a lot from him. His hard work, motivation and vision guided me through my Ph.D. process.

Especially, I would like to thank Prof. Wei GUO (Shanghai Jiao Tong Univ.) and Professor Wen-De ZHONG (Nanyang Technological Univ.) for their insightful discussion on my research work. I have benefited tremendously from their guidance. Without the endless their help and support, this work would not have come to fruition.

I would also like to thank Prof. Weisheng HU (Shanghai Jiao Tong Univ.), and Prof. Yaohui JIN (Shanghai Jiao Tong Univ.) give me a lot of help when I stay in Shanghai ; I also thank Prof. Prof. Anne WEI (CNAM Paris Univ.) helps me adapt French life when I study and research in France.

I want to thank all the co-authors of each paper of this thesis for our nice collaborations. Special thanks go to the students in State Key Lab of Advanced Optical Communication Systems and Networks (Shanghai Jiao Tong Univ.), including Dr. Zheng Liang, Dr. He Chen, Mr. Zhixin Liu, Mr. Lei Cai, Mr. Jie Shi, Ms. Meihua Bi, Mr. Zhao Zhou, Mr. Lingzhi Ge, Mr. Daozi Ding, Mr. Yi Xiang and Mr. Cheng Yang for helping me out in several tasks in the laboratory, entertainment and friendship.

Finally, I would like to deeply thank my father Mr. Yongqing ZHU and my mother Ms. Chenglan ZHU, who always encourage and support me throughout my whole life. Thanks to my dear wife Ms. Lei ZHOU for her everlasting love. This thesis is dedicated to them.

List of Acronyms

ADS	Availability-Driven Scheduling
APD	Avalanche Photodiode
APS	Automatic Protection Switching
ASE	Amplified Spontaneous Emission
ASK	Amplitude Shift Keying
ATM-PON	Asynchronous Transfer Mode PON
AWG	Array Waveguide Grating
BER	Bit Error Rate
BLS	Broadband Light Source
BPF	Band-Pass Filter
CCR	Communication Computation Ratio
CO	Central Office
CSR	Channel Switch Ratio
CW	Continuous Wave
DAG	Directed Acyclic Graph
DBA	Dynamic Bandwidth Allocation
DDMZM	Dual-Drive Mach-Zehnder Modulator
DFB	Distributed Feedback Laser
DF	Distributed Fiber
DI	Delay Interferometer
DPP	Dedicated Path Protection
DPMZM	Dual-Parallel Mach-Zehnder Modulator
DPSK	Differential Phase Shift Keying
DSL	Digital Subscriber Line
DWDM	Dense Wavelength Division Multiplexing

EDFA	Erbium-Doped Fiber Amplifier
ELS	Extended List Scheduling
ER	Extinction Ratio
FBG	Fiber Bragg Grating
FCFS	First Come First Serve
FF	Feeder Fiber
FP-LD	Fabry-Perot Laser Diode
FRM	Fiber Reflected Mirror
FSR	Free Spectral Range
GPON	Gigabit PON
GRP	Grid Resource Protection
HDTV	High-Definition Television
IF	Interconnection Fiber
IM	Intensity Modulator
IPACT	Interleaved Polling with Adaptive Cycle Time
IRZ	Inverse Return to Zero
MCC	Monitoring and Control Circuit
MZDI	Mach-Zehnder Delay Interferometer
MZM	Mach-Zehnder Modulator
NP	Nondeterministic Polynomial
NRZ	Non Return to Zero
OAM	Operation, Administration and Maintenance
OC	Optical Coupler
OCS	Optical Carrier Suppression
OLT	Optical Line Terminal
ONU	Optical Network Unit
OOK	On Off Keying
OS	Optical Switch
OXC	Optical Cross-Connect

PC	Polarization Controller
PD	Photo-Detector
PON	Passive Optical Network
POS	Power Optical Splitter
PPG	Pulse Pattern Generator
PRBS	Pseudo-Random Bit Sequence
QoS	Quality of Service
RBS	Rayleigh Back-Scattering
RF	Radio Frequency
RN	Remote Node
RSOA	Reflective Semiconductor Optical Amplifier
RWA	Routing and Wavelength Assignment
SCM	Sub-Carrier Multiplexing
SDH	Synchronous Digital Hierarchy
SLM	Single-Longitudinal-Mode
SL	Switch Latency
SMF	Single-Mode Fiber
SMSR	Side-Mode Suppression Ratio
SONET	Synchronous Optical Network
TDM-PON	Time Division Multiplexing PON
TLS	Tunable Laser Source
UMWS	Upstream Multi-Wavelength Shared
VCSEL	Vertical-Cavity Surface-Emitting Laser
VoD	Video-On-Demand
WC	Wavelength Converter
WDM-PON	Wavelength Division Multiplexing PON
WSS	Wavelength Selective Switch

Contents

Chapter 1. Introduction

In the current Information Age, optical communication has played an important role in the telecommunication networks, because it can transmit ultrahigh speed data over extremely long distance, due to the broad bandwidth and low transmission attenuation provided by optical fibers. A typical telecommunication network can be divided into three parts [1]: long-haul transport networks, metropolitan area networks and access networks. The long-haul transport networks, also known as backbone networks, usually span thousands of kilometers connecting major network hubs in different countries across different continents. Optical fibers have been the dominant media to support such long distance and high speed transmission systems. Metropolitan area networks, serving as feeder networks between the access networks and the long-haul networks, usually cover a range from 10km to 100km, which adopt a circuit-based synchronous optical network (SONET)/synchronous digital hierarchy (SDH) as its major technique to provide a high-speed data transmission. Access networks, covering a range of only tens of kilometers (0~20km), provide connections for end users. They have to deliver the end-user data and applications to a large number of subscribers. The first half (charpter-2 to Charpter-4) of this thesis will focus on access networks and the second half (charpter-5) will discuss the optical Grid applications in the backbone networks.

1.1 Passive Optical Networks

1.1.1 Broadband optical access networks

Access network, which is also called “first-mile network”, connects service providers at central offices to the end subscribers. With the rapidly increasing bandwidth demand mainly driven by the development of advanced broadband multimedia application, such as video-on-demand (VoD), interactive high-definition digital television (HDTV) and video conference, novel broadband access network solutions that provide high capacity is highly desirable to satisfy these emerging services. Given the cost-sensitivity of access networks, the copper wire based access network technologies, such as digital subscriber line (DSL), are currently the predominant access network solutions. However, they are not considered as future-proof solutions, because these copper wire based infrastructures have been approaching their own fundamental speed limitation. For instance, the most recent DSL scheme, very-high-bit-rate DSL, version 2 (VDSL2) [2] permits the transmission of asymmetric and symmetric aggregate data rates up to 200Mbit/s but with severe distance limitations shorter than ~300 meters. As a result, the traditional copper-based access networks cannot meet the rapidly increasing bandwidth demand.

Passive optical network (PON) based access network is an efficient and vibrant technology which can meet the ever increasing bandwidth demand. PON has been extensively investigated due to its high bandwidth, cost sharing of infrastructure and absence of active components. So far, there are some different PONs that have been deployed or are being deployed, including asynchronous transfer mode PON/broadband

PON (APON/BPON), Gigabit PON (GPON) and Ethernet PON (EPON), as shown in Fig. 1.1 [3-4]. A typical APON/BPON provides 622Mbit/s of downstream bandwidth and 155Mbit/s of upstream traffic [5]. The GPON standard represents a boost in both the total bandwidth and bandwidth efficiency through the use of larger, variable-length packets. A GPON network delivers up to 2.5Gbit/s downstream data rate and 1.25Gbit/s upstream data rate [6]. EPON uses standard 802.3 Ethernet frames with a symmetrical 1.25Gbit/s up- and down- stream data rates [7]. All these PONs use the time division multiplexing (TDM) access technology, where the bandwidth of a single wavelength is shared among all users (typically 32 users in a PON), and hence are referred to as TDM-PON. As a result, although GPON and EPON can offer an aggregated bandwidth over 1Gbit/s, the bandwidth for each user may be not higher than 100Mbit/s, as shown in Fig. 1.1.

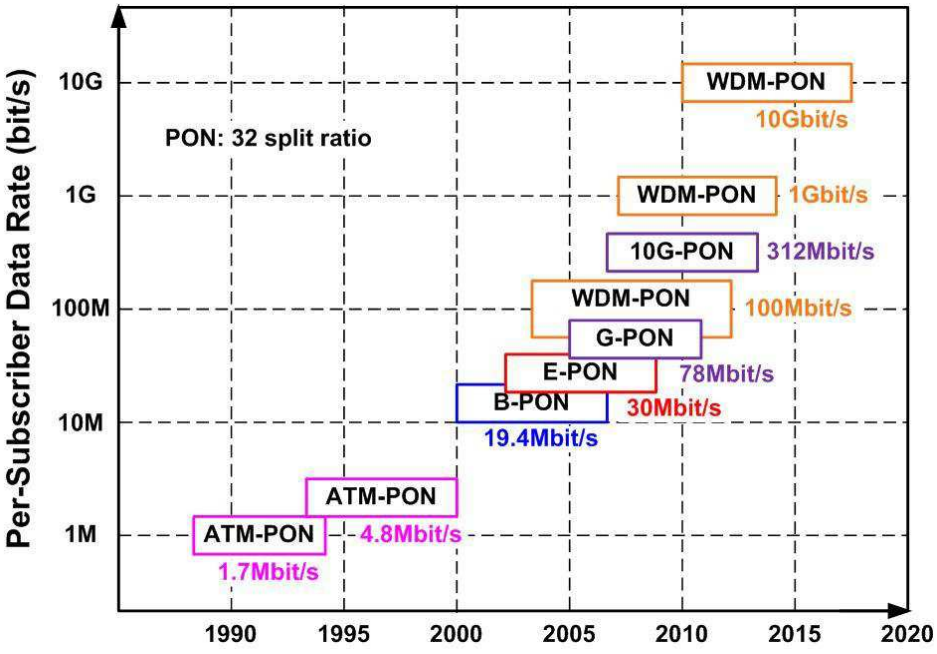

Fig. 1.1 Evolution of optical access networks [3-4].

1.1.2 WDM-PON Architecture

Today the telecommunications industry is looking into ways to deliver even more bandwidth over longer distances than ever before to meet the bandwidth demand of near future, e.g. more than 1Gbit/s per user in 2020 as predicted in [8]. The exploration of wavelength division Multiplexing (WDM) technology can tremendously increase the bandwidth offered by a PON.

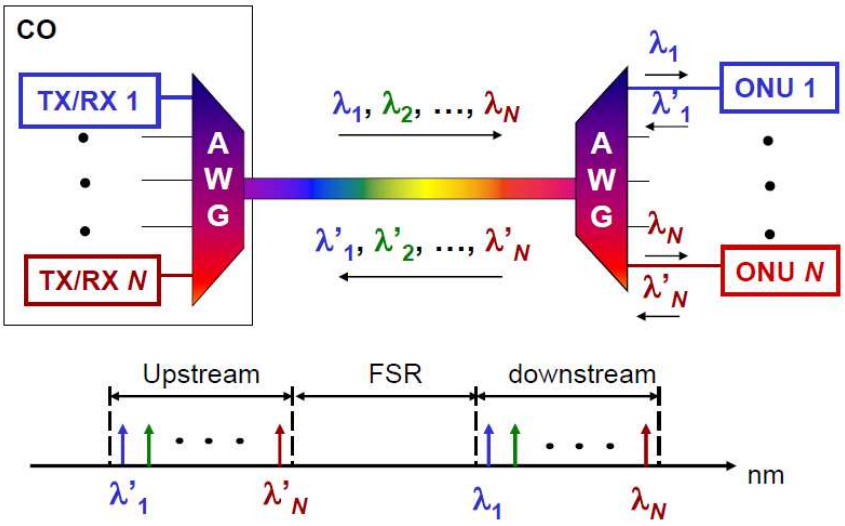

Fig. 1.2 The architecture of a WDM-PON

In a typical WDM-PON, each optical network unit (ONU) uses separate dedicated wavelengths to communicate with the OLT. It has a similar architecture with TDM-PON, except that a WDM multiplexer or de-multiplexer replaces the power splitter at the remote node (RN). The WDM multiplexer or de-multiplexer usually made of an array waveguide grating (AWG) [9] or thin-film filter, routes different wavelengths to their destined ONUs. At each ONU, the downstream data carried on the destined downstream wavelength are detected, while the upstream data are modulated onto the designated upstream wavelength before being transmitted back to the OLT, via the RN. With this

method, the bandwidth for each user can easily reach 1Gbit/s and beyond. Another advantage offered by the WDM-PON technology is network security. Unlike TDM-PON, in which a point to multipoint (P2MP) network topology is implemented with passive optical splitters located at the RN [7], a WDM-PON offers the point to point connection for each user through dedicated wavelengths, which considerably enhances network security. Besides, the WDM-PON makes it more convenient for capacity upgrade. Its bit rate can be easily upgraded by replacing an old transceiver with a higher speed one. In addition; the WDM-PON is a protocol and line-rate transparent system. All these advantages make WDM-PON be the ultimate solution for future broadband access networks. The nascent WDM-PON offers lots of opportunities for carriers and vendors. So far, Korea Telecom is leading the charge in the development and deployment of WDM-PONs [10].

1.1.3 Challenging issues in WDM-PONs

As discussed, WDM-PON has been considered as an ultimate solution for the access networks due to its large capacity, easy management, network security and upgradeability. However, there are still many challenging issues to be addressed before it can be deployed widely round the world.

Compared with the TDM-PON, the WDM-PON may be not cost-effective due to the relative higher costs for the wavelength-specific and stable light sources that are required at respective ONU. The cost is the key issue for the implementation and deployment of WDM-PONs. Moreover, the craftsman has to make sure that he/she is dealing with the

correct wavelength during the installing and maintaining of the WDM-PON. Hence, it is desirable to use low-cost wavelength independent operation (also known as colorless operation) of light source at each ONU.

With the development of diverse Internet based applications, such as IPTV and video conference, a large amount of data are transmitted through the access network, which not only requires broadband transmission but also a flexible and reliable transmission to enrich its networking capability. Traditional WDM-PONs support only point-to-point transmissions between the OLT and ONUs by employing dedicated wavelength for each ONU. Therefore, a basic WDM-PON suffers from the sole data delivery mode and limits the networking capability when different modes of data or video delivery such as broadcast and multicast are necessary to cope with more diverse multimedia and data services available for broadband access.

Another noteworthy issue is that the point-to-multipoint tree architecture further limits the networking capability since it has limited protection feature, which may cause enormous loss of data or even business during any failure of component or fiber.

1.1.4 Colorless ONUs

In terms of low-cost and colorless light source in WDM-PONs, the initial efforts involved a tunable laser incorporated in an ONU, but the key challenge exists in how to reduce the cost of a wavelength-tunable laser source to be commercially available for access network applications. Some low-cost wavelength-tunable transceivers have been proposed in [11-12]. Spectrum-slicing is another typical way to realize colorless ONUs,

in which the centralized broadband light source at the OLT, is spectrally-sliced at the RN before being distributed to each ONU as upstream carriers for data modulation. In such schemes, no light sources are required at the ONUs, but only one cost effective broadband light source is needed for upstream transmission instead, which can be LED [13-17], Fabry-Perot (FP) laser [16], or super-continuum-based broadband light source [13]. However the centralized broadband light sources usually have limited system performance due to its incoherent nature. In order to improve the system performance, injection-locking and wavelength seeding schemes have been proposed, in which FP laser diodes [17-18], reflective semiconductor optical amplifiers (RSOA) [19-22] or vertical-cavity surface-emitting laser (VCSEL) [23] were employed at the ONUs and injected by the spectrum-sliced seeding wavelengths from a broadband light source based on the amplified spontaneous emission (ASE) at the OLT. However, the data rates of such schemes were limited to around 1.25Gbit/s. The re-modulation schemes proposed in [24-28] was another approach to realize colorless ONUs, and could provide higher data rates for upstream traffic. In such architectures, the downstream data carried on the dedicated downstream wavelengths were delivered to their destined ONUs, at which the downstream power was split into two parts. One part was used for downstream data reception, while the other part was used as the light source for the upstream transmission and re-modulated by the upstream data via an optical modulator. Since the downstream carrier was reused for upstream transmission, the downstream data should be erased at the upstream transmitter so as not to affect the upstream traffic. The downstream data

could be erased from upstream transmission either by pre-coding upstream data with downstream data [24] or utilizing the orthogonality between different modulation formats, such as OOK versus DPSK [25], OOK versus FSK [26], OOK versus inverse-RZ [27], and DPSK versus dark (inverse)-RZ [28].

1.1.5 Multicast Overlay Scheme

WDM-PONs support two-way point-to-point data transmission between the OLT and the individual subscribers, via the respective designated set of wavelengths. However, with more diverse multimedia and data services available for broadband access, the access network has to be flexible enough to cope with various different modes of data or video delivery such as broadcast and multicast, in addition to point-to-point transmissions. Hence, the same data or video service can be delivered to a designated subset of subscribers or ONUs, and the connections can also be flexibly reconfigured at the OLT. Multicast transmission in a WDM-PON significantly enhances the network resource utilization efficiency for multiple destination traffic and improves the networking capability. Optical multicast can be realized by establishing one-to-many lightpaths on the optical layer, and thus reduces the loading of the electronic network processors or routers on the network layer and achieves much higher processing speed. Several interesting schemes have been proposed to overlay optical multicast onto a WDM-PON, either by using additional light sources [29], subcarrier multiplexing technique [30-32], or the characteristics of specific modulation formats [33-35].

1.1.6 Protection Switching Scheme

WDM-PON is an attractive solution to realize optical broadband access. However, the PON architecture employed in a WDM-PON limits its protection characteristics. In order to avoid enormous loss in data and business due to any possible fiber cuts, survivable network architecture is highly desirable. The survivable architecture can be designed into a tree topology and utilize group protection mechanism [36-40] or the cycling property of an AWG [41-43] for traffic protection. Besides, ring structure is also considered when designing survivable architectures for WDM-PONs [44-51], since a ring structure can provide a good property of protection by duplicating protection fibers to offer redundant paths, and locating path protection switching at both the CO and the subscribers.

1.2 Optical Grids

The section introduces some background information and network architectures related to Grid computing, with a specific focus on Grid applications based on wavelength-division multiplexing (WDM) optical networking technology.

1.2.1 Grid Computing

Due to advances in data network communication technology and the availability of powerful computer resources, Grid computing [52-53] has emerged and has led to the possibility of using a collection of resources that are shared and owned by different organizations to solve large scale problems, such as earthquake simulation, financial modeling, and motion picture animation. A Grid is a resource sharing service that is implemented through the deployment of standards-based infrastructure that coordinates

various types of resources among distributed communities. These shared resources can be computing cycles, storage space, network bandwidth, applications, scientific equipment, or data. These resources are interconnected via a wide area network, and they may be owned by various organizations and managed under locally defined policies.

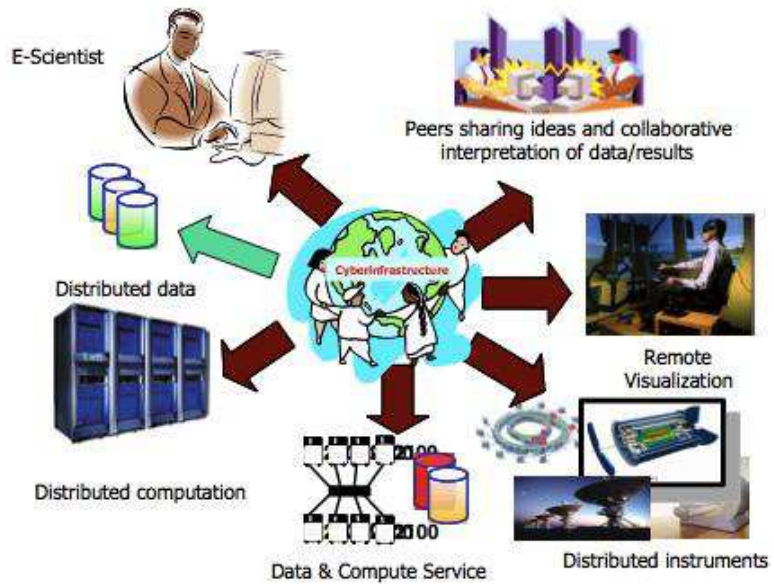

Fig. 1.3 Grid Computing Applications

Fig. 1.3 shows an overview of Grid computing. Grid services offer a number of benefits [54] such as: 1) on-demand coordination and aggregation of various types of resources located at different organizations, 2) improved utilization of underutilized and unused resources, 3) transparent access to those distributed and highly heterogeneous resources, 4) reduced operation and management cost with integration of resources.

1.2.2 Optical Grid

In general, Grid applications involve a huge amount of information and computation, and thus the bandwidth requirements of most Grid applications, especially in the

scientific computing, have increased rapidly during recent years. For example, aerodynamic simulation in transportation industry can produce vast amounts of data, and may require transferring of the data in real time [55]. Grid applications may range from the simple transfer of a large data set to the complex execution of a collection of interdependent tasks that have varying requirements with respect to processing, storage, communication, reliability, and quality of service (QoS). The support of such services requires a reliable computing and network infrastructure that can provide dynamic on-demand provisioning of bandwidth and computing resources, which span across multiple network domains.

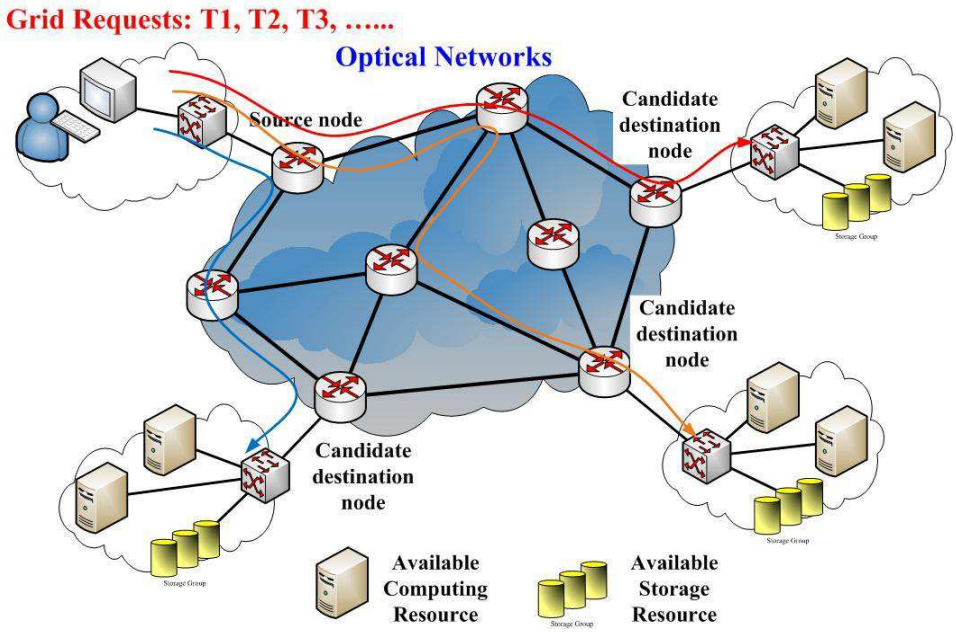

Fig. 1.4 Grid computing over optical networks

With advances in optical communication technology, an optical network infrastructure endowed with the wavelength-division multiplexing (WDM) technology, in which the

optical fiber capacity is divided into many wavelength channels, could support highly data-intensive Grid applications, which is called optical Grid. An optical Grid is a collection of computing resources that are interconnected by optical networks, and on which enhanced services are provided through the intelligent control and management of the underlying physical resources. Figure 1.4 shows the overview of a Grid over optical network architecture. An optical Grid is expected to be an efficient infrastructure to support advanced data-intensive Grid applications. Optical Grids offer huge data transfer capacity with relatively low latency and guaranteed delay. There has been significant research effort to enable Grid services over optical networks, and a number of test-beds and architectures for optical Grid applications have been developed [56-57].

1.2.3 WDM Optical Networks

WDM has the capability to provide an enormous amount of communication bandwidth on a single fiber. WDM is one type of frequency division multiplexing where each wavelength corresponds to a band of frequency, and huge capacity is provided by simultaneously carrying multiple wavelengths on a single fiber [58]. WDM systems can support 160 wavelengths each with gigabit bandwidths. According to [59], the total bandwidth of a single mode fiber is in the range of terabits per second. WDM optical networks have seen increased deployment over the years, and have contributed to the rapid growth of the Internet. In WDM networks, a “lightpath” is required to be set up between a source-destination node pair at the beginning of each communication.

1.2.4 Lightpath Connectivity and Switching Nodes

When establishing an end-to-end lightpath over multiple hops in WDM optical networks, switching nodes are needed. This function is performed by an optical cross-connect (OXC), and can be implemented in either the electronic or the optical domain. An electronic or opaque OXC converts the incoming optical signal to the electronic domain (O/E), performs the switching electronically, and finally transforms the signal back in an optical format (E/O). The availability of data in an electronic form allows, next to switching, additional electronic processing operations (for instance, data analysis, monitoring, traffic reshaping, etc.). However, the main drawback is that electronic switching speeds cannot scale proportionally to the growing fiber capacity. In contrast, an optical or transparent OXC can switch the optical signal directly, by using switching fabrics based on micro-electro-mechanical systems (MEMS) or semiconductor optical amplifier (SOA) technologies [60].

It should be noted that, due to high cost and technical issues, it is difficult to create an all-optical (i.e. without O/E/O conversions) wavelength convertor, and thus an end-to-end lightpath connection over multiple hops usually remains on the same wavelength from source to destination. As a result, the so-called wavelength continuity constraint has important consequences for the design and operation of optical networks, a research track denoted as the routing and wavelength assignment (RWA) problem [61-63]. However, previous research has demonstrated that only a small number of intelligently placed wavelength convertors suffice to significantly improve network performance [64-66].

1.2.5 Optical Network Survivability

Given the huge amount of traffic on the optical fiber, the data loss would be disastrous if a failure occurs in the optical network. Therefore the survivability of WDM optical networks is a very important issue. The survivable WDM optical networks can be achieved through various protection and restoration mechanisms. Protection mechanisms [67-68] in general provide data recovery resources before a failure actually occurs, while restoration mechanisms try to allocate the necessary network resources after a failure occurs. For protection, the interruption of the connection service can be very short, for example, if the data is sent simultaneously on the backup path or detour paths, almost no service interruption at all can be achieved assuming a single failure model. However this performance is obtained at the price of allocating the backup resource for the connection even when there is no failure. In comparison, restoration schemes [69-70] do not allocate resources for recovery until the failure occurs. In that case, a backup path or detour path is routed on runtime. Hence there is a short time service interruption before the connection works again and there might be some data loss due to the service interruption.

1.3 Problem Statement and Contributions

As mentioned above, a traditional WDM-PON is currently faced with the challenge to increase its networking capability and bandwidth capacity. This thesis will cover three technologies, including optical multicast overlay scheme, automatic protection switching scheme and tunable FP-LD self-seeding scheme. Optical multicast overlay scheme can support the additional multicast transmission on the existing point-to-point data services,

while automatic protection switching can enhance network availability with short traffic restoration time. The tunable self-seeding FP-LD scheme not only upgrades the present TDM-PON in the upstream capacity, but also improves bandwidth utilization by using inter-channel statistical multiplexing. Besides, this thesis will address the issue of maximizing grid application availability in a real-time optical Grid system through fault-tolerant scheduling. This thesis is based on the research papers that have been published in international research journals and conferences. More specifically, the following novel research contributions are presented in this thesis.

1.3.1 Multicast Overlay Schemes in WDM-PONs

Multicast overlay scheme in a WDM-PON can be realized by establishing one-to-many light paths on the optical layer, and thus reduces the loading of the electronic network processors or routers on the network layer and achieves much higher processing speed. In this thesis, we have proposed our two feasible schemes to overlay multicast transmission onto the existing point-to-point traffic in a WDM-PON.

1) In the first approach, the control of the multicast transmission is achieved by a simple dynamic wavelength reflection scheme at the OLT. By using a dynamic wavelength reflector in each WDM channel, OLT selectively enable the multicast data imposed on the corresponding downstream unicast carrier. We have also provided several different configurations of the wavelength reflector. By employing re-modulation technique, no light sources and colored components are needed in the ONUs, which effectively reduce the cost and complexity.

2) The second approach uses a dual-parallel MZM (DPMZM) to generate the optical subcarriers or sidebands for multicast DPSK data modulation. The downstream unicast data is modulated in NRZ format carried on the optical baseband carrier, which will be re-modulated with the upstream NRZ data at the respective ONU. By simply switching the RF control signal on or off in each wavelength channel, the multicast data can be enabled to realize a flexible multicast overlay. The multicast function for all wavelength channels can be reconfigured dynamically through simple and centralized management in the OLT. As the downstream unicast signal and the upstream signal are carried on different fiber feeders, while the upstream signal and the multicast signal are carried on different subcarriers, though on the same fiber feeder, the possible Rayleigh backscattering effect is much alleviated.

1.3.2 Protection Switching Schemes in WDM-PONs

A survivable WDM-PON architecture which provides automatic protection switching (APS) capability is attractive to avoid enormous loss in data and business due to fiber cuts. We have proposed and demonstrated two novel APS schemes: one is used in single WDM-PON and the other is suitable for dual-PON architecture.

1) Centrally-controlled intelligent protection scheme in a single WDM-PON: By monitoring the optical power of each channel on both the working and protection paths, the proposed scheme can tell the connection status of both the working and protection paths of each channel, and hence can perform an effective protection switching with the aid of the proposed logic decision unit in more practical operation

scenarios. The protection switching is performed and implemented at the OLT. The fiber failure localization and repair would be made easier, since the OLT monitors would have the collection of all individual channels' status information.

2) Cross-protection dual-PON-based architecture: It can provide 1+1 protection for downstream traffic and 1:1 protection for upstream data against both feeder fiber and distribution fiber failures by using the fiber links and AWGs of the neighboring WDM-PON. No additional dedicated light source for protection switching is needed by using re-modulation technique. It has the minimum number of extra protection fibers, much improved wavelength utilization and better transmission performance compared with the other existing protection schemes.

1.3.3 Upstream Multi-Wavelength Shared PON

Providing cost-effective, smooth capacity upgrades while maintaining compatibility with existing PON standards will be of great concern for network operators. We propose a novel UMWS-PON based on the tunable FP-LD self-seeding module at ONU. The PON not only upgrades easily upstream capacity by introducing multiple wavelengths, but also improves greatly bandwidth utilization with inter-channel statistical multiplexing. We for the first time investigate the impact of channel SL on the network performance. The extensive simulations show that the enhanced performance of UMWS-PON is obtained when the condition that the channel SL is relative small.

1.3.4 DAG Applications in Optical Grids

Optical Grid systems have been viewed as a promising virtual computing environment

to support large-scale distributed computing applications. For such a system involving many heterogeneous computing and network resources, faults seem to be inevitable. We have proposed two fault-tolerant scheduling schemes for optical Grid applications:

1) The first one focus on optical link failures with application deadline requirement, the proposed Availability-Driven Scheduling (ADS) scheme can provide better performances in terms of application availability and network resource utilization, while satisfying given deadline. We hence concluded that the ADS scheme is a good candidate to provide reliable real-time DAG applications over optical Grids.
2) The second one focuses on issue of handling grid resource failures in optical Grids by using a primary-backup approach to allocate simultaneously two copies of each computation task to two different Grid resources for data process. It improves greatly application availability and induces less the overhead in scheduling length when much more network resources are available.

1.4 Outline of the Thesis

The organization of the remaining chapters of this thesis will be as follows:

The introduction to the subject area covered by this thesis has already been presented in Chapter 1. Then the problem statement of four different research works and their major contributions are also briefly presented.

Chapter 2 reviews previously proposed multicast enabled WDM-PON architectures and proposes our novel optical multicast overlays onto the existing point-to-point traffic.

The operation principles are explained and experiments are demonstrated.

Chapter 3 first reviews several survivable architectures for WDM-PONs. Then, we proposed a centrally-controlled intelligent protection scheme in a single WDM-PON and another cross-protection dual-PON-based survivable architecture. The experiments for both architectures are demonstrated to verify their fast recovering time.

Chapter 4 first reviews several upstream multiple wavelength PON architectures. We then propose a novel UMWS-PON based on the tunable self-seeding FP-LD module at ONU. The performances of the wavelength and power stability, side-mode suppression ratio (SMSR), tuning range for the proposed tunable self-seeding laser module at ONU are experimentally investigated. We for the first time investigate the impact of channel SL on the network performance.

Chapter 5 provides a survey of allocation and scheduling problem in Grid computing over optical networks. Then we proposed two fault-tolerant scheduling schemes for optical Grid applications. Two extended scheduling models taking into account the optical link protection and grid resource protection are developed. The performances of our proposed schemes are evaluated in different network scenarios.

Chapter 6 summarizes the work in this thesis and gives some suggestions for the future research in the area.

References

[1] I. Kaminow and T. Li, "Optical Fiber Telecommunications IVB," San Diego: Academic Press, 2002.

[2] "Very high speed digital subscriber line transceivers 2 (VDSL2)," ITU-T Recommendation G.993.2, 2006.

[3] R. E. Wagner, J. R. Igel, R. Whitman, M. D. Vaughn, A. B. Ruffin, and S. Bickham, "Fiber-based broadband-access deployment in the United States," *IEEE Journal of Lightwave Technology*, vol.24, pp. 4526-4540, 2006.

[4] C-H. Lee, W. V. Sorin, and B. Y. Kim, "Fiber to the home using a PON infrastructure," *IEEE Journal of Lightwave Technology*, vol. 24, pp. 4568-4583, 2006.

[5] ITUT standard G.983.1.

[6] ITUT standard G.984.1.

[7] Institute of Electrical and Electronics Engineers (IEEE) 802.3ah. Available online: http://www.ieee802.org/3/ah/index.html.

[8] J. George, "FTTH design with the future in mind: optical infrastructure scalable to 25 year bandwidth demands," *Digest FTTH conference*, Session 7D, 2005.

[9] C. Dragone, C. A. Edwards, and R. C. Kistler, "Integrated optics N×N multiplexer on silicon," *IEEE Photonic Technology Letters*, vol. 4, pp.896-899, 1991.

[10] Press Release of Novera Optics Inc. "Novera optics expands Korea telecom engagement with new 30,000-line DWDM PON deployment in Q1/2007," Available online: http://www.noveraoptics.com/news/index.php#turbolight.

[11] H. Suzuki, M. Fujiwara, T. Suzuki, N. Yoshimoto, H. Kimura, and M. Tsubokawa, "Wavelength-tunable DWDM-SFP transceiver with a signal monitoring interface and its application to coexistence-type colorless WDM-PON," *European Conference on Optical Communications (ECOC)*, Berlin, Germany, Post-deadline paper PD3.4, 2007.

[12] J. Kani and K. Iwatsuki, "A wavelength-tunable optical transmitter using semiconductor optical amplifiers and an optical tunable filter for metro/access DWDM applications," *IEEE J. Lightwave Technol.*, vol. 23, no. 3, pp. 1164–1169, Mar. 2005.

[13] B. Zhang, Chinlon Lin, L. Huo, Z. X. Wang, C. K. Chan, "A simple high-speed WDM PON utilizing a centralized super-continuum broadband light source for colorless ONUs," *IEEE/OSA*

Optical Fiber Communication Conference / National Fiber Optic Engineers Conference (OFC/ NFOEC), Paper OTuC6, Anaheim, California, USA, 2006.

[14] M. Zirngibl, C. R. Doerr, and L. W. Stulz, "Study of spectral slicing for local access applications," *IEEE Photon. Tech. Lett.*, vol. 8, pp. 721–723, 1996.

[15] D. K. Jung, S. K. Shin, C. –H. Lee, and Y. C. Chung, "Wavelength-division-multiplexed passive optical network based on spectrum-slicing techniques," *IEEE Photonic Technology Letters*, vol. 10, no. 9, pp. 1334-1336, 1998.

[16] S. L. Woodward, P. P. Iannone, K. C. Reichmann, and N. J. Frigo, "A spectrally sliced PON employing Fabry-Perot Lasers," *IEEE Photonic Technology Letters*, vol. 10, no. 9, pp. 1337-1339, 1998.

[17] D. J. Shin, Y. C. Yeh, J. W. Kwon, E. H. Lee, J. K. Lee, M. K. Park, J. W. Park, Y. K. Oh, S. W. Kim, I. K. Yun, H. C. Shin, D. Heo, J. S. Lee, H. S. Shin, H. S. Kim, S. B. Park, D. K. Jung, S. T. Hwang, Y. J. Oh, and C. S. Shim, "Low-cost WDM-PON with colorless bi-directional transceivers," *IEEE J. Lightwave Technol.*, vol. 24, no. 1, pp 158-165, Jan. 2006.

[18] K. M. Choi, C. H. Lee, "Colorless operation of WDM-PON based on wavelength locked Fabry-Perot laser diode," *European Conference on Optical Communications (ECOC)*, Paper We3.3.4, Glasgow, UK, 2005.

[19] P. Healy, P. Townsend, C. Ford, L. Johnston, P. Townley, I. Lealman, L. Rivers, S. Perrin, R. Moore, "Spectral slicing WDM-PON using wavelength-seeded reflective SOAs," *IEE Electron. Lett.*, vol. 37, no. 19, pp1181-1182, 2001.

[20] S. J. Park, G. Y. Kim, T. Park, E. H. Choi, et al., "WDM-PON system based on the laser light injected reflective semiconductor optical amplifier," *European Conference on Optical Communications (ECOC)*, Paper We3.3.6, Glasgow, UK, 2005.

[21] C. Arellano, C. Bock, and J. Prat, "RSOA-based optical network units for WDM-PON," *IEEE/OSA Optical Fiber Communication Conference / National Fiber Optic Engineers Conference (OFC/NFOEC)*, Paper OTuC1, Anaheim, California, USA, 2006.

[22] E. Wong, K. L. Lee, T. Anderson, "Directly modulated self-seeding reflective SOAs as colorless transmitters for WDM passive optical networks," *IEEE/OSA Optical Fiber Communication Conference / National Fiber Optic Engineers Conference (OFC/NFOEC)*, Paper PDP49, Anaheim, California, USA, 2006.

[23] E. Wong, X. Zhao, C. J. Chang-Hasnain, W. Hoffman, and M. C. Amann, "Uncooled, Optical Injection-Locked 1.55 μm VCSELs for Upstream Transmitters in WDM-PONs," *IEEE/OSA*

Optical Fiber Communication Conference / National Fiber Optic Engineers Conference (OFC/NFOEC), paper PDP50, Anaheim, California, USA, 2006.

[24] C. W. Chow, "Wavelength Remodulation Using DPSK Down-and-Upstream With High Extinction Ratio for 10-Gb/s DWDM-Passive Optical Networks," *IEEE Photon. Tech. Lett.*, vol. 20, no. 1, pp. 12-14, Jan. 2008.

[25] W. Hung, C. K. Chan, L. K. Chen, F. Tong, "An optical network unit for WDM access networks with downstream DPSK and upstream re-modulated OOK data using injection-locked FP laser," *IEEE Photon. Tech. Lett.*, vol. 15, no. 10, pp. 1476-1478, Oct. 2003.

[26] N. Deng, C. K. Chan, L. K. Chen, F. Tong, "Data re-modulation on downstream OFSK signal for upstream transmission in WDM a passive optical network," *IEE Electron. Lett.*, vol. 39, no. 24, pp. 1741-1742, Nov. 2003.

[27] G. W. Lu, N. Deng, C. K. Chan, L. K. Chen, "Use of downstream inverse-RZ signal for upstream data re-modulation in a WDM passive optical network," *IEEE/OSA Optical Fiber Communication Conference / National Fiber Optic Engineers Conference (OFC/NFOEC)*, Paper OFI8, Anaheim, California, USA, Mar. 2005.

[28] L. Xu and H. K. Tsang, "Differential Phase Shift Keying for Asynchronous Upstream Remodulation of Dark Return-to-Zero Downstream Channel," *IEEE/OSA Optical Fiber Communication Conference / National Fiber Optic Engineers Conference (OFC/NFOEC)*, Paper OWH6, San Diego, USA, 2008.

[29] C. Bock and J. Prat , "WDM/TDM PON experiments using the AWG free spectral range periodicity to transmit unicast and multicast data," *OSA Opt. Express*, vol. 13, no. 8, pp. 2887-2891, April. 2005.

[30] M. Khanal, C. J. Chae, R. S. Tucker, "Selective broadcasting of digital video signals over a WDM passive optical network," *IEEE Photon. Technol. Lett.*, vol. 17, no. 9, pp. 1992-1994, Sept. 2005.

[31] Q. J. Chang, J. M. Gao, Q. Li, Y. K. Su, "Simultaneous transmission of point-to-point data and selective delivery of video services in a WDM-PON Using ASK/SCM Modulation Format," *IEEE/OSA Optical Fiber Communication Conference / National Fiber Optic Engineers Conference (OFC/NFOEC)*, Paper OWH2, San Diego, California, USA, 2008.

[32] Y. Tian, Q. J. Chang, Y. K. Su, "A WDM passive optical network enabling multicasting with color-free ONUs," *OSA Opt. Express*, vol. 16, no. 14, pp. 10434-10439, Jul. 2008.

[33] N. Deng, C. K. Chan, L. K. Chen, and C. Lin, "A WDM passive optical network with centralized light sources and multicast overlay," IEEE Photon. Technol. Lett., vol. 20, no. 2, pp. 114–116, Jan.

2008.

[34] L. Cai, Z. Liu, S, Xiao, M. Zhu, R. Li and W. Hu, "Video-service-overlaid wavelength-division-multiplexed passive optical network," *IEEE Photon. Technol. Lett.*, vol. 21, no. 14, pp. 990-992, 2009.

[35] Y. Zhang, N. Deng, C. K. Chan, and L. K. Chen, "A multicast WDM-PON architecture using DPSK/NRZ orthogonal modulation," *IEEE Photon. Technol. Lett.*, vol. 20, no. 17, pp. 1479-1481, 2008.

[36] T. J. Chan, C. K. Chan, L. K. Chen, and F. Tong, "A self-protected architecture for wavelength division multiplexed passive optical networks," *IEEE Photon. Technol. Lett.*, vol. 15, no. 11, pp. 1660–1662, Nov. 2003.

[37] C.M. Lee, T.J. Chan, C.K. Chan, L.K. Chen, C.L. Lin, "A Group Protection Architecture (GPA) for Traffic Restoration in Multi-wavelength Passive Optical Networks," *European Conference on Optical Communications (ECOC)*, Paper Th2.4.2, Rimini, Italy, Sept, 2003.

[38] Z.X. Wang, B. Zhang, C.L. Lin, C.K. Chan; "A Broadcast and Select WDM-PON and its Protection," *European Conference on Optical Communications (ECOC)*, Paper We4.P.24, Glasgow, United Kingdom, Sep. 2005.

[39] Z. X. Wang, X. F. Sun, C. Lin, C. K Chan, and L. K. Chen, "A novel centrally controlled protection scheme for traffic restoration in WDM passive optical networks," *IEEE Photon. Technol. Lett.*, vol. 17, no. 3, pp. 717–719, Mar. 2005.

[40] X.F. Sun, C.K. Chan, L.K. Chen; "A Survivable WDM PON Architecture with Centralized Alternate-Path Protection Switching for Traffic Restoration," *IEEE Photon. Technol. Lett.*, vol. 18, no. 4, pp.631-633, Feb. 2006.

[41] E. S. Son, K. H. Han, J. H. Lee, and Y. C. Chung, "Survivable network architectures for WDM PON", *IEEE/OSA Optical Fiber Communication Conference / National Fiber Optic Engineers Conference (OFC/NFOEC)*, Paper OFI4, Anaheim, California, USA, 2005.

[42] K. Lee, S. G. Mun, C. H. Lee, and S. B. Lee, "Reliable Wavelength-Division-Multiplexed Passive Optical Network Using Novel Protection Scheme," *IEEE Photon. Technol. Lett.*, vol. 20, no. 9, pp.679-681, May. 2008.

[43] A. Chowdhury, M. F. Huang, H. –C. Chien, G. Ellinas, and G. K. Chang, "A Self-Survivable WDM-PON Architecture with Centralized Wavelength Monitoring, Protection and Restoration for both Upstream and Downstream Links," *IEEE/OSA Optical Fiber Communication Conference / National Fiber Optic Engineers Conference (OFC/NFOEC)*, San Diego, Paper JThA95, 2008.

[44] B. Glance, C. R. Doerr, I. P. Kaminow, and R. Montagne, "Optically restorable WDM ring networks using simple add/drop circuitry," *IEEE J. Lightwave Technol.*, vol. 14, no. 11, pp. 2453-2456, 1996.

[45] C. H. Kim, C.-H. Lee, and Y. C. Chung, "Bidirectional WDM self-healing ring network based on simple bidirectional add/drop amplifier modules," *IEEE Photon. Technol. Lett.*, vol. 10, pp. 1340-1342, Sept.1998.

[46] Y. H. Joo, G. W. Lee, R. K. Kim, S. H. Park, K. W. Song, J. Koh, S. T. Hwang, Y. Oh, and C. Shim, "1-fiber WDM self-healing ring with bidirectional optical add/drop multiplexers," *IEEE Photon. Technol. Lett.*, vol. 16, pp. 683-685, Feb. 2004.

[47] S. B. Park, C. H. Lee, S. G. Kang, and S. B. Lee, "Bidirectional WDM self-healing ring network for hub/remote nodes," *IEEE Photon. Technol. Lett.*, vol. 15, pp. 1657-1659, Nov. 2003.

[48] Z.X. Wang, C.L. Lin, C.K. Chan; "Demonstration of a Single-Fiber Self-Healing CWDM Metro Access Ring Network with Uni-directional OADM," *IEEE Photon. Technol. Lett.*, vol. 18, no. 1, pp. 163-165, Jan. 2006.

[49] X. F. Sun, C.K. Chan, Z.X. Wang, C.L. Lin, L.K. Chen; "A Single-Fiber Bi-directional WDM Self-Healing Ring Network with Bi-directional OADM for Metro-Access Applications," *IEEE Journal of Selected Areas on Communications*, vol. 25, no. 4, pp. 18-24, Apr. 2007.

[50] C. J. Chae and R. S. Tucker, "A protected optical star-shaped ring network using an N×N arrayed waveguide grating and incoherent light sources," *IEEE Photon. Technol. Lett.*, vol. 13, no. 8, pp. 878–880, Aug. 2001.

[51] C. J. Chae, "A Flexible and Protected Virtual Optical Ring Network," *IEEE Photon. Technol. Lett.*, vol. 14, no. 11, pp. 1626-1628, 2002.

[52] K. Czajkowsk, S. Fitzgerald, I. Foster, and C. Ke, "Grid Information Services for Distributed Resource Sharing," *IEEE High Performance Distributed Computing (HPDC-10)*, 2001.

[53] I. Foster, C. Kesselman, and S. Tuecke, "The Anatomy of the Grid: Enabling Scalable Virtual Organizations," *International Journal of High Performance Computing Applications*, vol. 15, no. 3, pp. 200-222, Aug. 2001.

[54] R. Buyya and A. Sulistio, "Service and Utility Oriented Distributed Computing Systems: Challenges and Opportunities for Modeling and Simulation Communities," *Annual Simulation Symposium (ANSS)*, 2008.

[55] Z. Sun, W. Guo, Z. Wang, Y. Jin, W. Sun, W. Hu, and C. M. Qiao, "Scheduling Algorithm for Workflow-Based Applications in Optical Grid," *IEEE Journal of Lightwave Technology*, vol. 26,

no. 17, pp. 3011-3020, 2008.

[56] F. Baroncelli, B. Martini, L. Valcarenghi, and P. Castoldi, "A Service Oriented Network Architecture suitable for Global Grid Computing," *Optical Network Design and Modeling (ONDM)*, 2005.

[57] T. Lehman, J. Sobieski, and B. Jabbari, "DRAGON: a framework for service provisioning in heterogeneous grid networks," *IEEE Communications Magazine*, vol. 44, pp. 84 - 90, 2006.

[58] R. Ramaswami and K.N. Sivarajan, "Optical Networks: A Practical Perspective," Morgan Kaufmann Publishers, 1998.

[59] B. Mukherjee, "Optical WDM Networks," Springer, 2006.

[60] G. I. Papadimitriou, C. Papazoglou, and A.S. Pomportsis, "Optical Switching: Switch Fabrics, Techniques, and Architectures," *IEEE Journal of Lightwave Technology*, vol. 21, no. 2, pp. 384-405, Feb 2003.

[61] D. Banerjee and B. Mukherjee, "Practical approaches for Routing and Wavelength Assignment in All-Optical Wavelength-Routed Networks," *IEEE Journal on Selected Areas in Communications*, vol. 14, no. 5, pp. 903-908, Jun 1996.

[62] H. Zhang, J.P. Jue, and B. Mukherjee, "A Review of Routing and Wavelength Assignment Approaches for Wavelength-Routed Optical WDM Networks," *Optical Networks Magazine*, vol. 1, no. 1, pp. 47-60, Jan 2000.

[63] P.H. Ho and H.T. Mouftah, "Routing and Wavelength Assignment with Multi-granularity Traffic in Optical Networks," *IEEE Journal of Lightwave Technology*, vol. 20, no. 8, pp. 1292-1303, Aug 2002.

[64] J. Iness and B. Mukherjee, "Sparse Wavelength Conversion in Wavelength-Routed WDM Networks," *Photonic Network Communications*, vol. 1, no. 3, pp. 183-205, Nov 1999.

[65] S. Subramaniam, M. Azizoglu, and A.K. Somani, "All-Optical Networks with Sparse Wavelength Conversion," *IEEE/ACM Transactions on Networking*, vol. 4, no. 4, pp. 544-557, Aug 1996.

[66] X. Chu, J. Liu, and Z. Zhang, "Analysis of Sparse-Partial Wavelength Conversion in Wavelength-Routed WDM Networks," In Proc. *IEEE INFOCOM*, Mar 2004. Paper 29.3.

[67] S. Ramamurthy, B. Mukherjee, "Survivable WDM mesh networks – Part I: protection," in: Proc. *IEEE INFOCOM*, pp. 744-751, Mar. 1999.

[68] E. Bouillet and J. F. Labourdette, "Distributed computation of shared backup path in mesh optical networks using probabilistic methods," *IEEE/ACM Transactions on Networking*, Vol. 12, 2004, pp. 920-930.

[69] S. Ramamurthy, B. Mukherjee, “Survivable WDM mesh networks – Part II: restoration,” in: Proc. *IEEE Integrated Circuits Conf.*, pp. 2023–2030, June 1999.

[70] Y. Sone, A. Watanabe, W. Imajuku, Y. Tsukishima, B. Kozicki, H. Takara, and M. Jinno, “Highly survivable restoration scheme employing optical bandwidth squeezing in spectrum-sliced elastic optical path SLICE network,” *IEEE/OSA Optical Fiber Communication Conference / National Fiber Optic Engineers Conference (OFC/NFOEC)*, Paper OThO2, 2009.

Chapter 2. Multicast Overlay Schemes in WDM-PONs

In this chapter, we will first review several typical multicast overlay schemes proposed in the physically optical layer to overlay the multicast data onto the existing unicast wavelengths in WDM-PONs. We have grouped the previous schemes into two categories: In-band transmission and Out-band transmission. Then we will propose our own two multicast overlay schemes in a WDM-PON: 1) A multicast-enable WDM-PON with dynamic wavelength reflection scheme; 2) An optical multicast overlay scheme by simply switching the radio frequency (RF) control signal on or off in each wavelength channel. These novel schemes show several attractive features: 1) it provides a flexible, centralized and dynamically reconfigurable multicast overlay over the conventional unicast service; 2) simple multicast architecture with the wavelength reflectors, which are composed by some mature and simple devices; 3) the multicast and unicast data transmissions differ in both frequency and modulation format, which reduces the inference between them; 4) no high-frequency electrical components and no light source are needed in the ONUs.

2.1 Introduction

Conventionally, a wavelength-division-multiplexed (WDM) passive optical network (PON) utilizes arrayed waveguide gratings (AWGs) to provide virtual point-to-point connectivity between the OLT and the different ONU, via the respective designated set of

wavelengths. However, with more diverse multimedia and point-to-multipoint data services such as video-on-demand and high-definition television (HDTV) broadcasting for broadband access, the access network has to be flexible enough to cope with various different modes of data or video delivery such as broadcast and multicast, in addition to point-to-point transmissions to enrich the networking capability.

Broadcast transmission in a WDM-PON [1] increases the networking capability by delivering copies of information to all ONUs. Thus service providers may have to use much bandwidth resource to deliver unnecessary information to certain customers and some sensitive information may be leaked to others. On the contrary, in a multicast transmission [2] the same data or video service can be delivered to a designated subset of subscribers or ONUs, and the connections can also be flexibly reconfigured at the OLT, which significantly enhances the network resource utilization efficiency for multiple destination traffic and improves the cost effectiveness while keeping the security of information within the designated subset of subscribers or ONUs.

Multicast transmission in a WDM-PON can be realized by loading the electronic network processors or routers on the networking layer. The processing bandwidth of electronic components will limit the processing speed. Therefore, optical multicast realized by establishing one-to-many light paths on the optical layer, which can achieve much higher processing speed, is very attractive. In order to realize optical multicast overlay in a WDM-PON, the overlay control technique for connection reconfiguration is crucial to be carefully designed, so as to effectively overlay the multicast traffic to the

existing network infrastructure which is carrying the two-way unicast traffic.

2.2 Related works

Multicast Overlay Schemes in a WDM-PON

In-band Transmission	Extinction Ratio (ER)	DPSK over NRZ Y. Zhang [3], et al, IEEE PTL Vol.20(17), 2008	NRZ over IRZ L. Cai [4], et al, IEEE PTL Vol.21(14), 2009
	Modulation Format Conversion	DPSK over (NRZ or IRZ) N. Deng [5], et al, IEEE PTL Vol.20(2), 2008	
	(*Proposed*) Wavelength Deflection	Optical Switch, WSS, FBG or Interferometer M. Zhu, et al, OSA/IEEE ACP2009	
Out-band Transmission	Extinction Ratio (ER)	SCM over ASK M. Khanal [6], et al, IEEE PTL Vol.17(9), 2005	SCM over ASK Q. J. Chang [7], et al, OWH2, OSA/IEEE OFC2008
	Base Carrier Switching	DC carrier Switching Control Y. Tian [8], et al, OSA OE Vol.16(4), 2008	
	(*Proposed*) RF Carrier Switching	RF Carrier Switching Control M. Zhu, et al, OSA COL Vol.8(10), 2010	

Fig. 2.1 Summary of the reported multicast overlay schemes in a WDM-PON [3-8]

Several interesting schemes [3-8] have been proposed to overlay the multicast data onto the existing point-to-point or unicast wavelengths in WDM-PONs, using various feasible and practical optical overlay control techniques. The common principle is to selectively enable or disable the multicast data superimposed on each downstream wavelength at the OLT, such that only the designated subset of ONUs can properly retrieve the multicast service. We have grouped the previous schemes into two categories:

1) In-band transmission [3-5], where the multicast data are orthogonally modulated onto unicast signals by adjusting extinction ratios (ERs) of the unicast signals [3-4]; or

dynamically converting unicast data modulation format [5];

2) Out-band transmission [6-8], where multicast data in the sub-carrier multiplexing (SCM) format are overlaid on the baseband unicast data with the amplitude shift keying (ASK) modulation in the same wavelength channel by adjusting dynamically the ER of the unicast ASK signals [6-7]; or on the contrary, baseband multicast data are overlaid on the unicast data in the SCM format by dynamically controlling whether the central baseband carrier in the SCM signal is generated [8].

2.2.1 In-band transmission Schemes

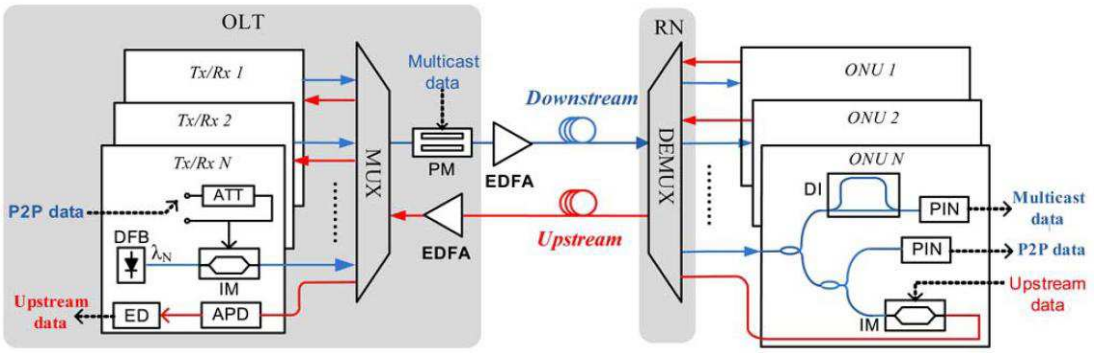

Fig. 2.2 A multicast architecture using DPSK/NRZ orthogonal modulation [3]

Fig. 2.2 depicts a multicast WDM-PON architecture using differential phase-shift keying (DPSK)/NRZ orthogonal modulation. At the OLT, each individual downstream channel was first modulated by the extinction ratio (ER)-controllable NRZ unicast signal via an intensity modulator and then combined with other downstream channels via an AWG before fed into a common phase modulator, where the DPSK multicast data was further superimposed onto them. The combined downstream wavelengths simultaneously delivered both unicast NRZ data and multicast DPSK signal to the ONUs after amplified

by an erbium-doped fiber amplifier (EDFA). At the ONU, due to the orthogonality of NRZ and DPSK formats, unicast and multicast data could be both recovered when the ER of NRZ signal remained low. On the contrary, only NRZ unicast could be recovered and multicast transmission was disabled. This ER control was realized at the OLT though a simple electrical switch, which changes the voltage peak-peak (Vpp) value of the NRZ unicast data. Although the multicast and unicast data could be both recovered when the multicast transmission was enabled, the performance of unicast data was sacrificed due to its low ER, while the multicast DPSK data suffered from the intensity fluctuation induced by unicast NRZ data. In addition, the ER of the downstream unicast data could not be very high to keep its reusability for upstream intensity modulated data. Therefore, the ONU could remain simple and colorless, but the performance of the system was limited.

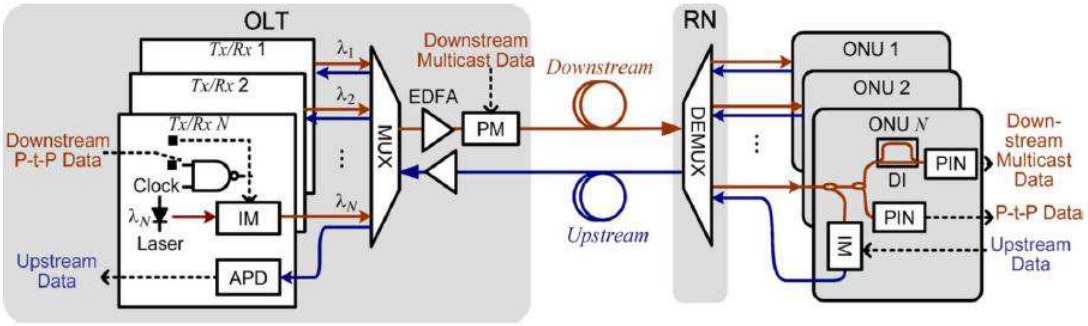

Fig. 2.3 A multicast enabled WDM-PON architecture employing IRZ [5]

Fig. 2.3 depicts a multicast enabled WDM-PON employing inverse return-to-zero (IRZ) format [5], which always has power in the second half of the transmitted bit implying the possibility to carry a second data stream onto this second half of the bit. Therefore, a single IRZ signal stream can simultaneously support two different data streams, one for

unicast and another for multicast transmission. On the contrary, non-return-to-zero (NRZ) with high ER is incapable to transmit second data stream on its own because there is negligible power existing when “0”s are transmitted. In this approach, the multicast control was realized by changing the modulation format of downstream unicast from IRZ to NRZ. When the unicast format was IRZ, the multicast differential phase-shift-keying (DPSK) video signal superimposed on it could be successfully received, but the multicast transmission would be disabled when unicast data was in high extinction ratio NRZ format. In the experiment, a logic NAND gate at the OLT driven by a combined signal of clock and the downstream unicast data was used to generate IRZ format signals for multicast enabled mode. In the multicast disabled mode, a simple electrical circuit implemented at each transceiver triggered the unicast to bypass the logic NAND gate, and only high ER NRZ could be generated. Multicast DPSK signals were superimposed onto the downstream unicast data via a common phase modulator after all the downstream channels were multiplexed at the AWG. At the ONU, half of downstream power was reused for upstream transmission. The transmission speed of the system increases to 10 Gbit/s, although some cost-effective electrical logic devices were still needed for multicast control. However, IRZ was not often employed in WDM-PONs, which makes it difficult to upgrade the existing system to multicast function as extra components were required to generate IRZ format.

2.2.2 Out-band transmission Schemes

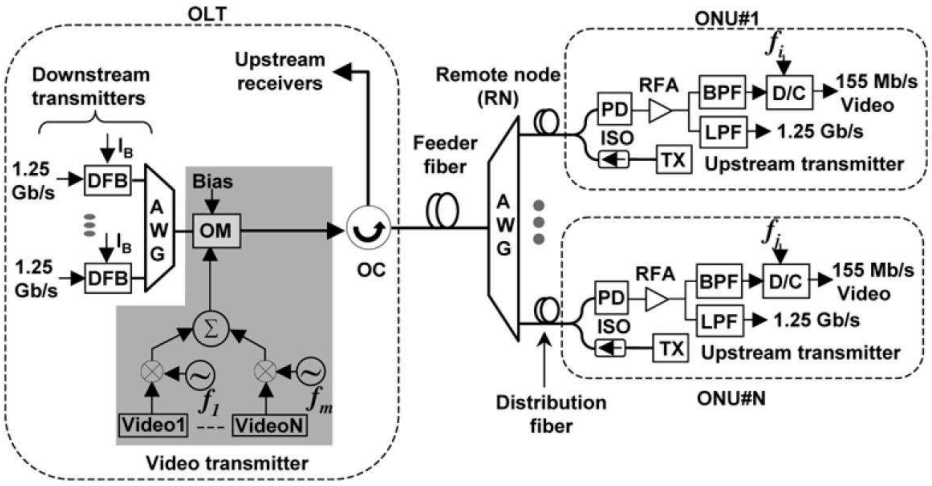

Fig. 2.4 Multicast enabled WDM-PON system utilizing subcarrier multiplexing (SCM) [6]

Fig. 2.4 shows a WDM-PON with multicast capability using subcarrier multiplexing (SCM) technology [6]. In this scheme, a set of directly-modulated distributed feedback (DFB) lasers located at the OLT carried the downstream unicast NRZ-ASK signals, while the downstream multicast SCM BPSK video signals generated by a common radio frequency (RF) video transmitter were superimposed onto the unicast channels, via a Mach-Zehnder modulator (MZM). All downstream channels from the OLT were fed into a feeder fiber before being delivered to the dedicated ONUs. At the ONU, the combined multicast SCM BPSK signal and the unicast NRZ-ASK signal were converted into electrical signals, via a wide-band photo detector, before being separated by different electrical filters. The multicast control was realized by changing the ER of the unicast NRZ-ASK signal, so that the multicast subcarrier signals could be enabled when the ER was low or disabled when the ER was high. The multicast control scheme was centralized at the OLT, which reduced the system cost and management difficulty. However, light

sources were needed for the upstream transmission which made ONUs complex and colored. Also the transmission capacity was limited since it provides only 1.25Gbit/s for unicast transmission and 155Mbit/s for multicast transmission. Moreover, several dedicated electronic devices, including subcarrier modulation module, local frequency synthesizer, and RF combiner were required at the transceivers to modulate and demodulate the subcarrier signals, which dramatically increased the system complexity.

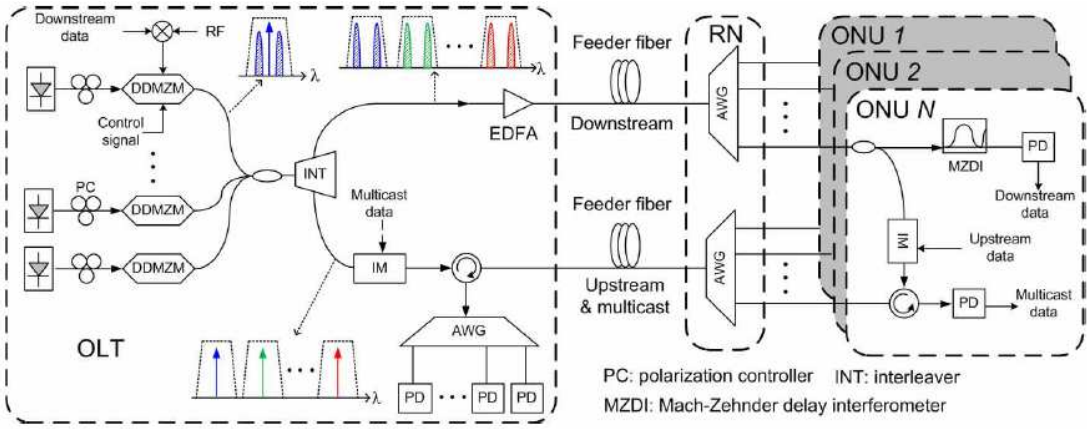

Fig. 2.5 Another SCM-based multicast architecture [8]

Another SCM based multicast architecture was proposed as shown in Fig. 2.5 [8]. Different from previous schemes, a SCM downstream signal was first generated by a dual-drive Mach-Zehnder modulator (DDMZM), driven by a combined signal of unicast data and a RF clock. The SCM downstream signal, comprising a central carrier and subcarriers with unicast data on it, were then separated through an optical interleaver (INT), where the central carrier was separated out onto a different transmission link for multicast traffic after intensity modulated by the multicast data via a common MZM. Meanwhile, the remained subcarriers carrying unicast signal were delivered to ONUs for

unicast data reception. At the ONU, half of unicast traffic power was reused for the upstream transmission. Because the unicast data and multicast data passed through two independent transmission links, the potential crosstalk or interference between them could be much reduced. The realization of multicast control was carried out by changing the bias current of the DDMZM which determined the generation of the central carrier in the SCM signal. Multicast transmission would be enabled if the SCM signal has central carrier but disabled without central carrier. The system could relieve the crosstalk between unicast and multicast to some extent through different transmission links, but the unicast signal might still leak to central carrier. In addition, the unicast data on the double-sideband subcarrier suffered from serious coherent beating noise and required additional electric low-pass filter at the ONU for data reception. Moreover，transmission speed of the subcarrier modulated signal in a SCM based system is limited due to the processing speed of electrical devices used in the SCM module.

2.3 Dynamic Wavelength Reflection Scheme

In this section, a simple scheme to overlay multicast service is proposed, which falls into the “In-band transmission” category. It uses a set of dynamic wavelength reflector added on each wavelength channel. By dynamically adjusting the state of the dynamic wavelength reflector, the multicast data can be enabled on a unicast wavelength channel to achieve flexible multicast function. The multicast function can be quickly and dynamically reconfigured with simple and centralized control in the OLT and is transparent for all

ONUs. The technique just adds a little complexity to the existing WDM-PON structure, and its feasibility is demonstrated with 5Gbit/s downstream unicast, multicast signal and 625Mbit/s upstream re-modulated data. By employing re-modulation technique, no light sources and colored components are needed in the ONUs, which effectively reduce the cost and complexity.

2.3.1 Proposed Scheme and Principle

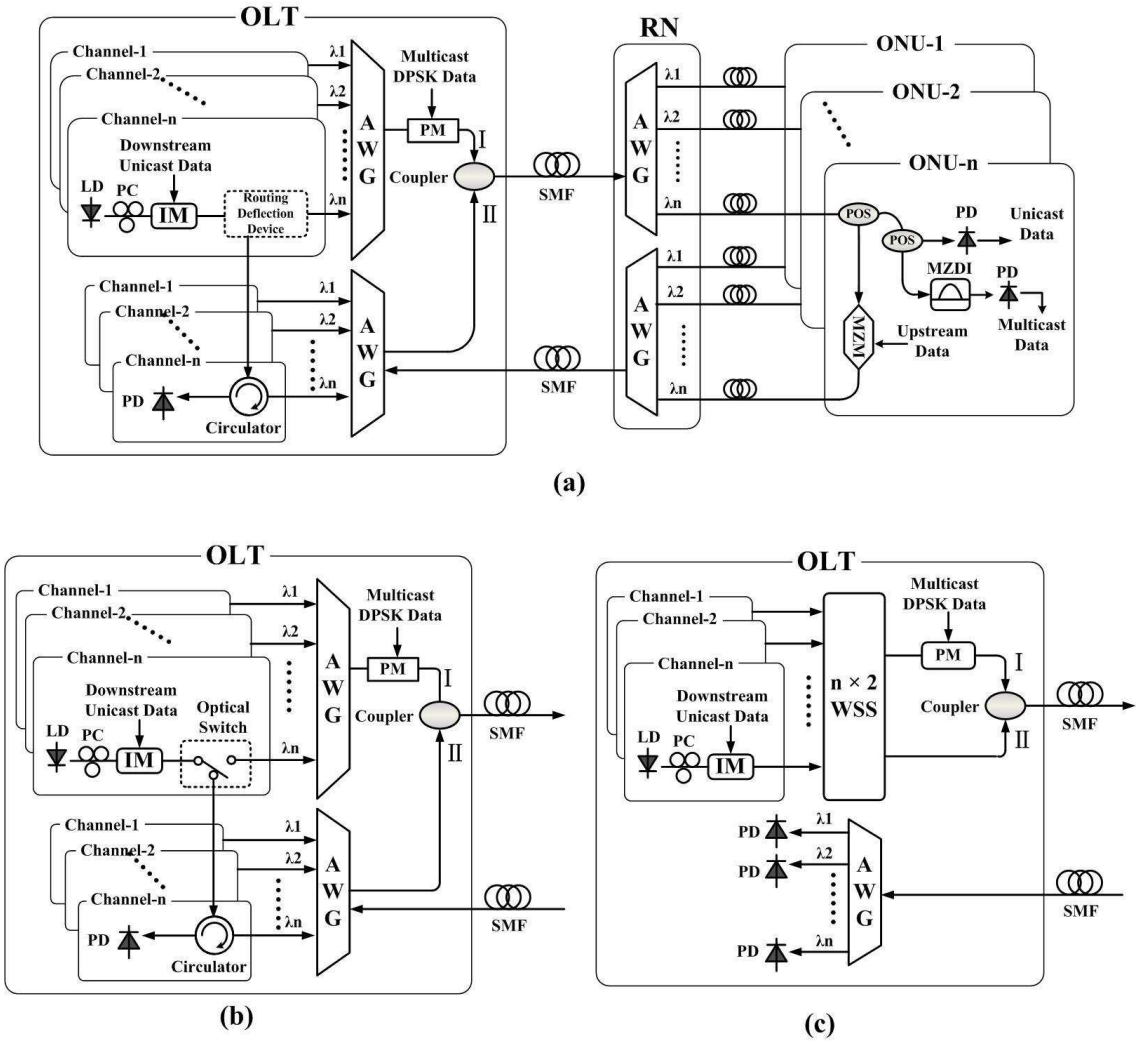

Fig. 2.6 (a) Schematic of the proposed WDM-PON architecture with multicast overlay, using (b) 1×2 optical switch, or (c) n×2 WSS as a dynamic wavelength reflector in OLT

The proposed WDM-PON architecture with multicast overlay is shown in Fig. 2.6. In the OLT, the downstream carrier of each wavelength channel is generated by a continuous-wave (CW) laser, and modulated by an optical intensity modulators (IMs), to generate NRZ unicast data, with an ER of around 3dB. The lower ER makes it easier that the successful superimposition of the DPSK multicast data and upstream data re-modulation [9]. To realize flexible multicast, the dynamic wavelength reflector can be added in between IM and AWG on each wavelength channel. In the scheme, the dynamic wavelength reflector can be realized as either an optical switch (OS), or wavelength selective switch (WSS) [10-11], or optical interferometer [12-13], or a set of an optical circulator and a controllable Fiber Bragg Grating (FBG) [14-15].

When an ONU makes a request for the multicast service, the controllable FBG in the corresponding wavelength channel is adjusted via the control circuit to deviate from center wavelength and to allow unicast data carrier go straight to the AWG. Thus multicast signal can be simultaneously modulated on the downstream unicast carrier by an optical phase modulator (PM). To disable the multicast signal for an ONU, the FBG is dynamically tuned and reflects the corresponding wavelength to 2×N AWG, so as to bypass multicast signal modulation. Hence the multicast signal can be selectively and dynamically superimposed onto downstream unicast signal on arbitrary wavelength channels. Then these two multiplexed signals I and II are combined by coupler and carried to remote node (RN) and finally routed to individual ONU. It is noted that all the multicast control

intelligence is deployed at OLT by adjusting a set of the dynamic wavelength reflectors, which are transparent to all ONUs and can be a cost-effective solution.

In ONU, one part of downstream power is tapped off by a power optical splitter (POS) for downstream unicast NRZ data and multicast DPSK data, respectively. For users who subscribe to multicast service, the optical carrier not only carries the downstream unicast data, but also contains the multicast data information. The remaining part is re-modulated by upstream data with higher ER and sent back to the OLT. In this way, colorless ONU without the need of light source could also be implemented.

2.3.2 Experimental Setup and Results

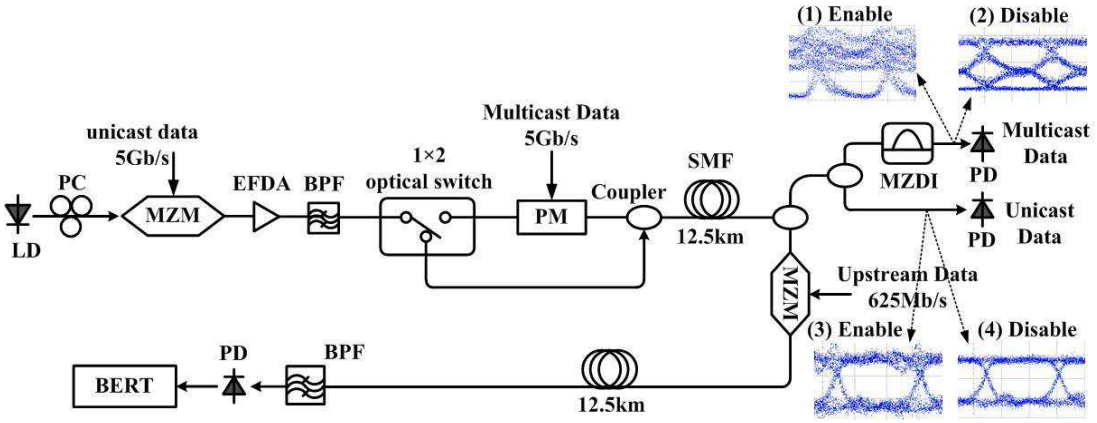

Fig. 2.7 Experimental setup using a 1×2 optical switch as a dynamic wavelength reflector.

To verify the feasibility of the proposed scheme, the downstream unicast/multicast transmission and upstream data re-modulation were demonstrated in Fig. 2.7. In the OLT, a CW in the 1551.95 nm wavelength is fed into a MZM which is biased at the transmission null point and is driven by a 5-Gb/s 2^{31}-1 pseudorandom binary sequence (PRBS) to generate downstream unicast NRZ signal, with 3dB ER. After an EDFA and a

tunable band-pass filter (BPF) with a bandwidth of 0.4 nm, the unicast NRZ signal is orthogonally phase-modulated by a PM to superimpose multicast data when the optical switch is in the bar state. To obtain better signal performance, downstream unicast data and multicast data signals need to be bit synchronized, which is adjusted by an electrical phase shifter. When the optical switch is in the cross state, the downstream optical carrier just contains unicast data with multicast service disabled. Then the both two optical links are connected via a 1×2 optical coupler with a piece of 12.5km single mode fiber (SMF) to reach respective ONU.

The four eye diagrams are shown in the insets of Fig. 2.7. The inset figure 1) shows the eye diagram of the demodulated multicast DPSK signal with downstream unicast NRZ signal, which has three folds of up-eyelids. The inset figures 3) and 4) display the eye diagrams for the demodulated NRZ with multicast DPSK signal enabled and with DPSK signal disabled, respectively. The eye diagram for the downstream unicast NRZ demodulated by DI without multicast DPSK signal is shown in the inset 2) of Fig. 2.7.

The bit-error-rate (BER) curves of the downstream unicast NRZ signal and multicast DPSK signal are provided in Fig. 2.8 (a). The power penalties of downstream unicast signal caused by the fiber transmission are ~0.8 dB with multicast data and ~1.3dB without multicast data, respectively. The power penalty is ~0.5 dB for the DPSK multicast signal. Fig. 2.8 (b) shows the BER of upstream re-modulated NRZ signal with higher ER, after the 25-km SMF transmission. We observe that the upstream transmission suffers ~0.5-dB penalty due to the dispersion. The insets of Fig. 2.8 (b) are eye diagrams of

upstream re-modulated NRZ signal.

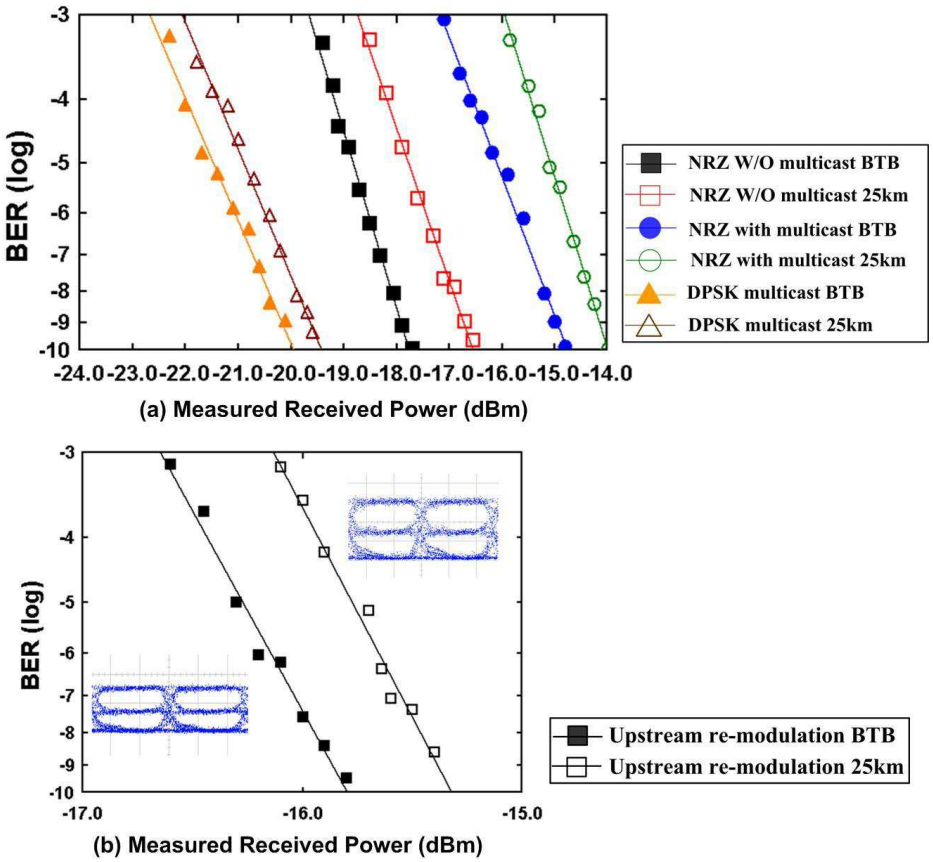

Fig. 2.8 BER curves (a) for the downstream NRZ/DPSK, (b) for upstream re-modulated signal

2.4 RF Control Scheme

In this section, we propose and demonstrate a novel WDM-PON with the "Out-band transmission" scheme to simultaneously deliver the downstream unicast data and multicast services along with upstream data re-modulation in ONUs. For each wavelength channel in the OLT, the downstream unicast data are applied to one arm of a dual-parallel MZM (DPMZM) to generate unicast NRZ signal carried on the optical baseband carrier, and a RF control signal is applied to the other arm to produce two un-modulated optical

sidebands for subsequent multicast DPSK data modulation. By simply switching the RF control signal on or off in each wavelength channel, the multicast data can be enabled to realize a flexible multicast overlay. Given that the RF control signal is transparent to all ONUs, the system can thus be considered a cost-effective solution.

2.4.1 Principle of proposed WDM-PON

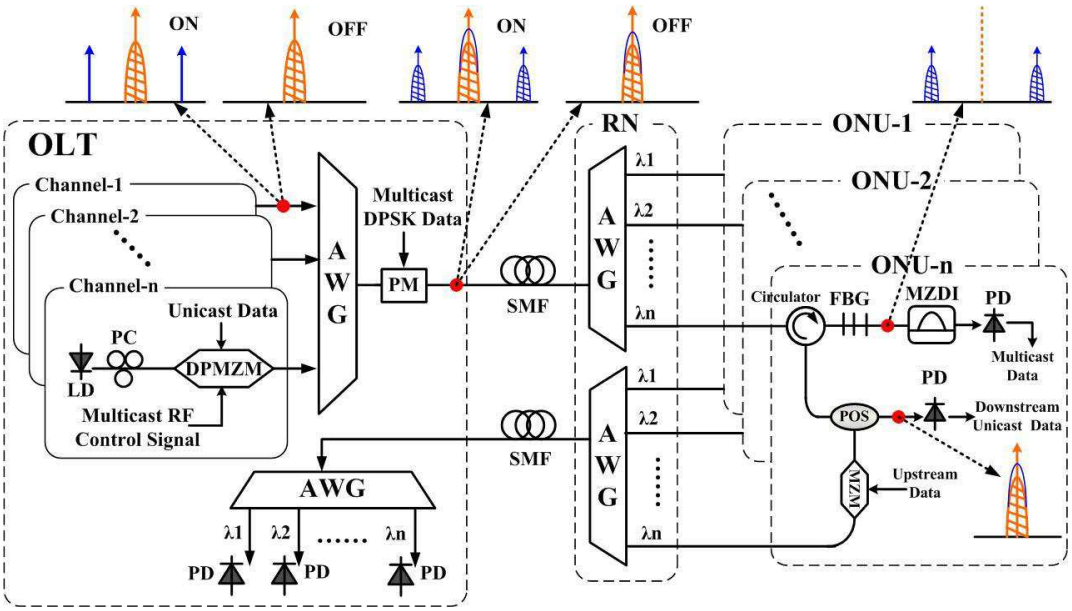

Fig. 2.9 Schematic of the proposed WDM-PON architecture with SCM multicast overlay.

The proposed WDM-PON architecture with SCM multicast overlay is shown in Fig. 2.9. In the OLT, the downstream carrier of each wavelength channel is generated by a CW laser and is modulated using a DPMZM [16-17]. The DPMZM consists of a pair of x-cut LiNbO3 MZMs embedded in the two arms of a main MZM structure. The DPMZM has three bias ports that belong to the two sub-MZMs and the main modulator. The downstream unicast data are then applied to one arm of a DPMZM, to generate a

downstream unicast NRZ signal with a lower ER, and a RF control signal is applied to the other arm of the DPMZM to switch two un-modulated optical sidebands on or off. These optical double-sideband signals in all wavelength channels are then coupled using an AWG and subsequently modulated through a common PM, which is driven by the multicast data to overlay a multicast DPSK signal on the optical sub-carriers. The multicast data are also superimposed onto the optical baseband carrier in the baseband carrier; however, the multicast data are not recovered in the ONU. Hence, the multicast and unicast data transmissions differ in both frequency and modulation formats, thereby avoiding the bit synchronization between them.

When an ONU on a wavelength makes a request for multicast services, the RF control signal on the corresponding wavelength channel is switched on, allowing the simultaneous modulation of multicast data on the optical sub-carriers. To disable the multicast data for a designated ONU user, the RF control signal can be simply switched off and consequently, the optical sub-carriers for multicast data modulation do not exist.

After transmission, an AWG in the RN is used to de-multiplex the downstream wavelengths and route them to individual ONUs. At the ONU, a circulator and fiber Bragg grating (FBG) are used to separate the downstream unicast NRZ data and the multicast DPSK data on different spectra. The multicast data are demodulated using a 1-bit Mach-Zehnder delay interferometer (MZDI) followed by a low-speed photo-detector (PD). The baseband optical carrier is then filtered and split into two parts, one is detected using a PD receiver for downstream unicast data, while the other part of the baseband carrier

power is fed into a single drive MZM for upstream data re-modulation and is sent back to the OLT through another feeder fiber. In this way, an ONU module without a light source deployment, which is an attractive feature of PON deployment, could also be implemented. All the multicast control intelligence data are deployed at the OLT by simply switching the RF control signal on or off. Given that the RF control signal is transparent to all ONUs, the system can thus be considered a cost-effective solution.

2.4.2 Experimental setup and results

To verify the feasibility of the proposed WDM-PON with SCM multicast overlay, we performed an experiment shown in Fig. 2.10. In the OLT, a CW light with the wavelength of 1561.16 nm was fed into a DPMZM. One arm of the DPMZM was biased at the transmission null point and was driven by 1.25Gitb/s data with a pseudo-random bit sequence (PRBS) length of 2^{31}-1 to generate downstream unicast NRZ signal with the lower ER around 3 dB. The 12.5GHz RF control signal was applied on the other arm of DPMZM also biased at the transmission null point; switching it on or off made it easy to control the presence of two un-modulated subcarriers. The bias of main MZM structure was adjusted to obtain zero phase difference between the two arms of the modulator. The two signals from two sub-MZMs were combined constructively to achieve a double-sideband signal at the output port of the main modulator. Another PM was driven by another 1.25Gitb/s 2^{31}-1 PRBS to generate multicast DPSK signal carried on the two optical sidebands. The sideband-to-carrier ratio (SCR) of an optical double-sideband signal was nearly 10 dB (see Fig. 2.11, inset (i)). Only the optical baseband carrier was

displayed in the inset (ii) of Fig. 2.11 with the multicast services switched off.

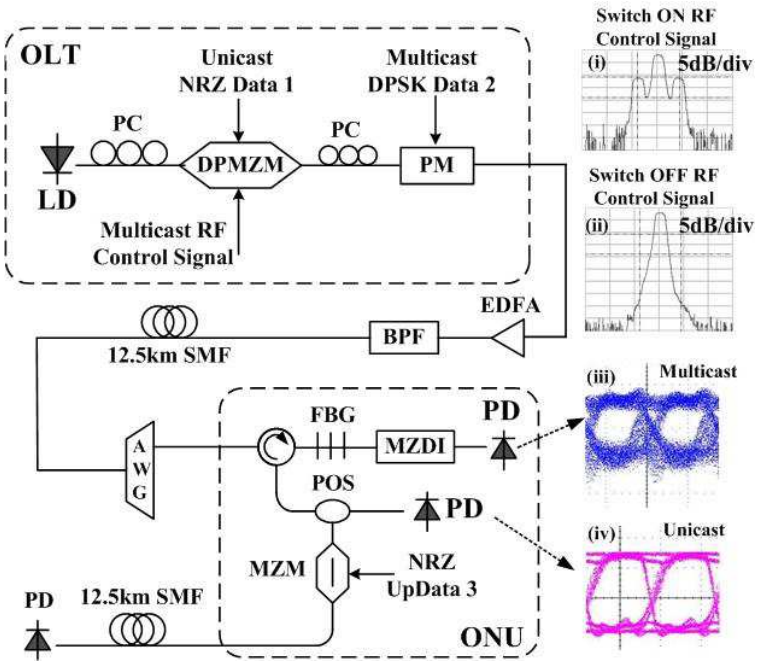

Fig. 2.10 Experimental setup of the proposed WDM-PON with SCM multicast overlay.

The output from the PM was amplified by an EDFA and filtered by a tunable band-pass filter (BPF) with the bandwidth of 0.4nm before a 12.5km single mode fiber (SMF) transmission. In the ONU, an optical circulator was connected to a FBG with a 3dB bandwidth of 0.15nm and a 90% reflection ratio. The FBG was used to reflect the baseband optical carrier of unicast NRZ data and bypass the two sideband optical carriers for multicast DPSK data. After being demodulated by 1 bit MZDI, followed by a low speed PD with a 2.5GHz bandwidth, the 25GHz oscillation of the SCM multicast data was filtered, and the electrical eye diagrams of multicast data are displayed (see Fig. 2.10, inset (iii)). The reflected optical power of the baseband NRZ signal was split into two parts using a POS. One half was converted into an electrical signal using a 2.5GHz PD receiver.

The detected electrical eye diagrams of downstream unicast NRZ data are shown in Fig. 2.10, inset (iv). The other half of baseband power was used for 1.25Gbit/s upstream data re-modulation in the NRZ format with the higher ER of around 10 dB and then sent back to the OLT, where it was detected by a PD.

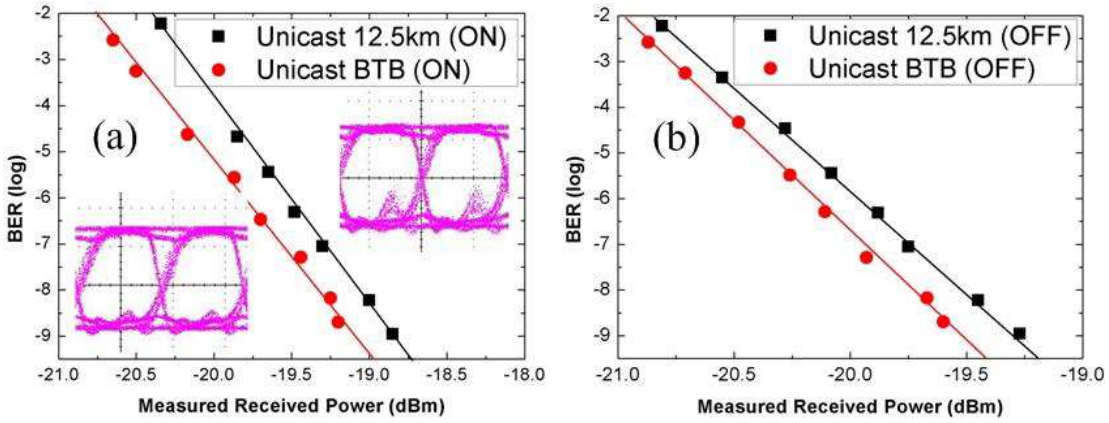

Fig. 2.11 BER curves and eye diagrams: (a) downstream unicast NRZ signal when the RF control signal is switched on; (b) downstream unicast NRZ signal when the RF control signal is switched off.

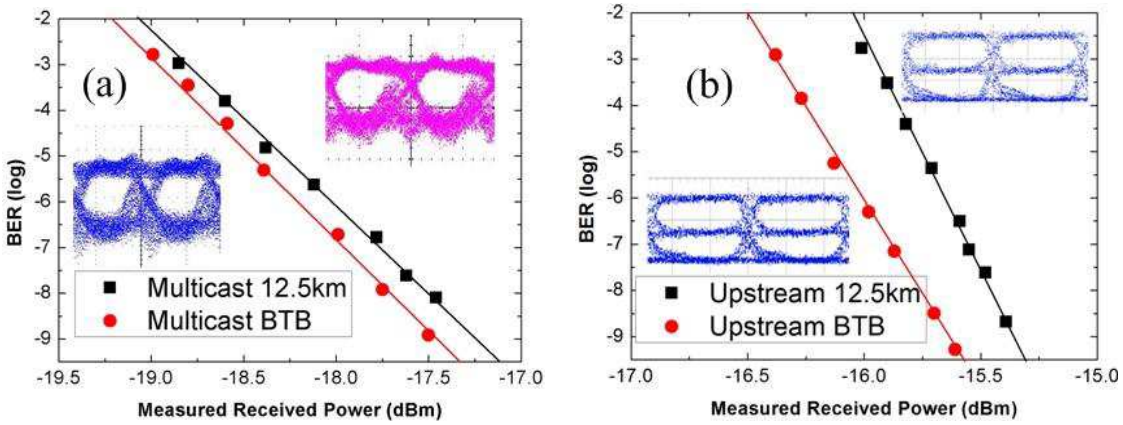

Fig. 2.12 BER curves and eye diagrams: (a) multicast DPSK data; (b) upstream re-modulated NRZ signal.

The BER measurement results are presented in Figs. 2.11 and Fig. 2.12. For the

downstream unicast NRZ data when the RF control signal is switched on and off, the power penalties are ~0.27 and ~0.23 dB, respectively. The detected electrical eye diagrams are also respectively provided in insets of Fig. 2.11 (a). For the multicast DPSK signal on the two optical sidebands, the power penalty is ~0.2dB; the eye diagrams are shown in Fig. 2.12 (a). The BER performance of upstream re-modulated NRZ signal shown in Fig. 2.12 (b) indicates that the upstream transmission suffered a ~0.35dB penalty due to the dispersion. The eye diagram of upstream data for back-to-back (BTB) transmission and after the 12.5km SMF transmission are also displayed in the inset of Fig. 2.12 (b).

Table. 2.1 Power margin calculation for downstream and upstream data

	Downstream Unicast Data	**Multicast Data**	**Upstream Unicast Data**
Modulated power at OLT (dBm)	-14	-16	----
Modulated power at ONU (dBm)	----		-19
EDFA amplifier gain (dB)	30	30	30
BPF loss (dB)	3	3	3
Phase modulator loss (dB)	6	6	----
AWG insertion loss (dB)	5×2 *	5×2 *	5×2 *
12.5km SMF loss (dB)	2.8	2.8	2.8
Circulator insertion loss (dB)	0.8	0.8	----
FBG insertion loss at ONU (dB)	0.6	0.6	----
Splitter insertion loss at ONU (dB)	3	----	----
MZDI insertion loss at ONU (dB)	----	6	----
Insertion loss (dB)	26.2	29.2	15.8
Receiver Sensitivity (dBm)	-18.85	-17.25	-15.35
Power Margin (dB)	8.65	2.05	10.55

* 2×2" means the optical signal experiences the loss twice.

To verify the feasibility of the downstream link, a power budget analysis for the downstream unicast and multicast data was carried out using the modulated optical power

of around -14dBm and -16dBm, respectively (see Table 2.1). In this analysis, EDFA gain reached about 30 dB in the OLT. The total losses consist of a 3dB BPF loss, a 6dB insert loss for PM, a 5dB insert loss for AWG, a 2.8dB transmission loss for a 12.5km optical fiber, a 0.8dB insert loss for the optical circulator, a 0.6dB FBG insert loss, a 6dB insertion loss for MZDI, and a 3dB splitter insertion loss at ONU. Consequently, in the upstream power budget analysis, a re-modulated upstream unicast signal showed an optical power of around -19dBm. According to the experiment data, the receiver sensitivity of the downstream unicast data, multicast data, and upstream unicast data are -18.85dBm, -17.25dBm, and -15.35dBm, respectively (see Figs. 2.12 (a), 2.13 (a), and 2.13 (b)). The power margin of about 8.65, 2.05, and 10.55dB are obtained for downstream unicast data, multicast data, and upstream signal, respectively, indicating the feasibility of the larger transmission scope in the proposed WDM-PON.

2.5 Conclusion

We have proposed and demonstrated novel two schemes to simultaneously deliver downstream unicast and multicast signal over WDM-PON architecture.

1) Dynamic wavelength reflection scheme: In each WDM channel, a dynamic wavelength reflector is used to selectively enable the multicast data superimposition on the corresponding downstream unicast carrier. The multicast function can be quickly and dynamically reconfigured with simple and centralized control in the OLT and is transparent for all ONUs. By employing re-modulation technique, no light

source is needed in the ONUs, which effectively reduces the cost and complexity.

2) RF Control Scheme: The baseband optical carrier bears the downstream unicast NRZ data, and the two optical sub-carriers only carry multicast DPSK data. The multicast function for all wavelength channels can be reconfigured quickly and dynamically through simple and centralized management in the OLT.

References

[1] P. P. Iannone, K. C. Reichmann, and N. J. Frigo, "Broadcast digital video delivered over WDM passive optical networks," *IEEE Photon. Technol. Lett.*, vol. 8, no. 7, pp. 930–932, Jul. 1996.

[2] C. Bock and J. Prat , "WDM/TDM PON experiments using the AWG free spectral range periodicity to transmit unicast and multicast data," *OSA Opt. Express*, vol. 13, no. 8, pp. 2887-2891, April. 2005.

[3] Y. Zhang, N. Deng, C. K. Chan, and L. K. Chen, "A multicast WDM-PON architecture using DPSK/NRZ orthogonal modulation," *IEEE Photon. Technol. Lett.*, vol. 20, no. 17, pp. 1479-1481, 2008.

[4] L. Cai, Z. Liu, S, Xiao, M. Zhu, R. Li and W. Hu, "Video-service-overlaid wavelength-division-multiplexed passive optical network," *IEEE Photon. Technol. Lett.*, vol. 21, no. 14, pp. 990-992, 2009.

[5] N. Deng, C. K. Chan, L. K. Chen, and C. Lin, "A WDM passive optical network with centralized light sources and multicast overlay," *IEEE Photon. Technol. Lett.*, vol. 20, no. 2, pp. 114–116, Jan. 2008.

[6] M. Khanal, C. J. Chae, R. S. Tucker, "Selective broadcasting of digital video signals over a WDM passive optical network," *IEEE Photon. Technol. Lett.*, vol. 17, no. 9, pp. 1992-1994, Sept. 2005.

[7] Q. J. Chang, J. M. Gao, Q. Li, Y. K. Su, "Simultaneous transmission of point-to-point data and selective delivery of video services in a WDM-PON Using ASK/SCM Modulation Format," *IEEE/OSA Optical Fiber Communication Conference / National Fiber Optic Engineers Conference (OFC/NFOEC)*, Paper OWH2, San Diego, California, USA, 2008.

[8] Y. Tian, Q. J. Chang, Y. K. Su, "A WDM passive optical network enabling multicasting with color-free ONUs," *OSA Opt. Express*, vol. 16, no. 14, pp. 10434-10439, Jul. 2008.

[9] M. Ohm, "Quaternary Optical ASK-DPSK and Receivers with Direct Detection," *IEEE Photon. Technol. Lett.*, vol. 15, no. 1, pp. 159-161, 2003.

[10] S. Frisken, G. Baxter, D. Abakoumov, H. Zhou, I. Clarke, and S. Poole, "Flexible and Grid-less Wavelength Selective Switch using LCOS Technology," *IEEE/OSA Optical Fiber Communication Conference/National Fiber Optic Engineers Conference (OFC/NFOEC)*, Paper OTuM3, California, USA, 2011.

[11] C. R. Doerr, L. L. Buhl, L. Chen, and N. Dupuis, "Monolithic Flexible-Grid 1×2 Wavelength-

Selective Switch in Silicon Photonics," *IEEE J. Lightwave Technol.*, vol. 30, no. 4, pp. 473-478, Apr. 2012.

[12] M. Sumetsky, Y. Dulashko, and A. Hale, "Fabrication and study of bent and coiled free silica nanowires: Self-coupling microloop optical interferometer," *OSA Opt. Express*, vol. 12, no. 15, pp. 3521-3531, 2004.

[13] M. B. Duhring and Ole Sigmund, "Improving the acousto-optical interaction in a mach-zehnder interferometer," *Journal of Applied Physics*, vol. 105, no. 8, pp. 083529- 1-9, Apr. 2009.

[14] K. O. Hill and G. Meltz, "Fiber Bragg grating technology fundamentals and overview," *IEEE J. Lightwave Technol.*, vol. 15, no. 8, pp. 1263-1276, Aug 1997.

[15] X. Fang, C. R. Liao, and D. N. Wang, "Femtosecond laser fabricated fiber Bragg grating in microfiber for refractive index sensing," *OSA Opt. Lett.*, vol. 35, no. 7, pp. 1007-1009, 2010.

[16] K. Higuma, S. Oikawa, Y. Hashimoto, H. Nagata, and M. Izutsu, "X-cut lithium niobate optical single-sideband modulator," *Electron. Lett.*, vol. 37, no. 8, pp. 515–516, Apr. 2001.

[17] Q. Chang, T. Ye, and Y. Su, "Generation of optical carrier suppressed-differential phase shift keying (OCS-DPSK) format using one dual-parallel Mach-Zehnder modulator in radio over fiber systems," OSA Opt. Express, vol. 16, no. 14, pp. 10421-10426, 2008.

Chapter 3. Protection Switching Schemes in WDM-PONs

In this chapter, we will first review several survivable WDM-PON architectures, which realize protection schemes in optical layer. We divided these reported protection schemes into three categories: group protection, ring protection and duplication protection. Then we will propose our own two automatic protection switching schemes: one is used in single WDM-PON, and the other is suitable for dual-PON architecture. The main contributions in this works are: 1) a novel logic decision unit in conjunction with a power monitoring unit is implemented in the OLT to enable the effective protection switching in more practical operation scenarios; 2) the detection results recorded by the power monitoring unit facilitate a faster failure recovery; 3) in dual-PON architecture, the number of extra protection fibers is minimized and the wavelength resource is much more efficiently utilized.

3.1 Introduction

Wavelength division multiplexed passive optical network (WDM-PON) is a promising broadband access solution, because it offers huge bandwidth, protocol transparency, excellent security and easy upgradeability [1-2]. As the data rate per user is getting to 1Gbit/s, 10Gbit/s and beyond in a WDM-PON, any possible failure of either feeder fibers (FFs) or distribution fibers (DFs) will lead to a large amount of data loss. Therefore, how

to increase the network survivability [3-4] has become an intensively-discussed issue in WDM-PON architecture design, since highly reliable data transmissions are required in nowadays networks even in some unpredicted scenarios, such as fire or flooding.

Fault management is one of the well-known crucial aspects in network management. Most of the conventional approaches of fault management rely on diagnosis in higher layers [5-6], based on the status reports collected from various checkpoints on the managed optical network. However, such high-level fault diagnosis would impose excessive overhead in network signaling as well as in the network management system (NMS). Yet there is no guarantee that higher layers can provide recovery from faults in the physical layer. Therefore, in order to facilitate effective and prompt network protection and restoration, it is highly desirable to perform network survivability measures in the optical layer. This can be achieved by simple fiber link or equipment duplication along with some protection switching schemes with minimal resource duplication or reservation for protection. For PON applications, equipment failure at either OLT or ONU can be easily remedied by having a backup unit in the controlled environment. However, for any fiber cut, it would take a relatively long time to perform the repair. Therefore, it is highly desirable to have survivable PON architectures with protection switching against any fiber cut.

3.2 Related Works

To date, many protection schemes based on automatic protection switching (APS)

[7-13] have been proposed. The APS unit consists of a monitoring and control circuit (MCC), which is responsible for failure monitoring and connection state control of optical switch (OS). The APS implies to switch automatically the affected data to an alternate protection path on the existing network architectures upon detection of a drastic power drop, in order to bypass the failed fiber links. The APS can be realized by either centralized or distributed control. In centralized control, all protection switching are performed at the OLT once a fiber failure is detected. The ONUs still stay connected with the OLT after the APS. On the contrary, protection switching can be performed at individual ONUs instead, to realize distributed control. In this case, individual ONUs continuously monitors the status of their attached fiber links. APS will be triggered only at the affected ONU when any fault is detected. The OLT does not need to perform any remedy and is transparent to such APS. However, this approach increases ONU complexity and costs.

We categorize the previous protection schemes into three categories as listed in Table 3.1: group protection [7-8], ring protection [9-10] and duplication protection [11-13]. In the first category, two adjacent optical network units (ONUs) can form a group to protect each other via an extra interconnection fiber (IF). Each ONU may also receive its signals from its adjacent ONU in the same group, thus the security advantage of the WDM-PON may be undermined. In the second category, all ONUs [9] or small regions of closely located ONUs [10] are connected one-by-one to provide alternate route for the next one following a certain direction along the protection ring and received backup wavelength

for itself from the prior one, thus the PON security was also sacrificed to a certain extent. For duplication protection, both working FFs and DFs in normal mode are duplicated for protection and connected to an $N \times N$ AWG located at RN [11-12]. Note that the working and protection fibers should be deployed separately. In [11-12], the distributed APS is performed at each ONU, where an optical switch and an optical monitor are installed. In [13], the OLT comprises two broadband light sources (BLS), two optical switches and an optical monitor to implement low-cost colorless transceivers and centrally-controlled APS. But it just offered protection against FFs.

Table. 3.1 Existing protection schemes in (a) single WDM-PON and (b) dual WDM-PONs

(a) Self-Protection Schemes in a Single WDM-PON			(b) Cross-Protection Schemes in Dual WDM-PONs
Distribution Fiber (DF) Protection Topology	Centrally-Controlled APS	Distributed-Controlled APS	
Duplication Protection Architecture 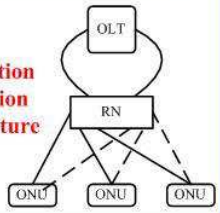	X. F. Sun, et al, IEEE PTL Vol.18(4), 2006 A. Chowdhury, et al, OFC2008, JThA95. Y. Qiu, et al, IEEE PTL Vol.23(6), 2011	S.-B. Park, et al, OFC2005, JWA57. K. Lee, et al, IEEE PTL Vol.20(9), 2008	E.S. Son, et al, OFC2005, OFI4.
Group Protection Architecture 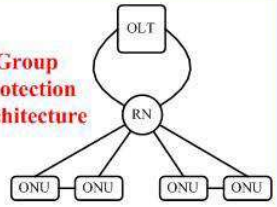	Z. X. Wang, et al, IEEE PTL Vol.17(3), 2005	T.-J. Chan, et al, IEEE PTL Vol.15(11), 2003 X. F. Cheng, et al, APOC2008. X. F. Cheng, et al, CHINACOM2010	X. F. Cheng, et al, Elsevier OC, vol. 281(18), 2008.
Ring Protection Architecture 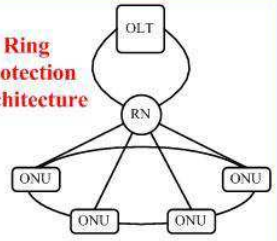		X. F. Sun, et al, OFC2004, JWA53. P. Fan, et al, OFC2011, JWA69.	

3.2.1 Duplication Protection Architecture

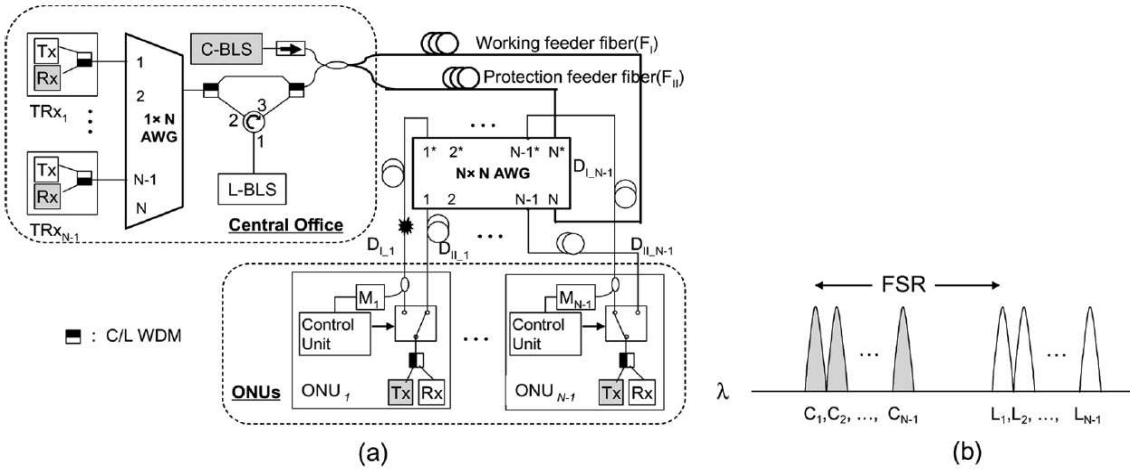

Fig. 3.1 A WDM-PON protection architecture and its wavelength assignment plan in [12]

A reliable WDM-PON architecture providing self-protection was demonstrated in Fig. 3.1 [12]. This architecture utilized the periodical and cyclical property of an N×N AWG for protection against any fiber failure in the transmission link including both FF and DF. The *N*×*N* AWG worked as a combination of two 1×(*N*-1) AWGs, which simultaneously provided two light paths between one ONU and OLT. In case of the fiber failure, the MCC unit at the ONU simply toggled the state of optical switch and the affected traffic could be rerouted to the protection link from the failed working link. The light sources were provided by two broadband light sources (BLS), L-band BLS for downstream traffic and C-band BLS for upstream traffic. They were separated by the multiple of free spectral range (FSR) of the AWG as shown in Fig. 3.2 (b). Since the two BLS were located at the central office, ONUs were kept colorless, which decreased the costs of operation, administration and maintenance (OAM). However, the use of BLS limited the data rate of the system.

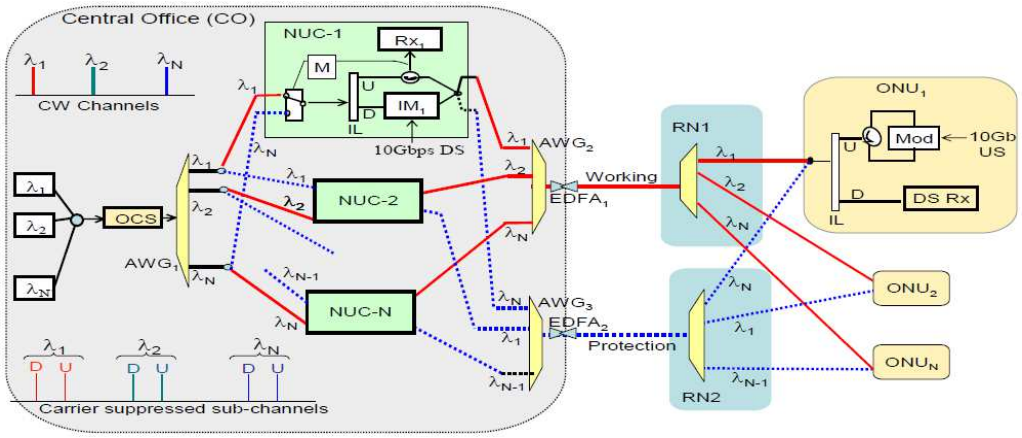

Fig. 3.2 A self-survivable WDM-PON architecture with centralized wavelength monitoring, protection and restoration [14]

A self-survivable WDM-PON architecture with centralized protection switching for both upstream and downstream links was proposed in [14] as shown in Fig. 3.2. At the CO, all the wavelengths were first fed into a common optical carrier suppression (OCS) unit to generate two subcarriers, one for downstream and the other for upstream transmission. Then each wavelength pair was divided into two parts before connected to two different network unit controllers (NUCs). Thus two wavelength pairs, implying two different transmission links, could be provided to each ONU. When a fiber failure was detected, the corresponding NUC would toggle the switch and the AWGs routed the affected traffic to the protection link. Because the light source for upstream was provided by OCS at the CO, the ONU kept colorless. In this configuration, OCS was only used for subcarrier generation for transmission. However, many optical interleavers (ILs) made the scheme complex although centrally-control APS was realized with colorless ONUs.

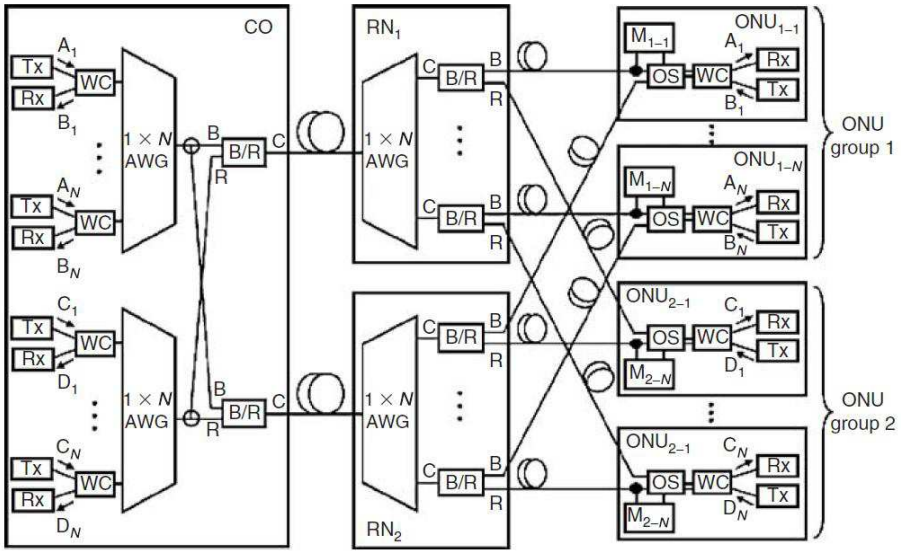

Fig. 3.3 A self-protected survivable WDM-PON in [15].

A self-protected survivable WDM-PON utilizing the cycling property of AWG was shown in Fig. 3.3 [15]. In this architecture, two WDM-PONs with different wavebands were connected together to provide mutual protection. When a fiber failure happened in one network either in feeder or distribution fiber, the transmission on the failed link could be rerouted to its protection link, which was reserved in the neighboring network. Because of the different wavebands used for two networks, the protection traffic would not affect the normal traffic even carried on the same network. The proposed architecture could successfully provide protection for both FF and DFs simultaneously. However, the MCC located at ONUs failed to realize centrally-control APS, which might make the network management difficult and increase the complexity of ONUs.

3.2.2 Group Protection Architecture

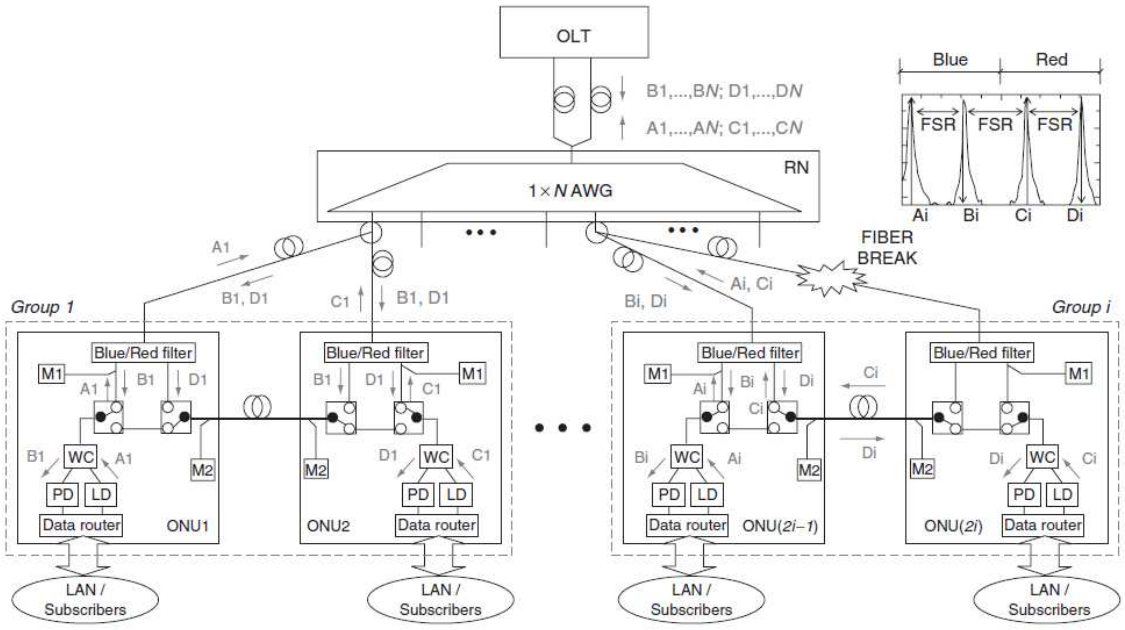

Fig. 3.4 A survivable architecture for WDM-PONs using group protection at the ONU and its wavelength assignment [7]

Fig. 3.4 shows a survivable architecture for WDM-PONs employing group protection scheme, in which two adjacent ONUs were grouped to provide mutual protection against any failure happened in the DFs [7]. The two ONUs in the same group were connected to the OLT via the same output port of the AWG at the RN. The same copy of the downstream signals of the group could reach both ONUs with proper wavelength assignment as shown in inset of Fig. 3.4. By the use of a blue/red filter and a pair of optical switches (OS) in each ONU, one ONU had preserved a potential transmission link via a piece of protection fiber for the other in the same group. In the working mode, the dedicated downstream and upstream wavelengths could be routed to the respective ONU. When there was fiber cut between a particular ONU and the RN as shown in Fig. 3.4, power loss could be detected by the monitoring units in the ONU group, which triggered

the OS states. Then the affected downstream and upstream wavelengths could be rerouted to the RN via its adjacent ONU without disturbing the normal traffic of the adjacent ONU. In this way, the ONUs in the same group provided mutual protection to each other and the OLT was kept transparent to such fiber failure.

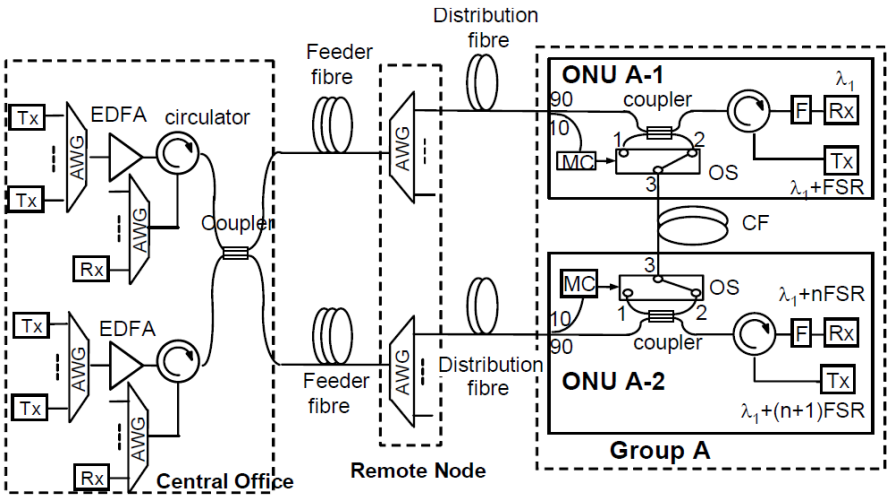

Fig. 3.5 Another survivable WDM-PON architecture using group protection at the ONU [16]

Fig. 3.5 shows another survivable WDM-PON architecture using group protection. The wavelength allocation for upstream and downstream signals in the dual WDM-PONs is similar to [15]. The four different wavelength bands are separated by a FSR of the AWGs in the RN. In the ONU, we group an ONU pair with wavelength spacing of n FSRs as an ONU group via a connection fiber (CF), where n is an integer (n>1). A sub-ring is formed, which includes the 3 dB coupler in the CO, feeder fibers, distribution fibers and an ONU pair. When any failure occurs and results in the loss of data for an ONU, the interrupted data will be recovered from the other direction of the sub-ring that the ONU belongs to. The protection procedure (i.e., failure monitoring and protection switching) is handled in

the local ONU, and no signaling of fault and OS control information needs to be remotely transmitted. Thus the protection switching time is very short.

3.2.3 Ring Protection Architecture

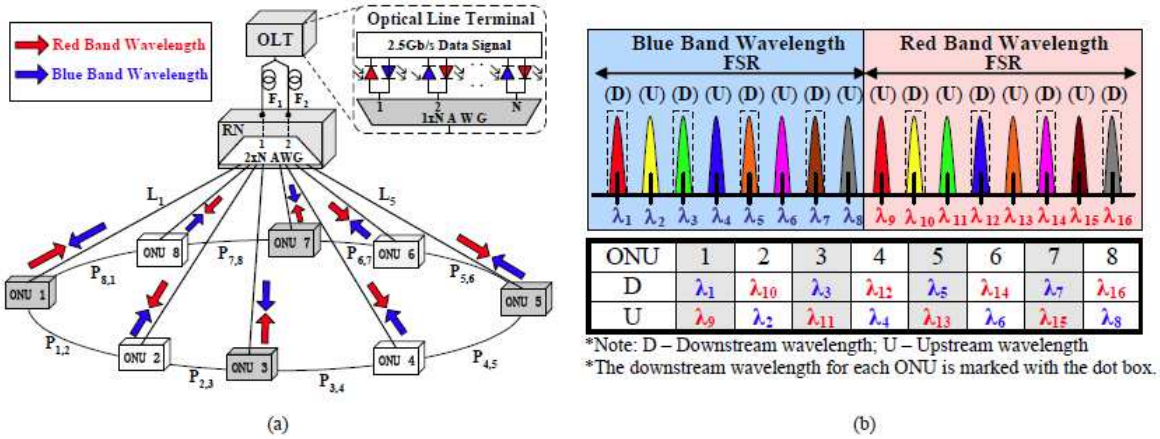

ONU	1	2	3	4	5	6	7	8
D	λ_1	λ_{10}	λ_3	λ_{12}	λ_5	λ_{14}	λ_7	λ_{16}
U	λ_9	λ_2	λ_{11}	λ_4	λ_{13}	λ_6	λ_{15}	λ_8

Fig. 3.6 (a) A star-ring protection architecture for WDM-PON; (b) wavelength assignment plan for eight ONUs.

Fig. 3.6 (a) presents a star-ring protection architecture for WDM-PON [9], which can protect against link failure of FF and DFs, simultaneously. At the RN, the two feeder fibers F1 and F2 are connected to input ports 1 and 2 of 2×*N* AWG, respectively, and those AWG input ports correspond to two adjacent passband channels. The value of *N* is chosen to be an even number. Fig. 3.6 (b) illustrates the wavelength assignment plan. The downstream and upstream wavelength channels are interleaved with each other for the ONUs. For each ONU, the up- and downstream wavelengths, of which one is in blue band while the other is in red band, are separated from each other by one FSR of the AWG. When a fiber failure between the RN and the ONU 2 occurs, a drastic drop in power at the monitoring unit (M) of ONU 2 will be detected. Thus, the optical switch in

the ONU 2 will be automatically reconfigured, so that the up-/downstream wavelengths of the ONU 2 will be routed to/from the ONU 1 via the protection fiber between them. With this protection scheme, a fast restoration of fiber failure can be achieved, without any disturbance on the existing traffic and other ONUs. The protection scheme is similar when fiber feeder F1 is broken, except that the monitoring units in all ONUs will trigger the respective optical switches simultaneously.

3.3 Self-Protection Single-PON Architecture

As we know, all the exiting protection schemes [7-16] based on simple power monitoring only work under the assumption that all the transmitters in the ONUs and the OLT continuously transmit optical signals. However, in practice, (i) some transmitters of ONUs or the OLT may frequently enter into sleep mode whenever there is no data to be sent in order to save power [17-18], (ii) some ONUs may be shut down whenever users are offline, (iii) fiber faults may occur during the time when ONUs are offline or when ONUs are in sleep mode. In the above cases, all the exiting protection schemes [7-16] do not work. For example, when an ONU is in sleep mode (or is offline), no optical signal is transmitted from that ONU. In such case, if one of the previous schemes is employed, since no optical signal is received from that ONU, the monitoring unit at the OLT would assume the DF of that ONU is faulty and may trigger protection switching, resulting in a malfunction.

In the section, we propose a centrally-controlled intelligent protection scheme in a

single WDM-PON with colorless ONUs, whereby the optical power on both the working and protection paths is monitored simultaneously. Note that in the existing schemes, the optical power of the working path only is monitored without any intelligent decision. In our scheme, a novel logic decision unit in conjunction with a power monitoring unit is implemented in the OLT to enable the protection switching in more practical operation scenarios described above. By monitoring the optical power of each channel on both the working and protection paths, the proposed scheme can tell the connection status of both the working and protection paths of each channel, and hence can perform an effective protection switching with the aid of the proposed logic decision unit. Moreover, the detection results recorded by the power monitoring unit facilitate a faster failure recovery.

3.3.1 Proposed Architecture and Operation Principle

The proposed centrally-controlled self-protected WDM-PON architecture with N colorless ONUs is shown in Fig. 3.7. The OLT has three function units: transceiver unit, power monitoring unit and logic decision unit, which are interconnected to realize intelligent protection switching. The transceiver unit includes N transceivers, supporting N ONUs. In each transceiver, a transmitter (TX) generates a downstream signal and an optical circulator is used to separate down-/up-stream signals. Apart from receiving the upstream signal, an upstream receiver (RX) also acts as a monitor for monitoring the upstream power in the working path in the normal mode and generates an electrical signal to the logic decision unit upon detecting a drastic power loss. The wavelengths of all channels are multiplexed by a $1\times N$ AWG at the OLT. The multiplexed signal is fed to port

1 of a 2×2 OS. Port 3 of the 2×2 OS is connected to another AWG with the same free spectral range (FSR) in the power monitoring unit. The power monitoring unit includes *N* power monitors for monitoring the power of respective upstream signals on the protection path and generating respective electrical logic signals to the logic decision unit.

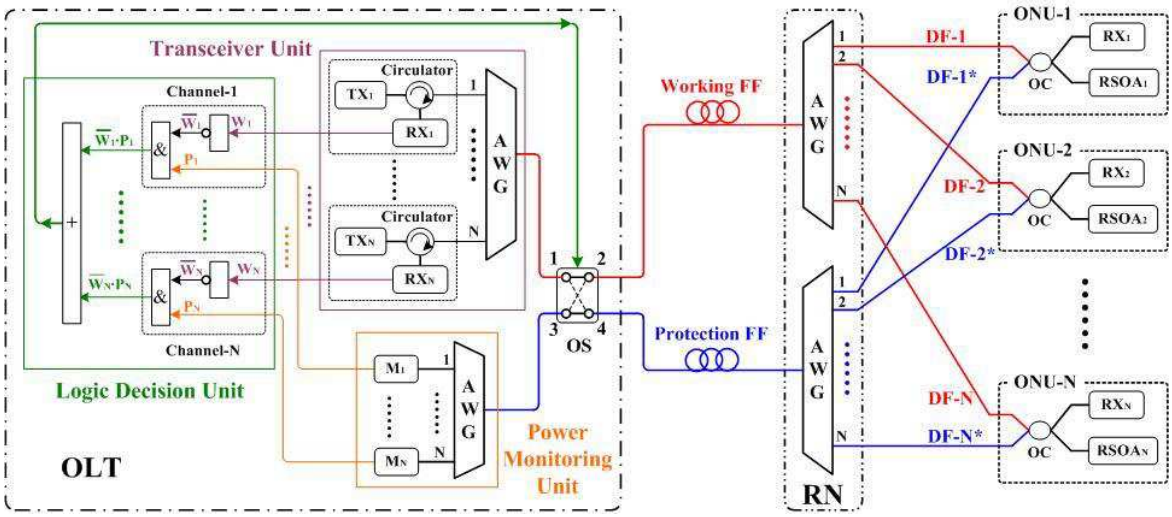

Fig. 3.7 Schematic diagram of the centrally-controlled intelligent self-protected WDM-PON

Ports 2 and 4 of the OS are connected respectively to the two 1×*N* AWGs with the same FSR at the RN, via two separate feeder fibers (working and protection FFs). After being de-multiplexed at the RN, each downstream signal is transmitted on one of the two alternate distribution fibers (DF-*i* and DF-*i**), which are connected to the corresponding ONU-*i*. In each ONU, a 2×2 optical coupler (OC) is used to combine two DFs and to split the downstream optical power into two parts: one part is fed to a downstream receiver (RX); the other is amplified and re-modulated with upstream data via a reflective semiconductor optical amplifier (RSOA) operating in its gain-saturated region.

As shown in Fig. 3.7, the novel logic decision unit consists of *N* identical logic

modules, each of which is related to a channel, and a multi-input-single-output logic OR gate. For each logic module, two input signals respectively come from the upstream RX and the monitor of the corresponding channel, and its output serves as one of the N input signals of the logic OR gate. The output of the logic OR gate controls the connection state (cross or bar) of the 2×2 OS. A single-link-failure scenario is assumed, because the chance of simultaneous multiple-link failures is negligibly small in an access network. Thus, when both the upstream RX and its associated monitor simultaneously experience a drastic power loss, it is assumed that the corresponding ONU either enters into sleep mode or is shut down. In such case, no protection switching will take place. It is also noted that the proposed protection scheme can also protect against simultaneous multiple link failures, except for a rare case that the two DFs for an ONU or the two FFs break down simultaneously. (In the rare case, that ONU or all the ONUs will completely lose the connection with the OLT, and hence any self-protection scheme would not work if no human intervention is involved.)

Table 3.2 provides the decision states of the logic decision unit based on the logic inputs on both the working and protection paths of each channel. In the normal working mode, the OS in the OLT is set to the bar state (i.e., 1-2 and 3-4 connection). Thus, a downstream signal is delivered only on the working path, consisting of the working FF and respective DF-i (red path). The downstream optical power is split into two parts by a 2×2 OC at each ONU, one of which is fed to a downstream RX, the other is amplified and re-modulated with upstream data via a gain-saturated RSOA. The upstream signal is

split into two copies by the 2×2 OC, one of which transmitted in the working path is sent to the transceiver unit in the OLT; the other in the protection path is fed into the power monitoring unit. Hence, the WDM-PON can offer 1:1 downstream protection and 1+1 upstream protection capability, respectively.

Table. 3.2 Truth table for the detection states of the upstream light on both working and protection paths of each channel

Detection state of the **upstream RX** in the working path	Detection state of the **monitor** in the protection path	Output of the **logic decision unit** for each channel
1 (with light)	1 (with light)	0 (normal working mode)
0 (no light)	1 (with light)	**1 (do switching)**
1 (with light)	0 (no light)	0 (no switching, but to repair protection fiber)
0 (no light)	0 (no light)	0 (ONU is in sleep mode or turned off)

In the case of any working DF failure, the corresponding upstream RX in the transceiver unit will detect the loss of that upstream signal, and hence a logic "0" signal will be generated to the logic decision unit. But, in this case, a monitor associated with the same channel in the power monitoring unit can detect light power, and a logic "1" signal will be generated. Consequently, the output of the logic decision unit will be logic "1" signal, which triggers the 2×2 OS to the cross state (i.e., 1-4 and 3-2 connections) to setup the alternate (protection) path. Hence, all of the bidirectional transmissions are switched from the working path (red path) to the protection path (blue path). After protection switching, based on the detection results of the *N* monitors, the power

monitoring unit can tell if it is a DF or the FF failure in the working path; if it is a DF failure, it can also tell which DF fails. Thus, a fast failure restoration can be performed. On the contrary, if an upstream RX detects the presence of light while its corresponding monitor detects no light, it indicates that the protection DF fails (and thus the network manager will be notified that the corresponding protection fiber link must be repaired in time), but in this case no protection switching will take place.

The logic expression of each logic module is $\left(\overline{w_i} \cdot p_i\right)$. If any of the above detection results occurs in all channels, it means the fiber failure take places in either the working or protection FF. A logic OR gate is used to synthetically respond to the detection states from all *N* logic modules. Therefore, the logic expression of the output of the whole logic decision unit is

$$\left[\left(\overline{w_1} \cdot p_1\right)+\left(\overline{w_2} \cdot p_2\right)+.....+\left(\overline{w_{N-1}} \cdot p_{N-1}\right)\right] \tag{3.1}$$

The proposed WDM-PON can provide centrally-controlled protection capability against the failures of both FFs and DFs. It should be mentioned that the proposed protection scheme is not restricted to a specific WDM-PON protection topology, and hence it is applicable to any protection topologies including group protection [7-8], ring protection [9-10], duplication protection [11-13].

3.3.2 Experimental Setup and Results

The transmission performance and the protection switching time of the proposed WDM-PON architecture were experimentally studied, using the setup shown in Fig. 3.8.

The ONU-1 was implemented to demonstrate the operation principle.

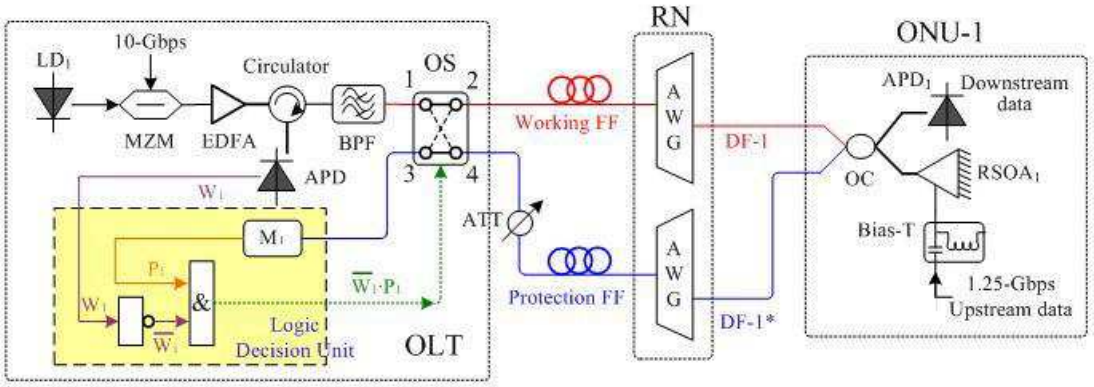

Fig. 3.8 Experimental setup for the centrally-controlled self-protection operation in WDM-PON

In the OLT, a continuous wave (CW) light from a laser diode at 1545.5nm was modulated via a Mach-Zehnder modulator (MZM), which was biased at the transmission null point and driven by a 10Gbit/s data with a pseudo-random bit sequence (PRBS) with length of 2^{31}-1 to generate downstream non-return-to-zero (NRZ) on-off key (OOK) signal. Note that since the downstream light is reused and re-modulated with upstream data, the downstream signal should have a low extinction ratio (ER) (e.g., up to 5 dB) so that the interference from the downstream to the upstream is minimized and the error-free upstream transmission can be achieved [19]. After being amplified by an erbium-doped fiber amplifier (EDFA), the downstream signal passed through an optical circulator and a band-pass filter (BPF) before it was fed to a 2×2 OS. The EDFA was used to compensate the downstream power loss and to improve the power budget. The optical circulator was used to separate the down-/up-stream signals. The BPF with an insertion loss of 3.5dB was used to emulate a 1×*N* AWG at the OLT. The 2×2 OS used in the experiment was an

optomechanical switch with a switching speed of 10 milliseconds, 1dB insertion loss and -70dB crosstalk. Two 1×16 AWGs located in the RN has a channel spacing of 100 GHz and a FSR of 31nm. The FF and DF were single mode fibers (SMF) with the lengths of 15km and 5km, respectively. At the ONU, one part of the downstream signal was detected by an avalanche photodiode (APD) receiver; the other was amplified and re-modulated with 1.25Gbit/s 2^{31}-1 PRBS upstream data via a gain-saturated RSOA, which was un-cooled and packaged in a TO-can. The RSOA was biased at 30mA via a Bias-T circuit and the optical power injected in to the RSOA was -15dBm. At these conditions, the RSOA was saturated with an output power of 7.5dBm (i.e., optical gain = 22.5dB), and its 3dB modulation bandwidth was measured to be 1.5GHz.

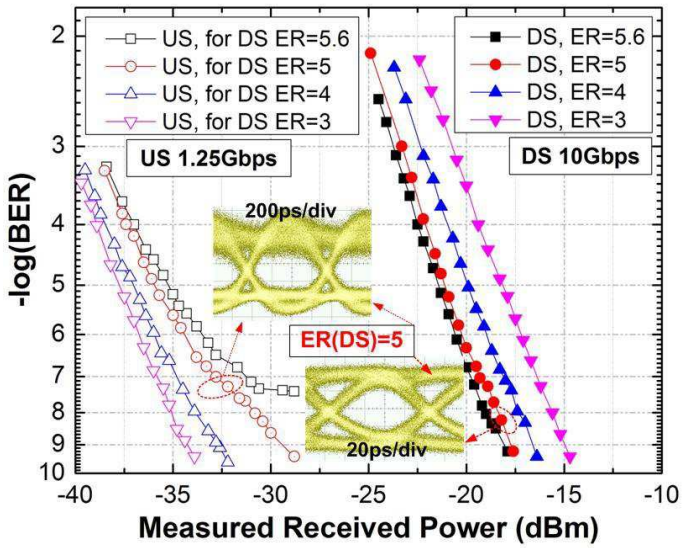

Fig. 3.9 Measured BER of the DS and US signals at 1545.5nm for different DS ERs. Insets show the eye patterns of DS and US signals when the DS ER is 5dB

We first investigated the effect of the downstream (DS) ER on the bit-error-rate (BER) performances for both DS and upstream (US) transmissions over 20-km (FF+DF) SMF.

The power injected into the RSOA was maintained at -15dBm so that the RSOA was operated in its saturation region. We were able to achieve the error-free upstream transmission with the DS ER of up to 5dB. An error floor at ~7.5×10^{-7} was observed for the upstream transmission when the DS ER was set to be 5.6. Fig. 3.9 shows the BER performances of the DS and US signals at 1545.5nm for different DS ERs. As shown in Fig. 3.9, when the DS ER was increased from 3dB to 5dB, the BER of the DS signal is improved, while the BER of the US signal is degraded due to the higher interference from the DS signal. The eye patterns of the DS and US signals when the DS ER was 5dB are shown in the insets of Fig. 3.9.

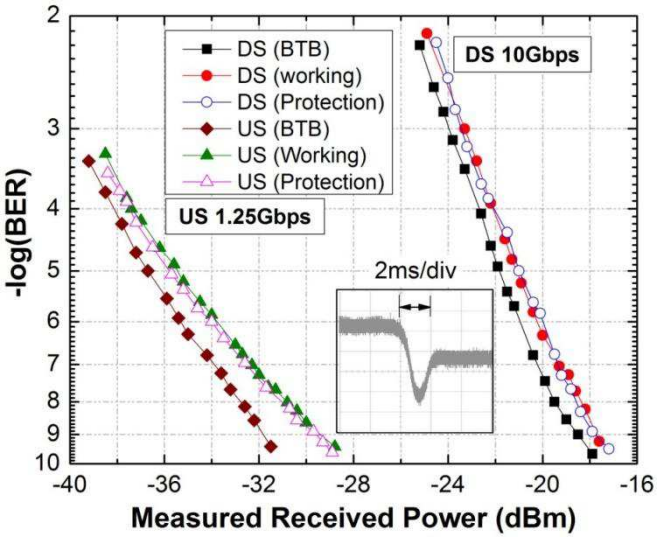

Fig. 3.10 Measured BER of the 10Gbit/s DS and 1.25Gbit/s US signals both in the working and protection modes at 1545.5nm. Inset shows the switching time during traffic restoration.

Fig. 3.10 shows the BER for down- and up-stream signals at 1545.5nm when the DS ER was 5. The receiver sensitivities of the DS signal in the working and protection paths were -17.7dBm and -17.9dBm, respectively. In US case the sensitivities in the working

and protection paths were -29.4dBm and -29.6dBm, respectively. To investigate the power penalties, the BER performances of the back-to-back (BTB) case are also shown in Fig.3.10. The power penalties between the BTB and the 20km SMF transmission cases in the working path were about 0.7dB and 2.3dB for the DS and US transmissions, respectively. The power penalty for the DS transmission is mainly due to the chromatic dispersion as the DS data rate is 10Gbit/s, while power penalty for the US transmission is attributed to the backscattering noise since the upstream reuses the downstream carrier.

Using the experimental setup, the fiber link (DF-1) between the AWG and the ONU-1 was intentionally disconnected to simulate the fiber cut scenario. Upon disconnecting DF-1, the US RX detected no optical power from the working path and hence generated a logic "0" signal (w_1=0), while the power monitor M_1 still detected optical power from the protection path and hence generated a logic "1" signal (p_1=1). As a result, the resultant output from the logic decision unit was a logic "1" signal $\left(\overline{w_1} \cdot p_1 = 1\right)$, which activated the protection switching by changing the connection state of the 2×2 OS from its bar state (1-2 and 3-4 connections) to the cross state (1-4 and 3-2 connections) (please refer to Fig. 3.8). The protection switching time was measured to be 2ms (see inset in Fig. 3.10), which is mainly determined by the switching response of the 2×2 OS used in the experiment. It is noted that the upper trace of the inset represents the US signal in the working path, while the lower trace is for the US signal in the protection path after the protection switching. The lower power level observed in the protection path is because an attenuator (ATT) was inserted in the protection path to distinguish two different paths.

3.3.3 Performance Analysis

Table. 3.3 Comparison of the Number of Elements and the Network Availabilities for Different Protection Schemes

Number of Elements			Scheme in [7]	Scheme in [12]	Scheme in [8]	Scheme in [13]	Our scheme
Shared Parts (including OLT, FF and RN)	OLT	Transceivers	N	N-1	N	N	***N***
		Circulators	0	1	0	0	***N***
		WDM	N	N+1	N	N	***0***
		1×N AWGs	1	1	1	2*	***2****
		OSs	1	0	1	2	***1***
	FFs		2	2	2	2	***2***
	RN	1×N AWGs	1	2*	2*	2*	***2***
		OCs	N+1	0	0	0	***0***
ONU Number			N	N-1	N	N	***N***
Dedicated Parts (including ONU, DF and IF)	ONU	Transceivers	1	1	1	1	***1***
		WDM	2	1	2	1	***0***
		OSs	2	1	0	0	***0***
		OCs	0	0	1	0	***1***
	DFs		1	2	1	1	***2***
	IFs		1/2	0	1	0	***0***
Wavelengths used per ONU			2	2	2	2	***1***
Centrally-controlled APS			No	No	Yes	Yes	***Yes***
Protection Capability			FF and DF	FF and DF	DF	FF	***FF and***
Overall Network Availability			99.99928%	99.99845%	99.94454%	99.99157%	***99.99949%***
Mean Down-Time (min/year)			3.80	8.16	291.48	44.32	***2.70***

* a 2×*N* AWG or *N*×*N* AWG are functionally equivalent to a pair of 1×*N* AWGs.

** In our scheme, two 1×*N* AWGs is used in OLT; one is in the transceiver unit and the other is in the power monitoring unit.

Table. 3.4 Unavailability of Different Elements

Elements	Unavailability	Elements	Unavailability
OLT (TX and RX)	$U_{TRX}^{OLT} = 5.12\times10^{-7}$	WDM filter	$U_{WDM} = 3\times10^{-7}$
ONU (TX and RX)	$U_{TRX}^{ONU} = 1.54\times10^{-6}$	OC	$U_{OC} = 3\times10^{-7}$
AWG	$U_{AWG} = 1.2\times10^{-6}$	Optical SW	$U_{OS} = 1.2\times10^{-6}$
Circulator	$U_{Circulator} = 3\times10^{-7}$	BLS *	$U_{BLS} = 4\times10^{-6}$
Fiber (/km)	$U_{F} = 1.37\times10^{-5}$ (/km)		

* BLS is the abbreviation of the “Broadband Light Source”.

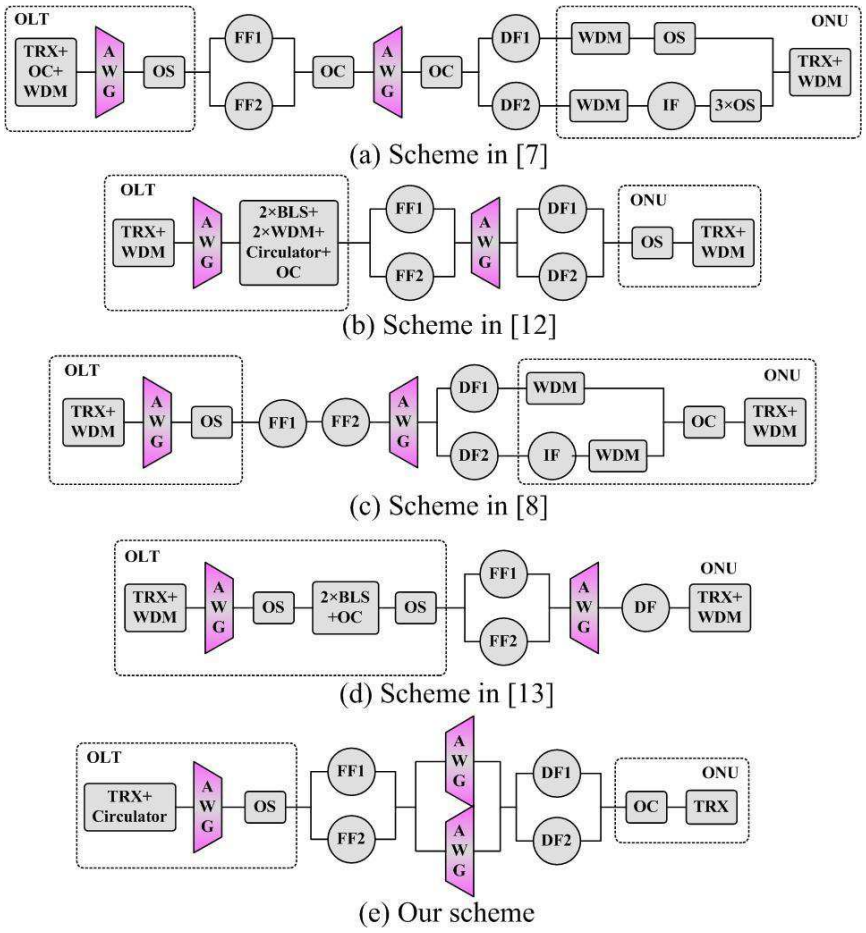

Fig. 3.11 Block diagrams for calculating the unavailability of different protection schemes: (a) scheme in [7], (b) scheme in [12], (c) scheme in [8], (d) scheme in [13] and (e) our proposed protection scheme.

To show the simplicity and effectiveness of the proposed architecture, we compare the proposed scheme to those in [7, 8, 12, 13] in terms of the number of elements and the network availabilities as shown in Table 3.3. In the proposed scheme, only one OS is used in the OLT, which is a significant reduction from $2N$+1 OS’s in [7] or N-1 OS’s in [12]. In each ONU, only one OC is required without WDM filter. Thus, the ONU

structure is much simplified, but also the device cost is greatly reduced. Meanwhile, the number of wavelengths used per ONU in our scheme is the minimized among all existing schemes. It means with the same total number of wavelengths, our proposed WDM-PON can support the most number of users and hence has the least investment cost per user. However, there are still some limitations in this scheme. One limitation of the proposed scheme as in the other schemes [7-16] is that it cannot support simultaneous multiple fiber cuts in a working path as well as a protection path, although the occurrence probability of simultaneous multiple fiber cuts is negligibly small in an access network. Besides, the protection switching for any DF failure will lead to a transient interruption to all the ONUs.

We next evaluate the overall network availability using the availability modeling methodology reported in [20-21]. The block diagrams for calculating the unavailability of different protection schemes are given in Fig. 3.11. Each block in the figure represents either a device/system or a fiber link. The unavailability of a block in Fig. 3.11 is denoted by $U_{BLOCK\ NAME}$. The description of symbols and their values of the typical element unavailability are listed in Table 3.4 [20-21]. The unavailabilities U_{FF}, U_{DF} and U_{IF} are calculated by multiplying the length of FF, DF and interconnection fiber (IF) by the fiber unavailability of the unit length U_F. The expressions of the connection unavailabilities for the considered protection schemes are given by the following equations:

$$\begin{aligned} U_{[4]} = & \left(U_{TRX}^{OLT} + U_{OC} + U_{WDM} + U_{AWG} + U_{OS}\right) + \left(U_{FF1} \times U_{FF2}\right) \\ & + U_{OC} + U_{AWG} + U_{OC} + \left(U_{DF1} + U_{WDM} + U_{OS}\right) \\ & \times \left(U_{DF2} + U_{WDM} + U_{IF} + 3 \times U_{OS}\right) + U_{TRX}^{ONU} + U_{WDM} \end{aligned} \tag{3.2}$$

$$U_{[6]} = U_{TRX}^{OLT} + U_{WDM} + U_{AWG} + 2\times U_{BLS} + 2\times U_{WDM} + U_{Circulator} + U_{OC} + \left(U_{FF1}\times U_{FF2}\right) + U_{AWG} + \left(U_{DF1}\times U_{DF2}\right) + U_{OS} + U_{TRX}^{ONU} + U_{WDM} \quad (3.3)$$

$$U_{[9]} = \left(U_{TRX}^{OLT} + U_{WDM} + U_{AWG} + U_{OS} + U_{OS}\right) + \left(U_{FF1} + U_{FF2}\right) + U_{AWG} + \left(U_{DF1} + U_{WDM}\right)\times\left(U_{DF2} + U_{IF} + U_{WDM}\right) + U_{OC} + U_{TRX}^{ONU} + U_{WDM} \quad (3.4)$$

$$U_{[10]} = \left(U_{TRX}^{OLT} + U_{WDM} + U_{AWG} + U_{OS} + 2\times U_{BLS} + U_{OC} + U_{OS}\right) + \left(U_{FF1}\times U_{FF2}\right) + U_{AWG} + U_{DF} + U_{TRX}^{ONU} + U_{WDM} \quad (3.5)$$

$$U_{proposed} = \left(U_{TRX}^{OLT} + U_{Circulator} + U_{AWG} + U_{OS}\right) + \left(U_{FF1}\times U_{FF2}\right) + U_{AWG}\times U_{AWG} + \left(U_{DF1}\times U_{DF2}\right) + U_{OC} + U_{TRX}^{ONU} \quad (3.6)$$

We assume that the average length of FF is 15km, DF 5km and protective IF 2km. Our calculations are based on un-availability data in Table 3.4 [20-21]. The results given in Table 3.3 show that our protection scheme achieves the highest availability, higher than 99.999% (5 nines) due to simple architecture and simultaneous protection against both FFs and DFs.

3.4 Cross-Protection Dual-PON Architecture

In this section, we propose a new cross-protection dual-PON-based architecture with carrier-reuse colorless ONUs. Our proposed architecture can provide 1+1 downstream protection and 1:1 upstream protection against both FF and DF failures by using the fiber links and AWGs of the neighboring WDM-PON. Only two different wavebands are utilized in dual-WDM-PONs where gain-saturated RSOAs are used as colorless

transmitters in ONUs. The number of extra protection fibers is minimized and the wavelength is much more efficiently utilized compared with other protection schemes [7-16].

3.4.1 Architecture and operation principle

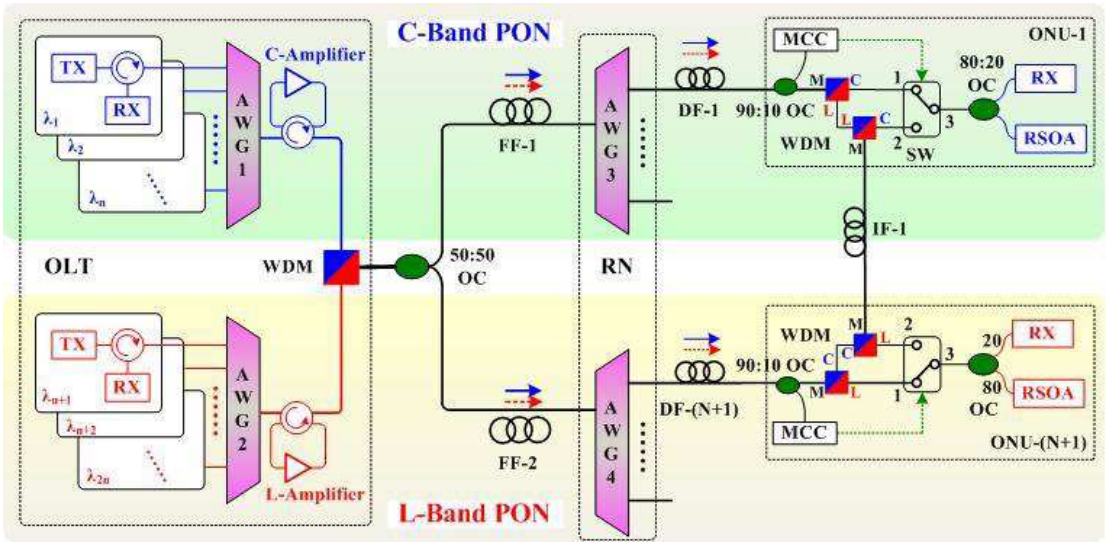

Fig. 3.12 Schematic of the proposed cross-protection colorless dual-WDM-PON architecture

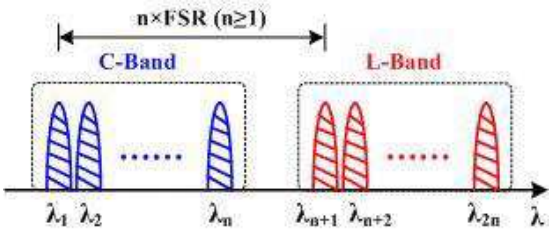

Fig. 3.13 Waveband allocation plan

Fig. 3.12 shows the proposed cross-protection dual-WDM-PON which consists of two WDM-PONs each with *N* colorless ONUs. As shown in Fig. 3.12, the 1st WDM-PON operates in the C-band and the 2nd WDM-PON in the L-band. In both WDM-PONs, the downstream wavelengths are reused for upstream transmission based on gain-saturated

RSOAs to efficiently utilize wavelength resource. In each WDM-PON, *N* transceivers are connected to an AWG which multiplexes the downstream signals and de-multiplexes the upstream signals. A circulator is used to separate down- and up-stream signals in each transceiver. The C- and L-bands are separated by *n* ($n \geq 1$) free spectral ranges (FSRs) of the AWGs as shown in Fig. 3.13. In the OLT located at central office (CO), the two waveband signals are combined by a coarse WDM and then power-split into the FF-1 and FF-2 by a 1×2 optical coupler (OC). An optical amplifier is used for each waveband to compensate the downstream power loss and to improve the power budget. The remote node (RN) consists of two periodical AWGs with the same FSR and links to each ONU via one DF. Each ONU in the C-band is connected with an ONU in the L-band via an interconnection fiber (IF); these two ONUs have a wavelength spacing of *n* FSRs of the AWG used. They form a group to protect each other. Inside each ONU, 10% of the downstream signal is tapped by a monitoring and control circuit (MCC). The MCC consists of a photo detector (PD) and a control circuit. The PD is used to monitor the optical power of downstream signals, and the control circuit is responsible for controlling the connection state of a local 1×2 optical switch (SW) according to the absence or presence of the power detected by the PD. Upon detection of fiber failure (loss of optical signal), the MCC generates an electrical signal to control the connection state (cross or bar) of the SW. Two coarse WDMs were used to separate and combine the C- and L-bands. Following the SW, a 1×2 OC is used to split the optical power into two parts: one part is fed to a downstream receiver (RX); the other is amplified and re-modulated

with upstream signal via a gain-saturated RSOA.

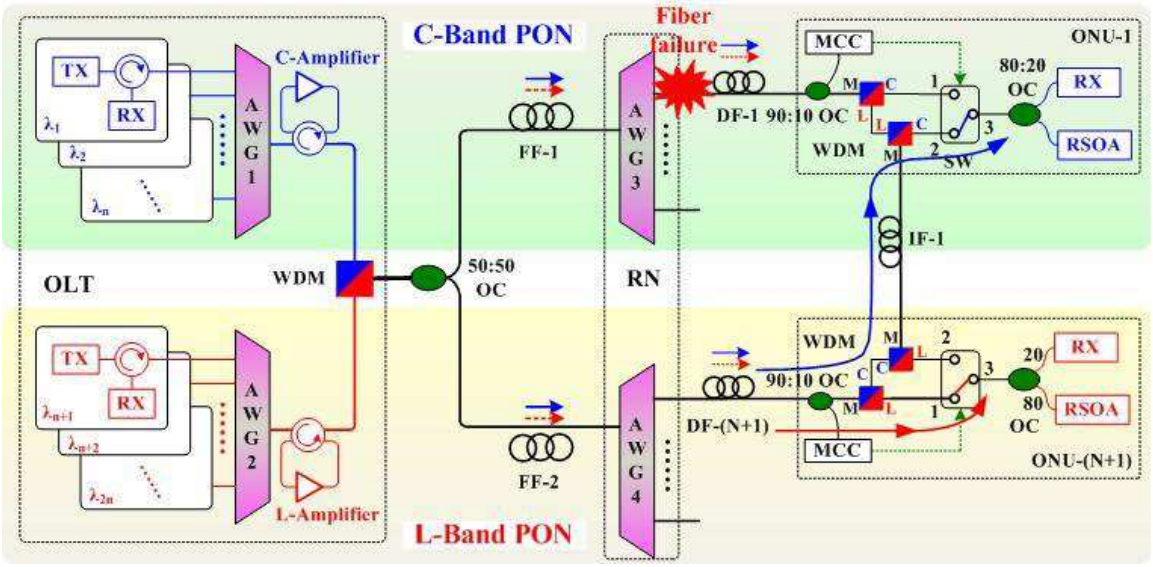

Fig. 3.14 Cross-protection colorless dual-WDM-PON under one distribution fiber (DF-1) failure

In the working mode, the 1st port of the SW is connected to the 3rd port of the SW in each ONU, and the down- and up-stream signals traverse the respective DF path from/to OLT. In case of any working DF failure (e.g., DF-1) as shown in Fig. 3.14, the corresponding MCC will detect the power loss and subsequently will reconfigure the SW in ONU-1 to the port 3-2 connection. Thus, the disrupted down- and up-stream signals in C-band are recovered through FF-2, AWG4, DF-(N+1) and ONU-(N+1) and IF-1 path. If FF-1 fails, the SW's connection states of the N ONUs in the C-band are changed and the bidirectional signals are transmitted through the neighboring PON in the L-band and the corresponding IFs. Thus, the architecture provides 1+1 downstream protection and 1:1 upstream protection against the failures of both FF and DF.

3.4.2 Experiment Setup and Results

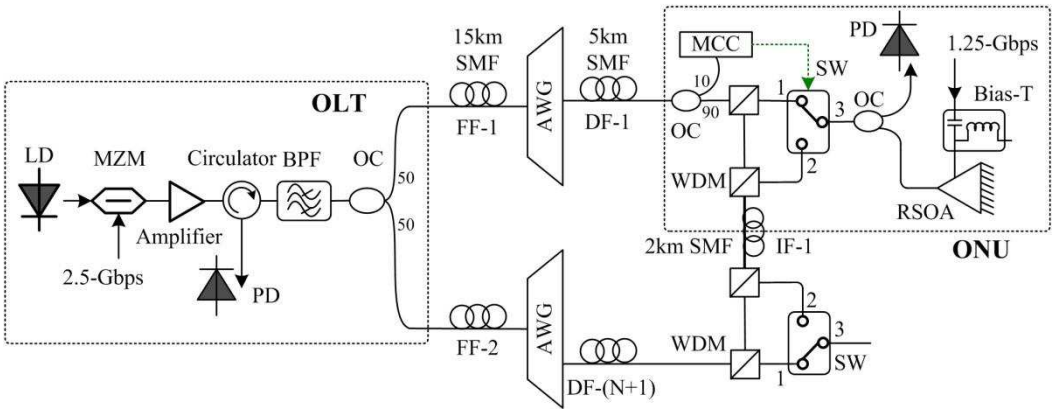

Fig. 3.15 Experimental setup for the proposed cross-protected colorless dual-WDM-PON

To verify the operation of the proposed cross-protection scheme, we performed an experiment as shown in Fig. 3.15. In the OLT, a continuous wave (CW) light from a laser diode at 1545.5nm is modulated via a Mach-Zehnder modulator (MZM), which was biased at the transmission null point and driven by a 2.5Gb/s data with a pseudo-random bit sequence (PRBS) with length of 2^{31}-1 to generate downstream non-return-to-zero (NRZ) signal with an extinction ratio (ER) of around 5. Note that since the downstream carrier is reused and re-modulated with upstream data, the downstream signal should have a low extinction ratio (ER) (e.g., up to 5 dB) so that the interference from the downstream signal to the upstream signal is minimized and the error-free upstream transmission can be achieved [22-24]. The downstream signal is amplified by an optical amplifier and then passes through an optical circulator and a band-pass filter (BPF) before it reaches an optical coupler (OC). The BPF emulates a 1×*N* AWG at the OLT and has an insertion loss of 3.5dB. Two 1×16 AWGs located in the RN have 100-GHz channel spacing and a FSR of 31-nm. The FF and DF are single mode fibers (SMFs) with

lengths of 15km and 5km, respectively. The IF is 2-km SMF. At the ONU, two coarse WDMs were used to separate and combine the C- and L-bands. The 2×2 optomechanical switch used in our experiment has a switching speed of milliseconds, 1-dB insertion loss and -70-dB crosstalk. One part of the downstream signal was detected by an avalanche photodiode (APD) receiver; the other was amplified and re-modulated by 1.25Gb/s 2^{31}-1 PRBS upstream data via a gain-saturated RSOA. The un-cooled RSOA is packaged in a TO-can. The optical gain of the device was 23.5dB when it was biased at 60mA via a Bias-T circuit and the optical power of the injected light was -15dBm. At these conditions, the RSOA got saturated (e.g., its optical gain decreases by 3 dB from the maximum value) with the output saturation power of 8.5dBm, and its 3-dB modulation bandwidth was measured to be 1.5GHz.

To achieve the error-free upstream transmission, we first set the downstream ER to be 5. The injected power to the RSOA was maintained to be -15dBm. Fig. 3.16 (a) shows the BER performance for downstream (DS) and upstream (US) signals at 1545.5nm (C-band). The receiver sensitivities of the DS signal in the working and protection modes were -30.2dBm and -30.1dBm, respectively. In US case the sensitivities in the working and protection modes were -29.8dBm and -29.6dBm, respectively. The power penalties between the BTB case and the case of 20km SMF transmission for DS and US in the working mode were about 0.4dB and 0.5dB, respectively. Fig. 3.16 (b) shows the BER curves at 1576.4nm (L-band). The sensitivity difference from the BTB case is 0.5dB both for DS and US cases, which is negligibly small due to the limited chromatic dispersion

and slight backscattering noise. The eye patterns of the DS and US signals in the C-band wavelength in the normal working mode are also included in the insets of Fig. 3.16 (a) when the downstream ER is 5dB.

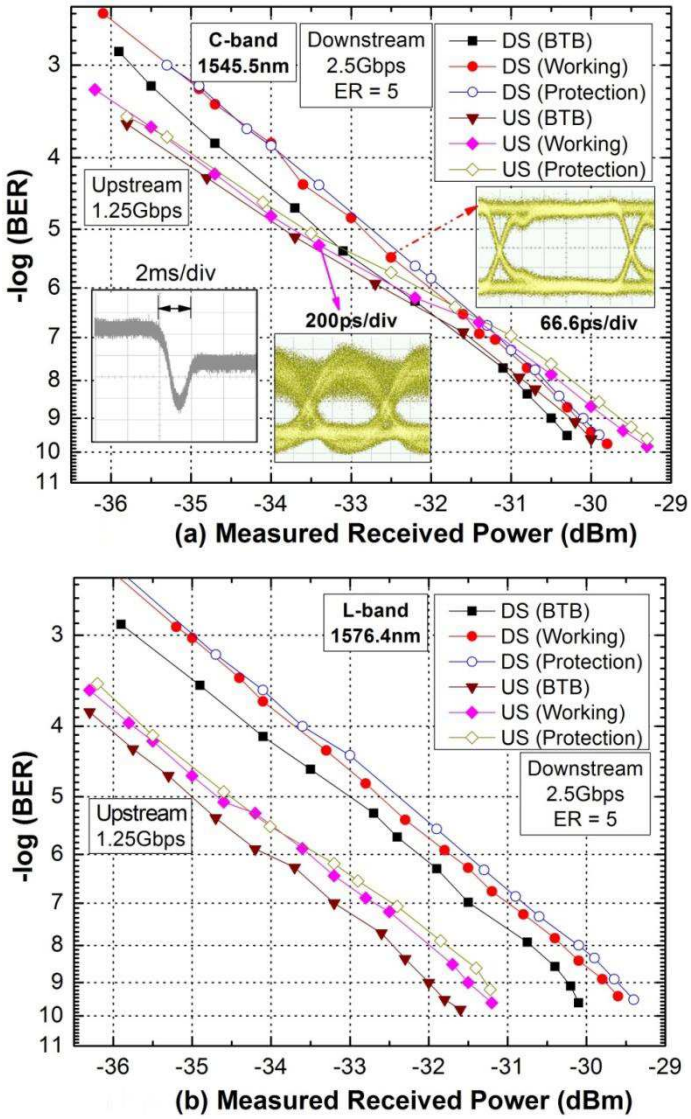

Fig. 3.16 Measured BER curves of the DS and US signals both in the working and protection modes at (a) C-band and (b) L-band. Inset in the (a) shows the switching time.

Using the experimental setup, the fiber link (DF-1) between the AWG and the ONU was then intentionally disconnected to simulate the fiber cut. Upon disconnecting DF-1,

MCC detected no optical power from the working path, and hence it activated the protection switching by changing the connection state of the 1×2 optical switch (SW) from 1-3 connection to 2-3 connection (please refer to Fig. 3.15). We also measured the protection switching time for re-modulated upstream signal, which is shown in the inset of Fig. 3.16 (a), where the upper trace represents the upstream signal in the working path, while the lower trace is for the upstream signal in the protection path after the protection switching. The lower power level observed in the protection path is because an attenuator (ATT) was inserted in the protection path to distinguish two different paths (working and protection). As shown in the inset of Fig. 3.16 (a), the protection switch time was measured to be 2ms in the case of the simulated fiber cut, which is mainly determined by the switching response of the opto-mechanical switch used in the experiment.

We also investigated the effect of the downstream ER on the BER performances for both down-/up-stream transmission over 20km SMF. Error-free upstream transmission was achieved when the downstream ER was varied from 3 to 5 dB. Fig. 3.17 (a) and (b) shows the measured BER performances for a C-band channel and a L-band channel, respectively. As shown in Fig.3.17 (a) and (b), when the downstream ER value is changed from 3 to 5, the BER of the DS signal is improved, while the BER of the US signal is degraded due to the higher interference from the DS signal. For the comparison purpose, Fig.3.17 (a) and (b) also shows the BER performance of the US signal when the light injected into the RSOA is a CW light; in this case, the US signal achieves the best BER performance with a sensitivity of about -33dBm at the BER of 10^{-9}.

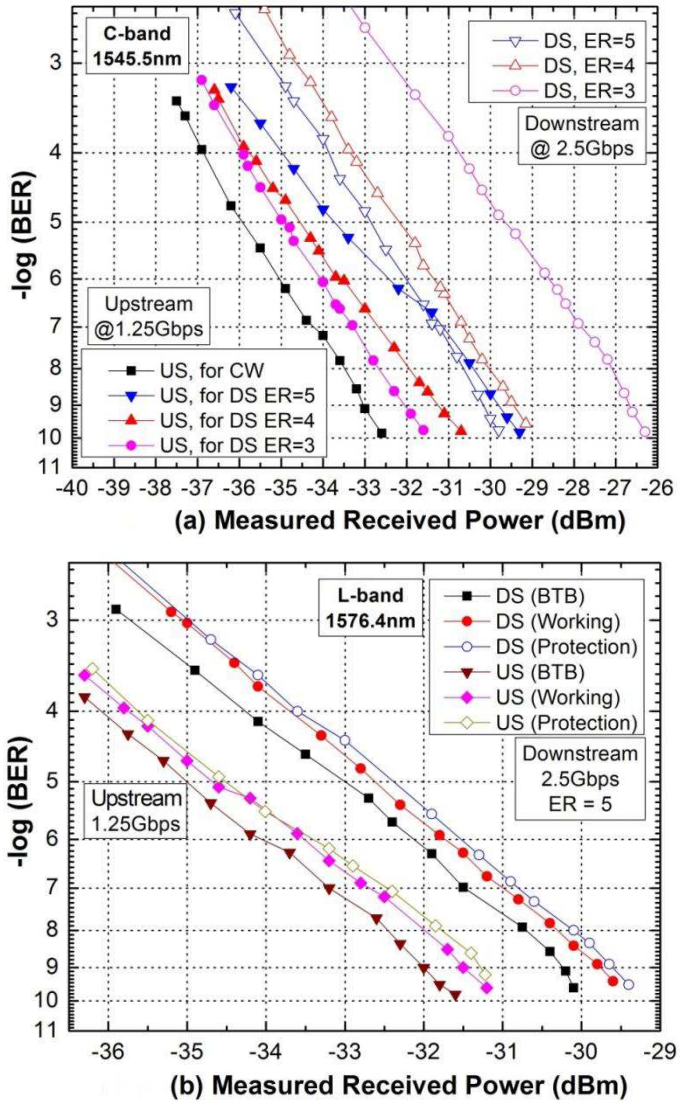

Fig. 3.17 Measured BER curves of the DS and US signals at (a) C-band and (b) L-band for different downstream ERs.

To show the improved network resource utilization and effective protection capability of the proposed architecture, we compare the proposed scheme to those in [7-16] as shown in Table 3.5. We assume that *N* ONUs are deployed in each PON, thus 2*N* ONUs are connected in the dual-PON architecture. The average lengths of FF, DF and IF fibers are assumed to be 20km, 5km and 2km, respectively. The used fiber link resource in our

scheme is minimized, which is the same as that in the scheme of [16]. Meanwhile, the wavelength utilization in our scheme is the highest among all existing schemes including the scheme of [16]. Note that the sub-ring structure designed in the scheme of [16] causes a half of the power of the downstream backup signals to go back to the OLT. As a result, two different wavelengths are needed for the down- and up-stream transmissions in each ONU. Hence the proposed dual-PON architecture can not only greatly reduce the implementation cost, but also use wavelength resource more efficiently.

Table. 3.5 Comparison of the Number of Network Resources and the Protection Capability

Number of Used Network Resources	**Single PON Architecture**			**Dual PON Architecture**		
	Duplication Protection in [12, 9]	Group Protection in [7, 8]	Ring Protection in [9, 10]	Scheme in [15]	Scheme in [16]	**Our scheme**
ONU Number	*N*	*N*	*N*	*2N*	*2N*	***2N***
FF (e.g., 20km) per PON	*2*	*2*	*2*	*1*	*1*	***1***
DF (e.g., 5km) per PON	*2N*	*N*	*N*	*2N*	*N*	***N***
IF (e.g., 2km) per PON	*0*	*N/2* [7], *N* [8]	*N*	*0*	*N/2*	***N/2***
Wavelength used per ONU	*2*	*2*	*2* [9], *1* [10]	*2*	*2* *	***1***
Protection Capability	FF and DF	DF	FF and DF	FF and DF	FF and DF	**FF and DF**

* The number of wavelength used per ONU of 2 could not be improved to 1.

3.5 Conclusions

We have proposed and demonstrated two novel protection switching schemes: one is used in single WDM-PON and the other is suitable for dual-PON architecture.

1) Centrally-controlled intelligent protection scheme in a single WDM-PON: By

monitoring the optical power of each channel on both the working and protection paths, the proposed scheme can tell the connection status of both the working and protection paths of each channel, and hence can perform an effective protection switching with the aid of the proposed logic decision unit in more practical operation scenarios. The fiber failure localization and repair would be made easier, since the OLT monitors every individual channel on both working and protection paths and would have the collection of all individual channels' status information. As such only one optical switch is required at the OLT, which can deal with both the feeder fiber and the distribution fiber failures.

2) Cross-protection dual-PON-based architecture: It can provide 1+1 protection capacity for downstream traffic and 1:1 protection for upstream data against both FF and DF failures by using the fiber links and AWGs of the neighboring WDM-PON. The architecture has the minimum number of extra protection fibers, much improved wavelength utilization and better transmission performance compared with the other existing protection schemes. No additional dedicated light source in ONUs is needed by using re-modulation technique.

References

[1] C.-H. Lee, W. V. Sorin, and B. Y. Kim, "Fiber to the home using a PON infrastructure," *IEEE J. Lightw. Technol.*, vol. 24, no. 12, pp. 4568–4583, Dec. 2006.

[2] S.-J. Park, C.-H. Lee, K.-T. Jeong, H.-J. Park, J.-G. Ahn, and K.-H. Song, "Fiber-to-the-home services based on wavelength- division-multiplexing passive optical network," *IEEE J. Lightw. Technol.*, vol. 22, no. 11, pp. 2582–2591, Nov. 2004.

[3] D. Zhou, S. Subramaniam, "Survivability in Optical Networks," *IEEE Network Magazine*, vol. 14, no. 6, pp. 16-23, 2000.

[4] T. H. Wu, ''Emerging technologies for fiber network survivability,'' *IEEE Communication Magazine*, vol.33, no.2, pp. 62–74, Feb., 1995.

[5] D. Colle, S. De Maesschalck, C. Develder, P. Van Heuven, A. Groebbens, J. Cheyns, I. Lievens, M. Pickavet, P. Lagasse, P. Demeester, "Data-centric optical networks and their survivability," *IEEE Journal on Selected Areas in Communications*, vol.20, no.1, pp. 6–20, 2002.

[6] L. Sahasrabuddhe, S. Ramamurthy, and B. Mukherjee, "Fault management in IP-over-WDM networks: WDM protection versus IP restoration," *IEEE Journal on Selected Areas in Communications*, vol.20, no.1, pp21–33, 2002.

[7] T. J. Chan, C. K. Chan, L. K. Chen, and F. Tong, "A self-protected architecture for wavelength division multiplexed passive optical networks," *IEEE Photon. Technol. Lett.*, vol. 15, no. 11, pp. 1660–1662, Nov. 2003.

[8] Z. X. Wang, X. F. Sun, C. L. Lin, C. K. Chan, and L. K. Chen, "A novel centrally controlled protection scheme for traffic restoration in WDM passive optical networks," *IEEE Photon. Technol. Lett.*, vol. 17, no. 3, pp. 717–719, Mar. 2005.

[9] X. F. Sun, C. K. Chan, and L. K. Chen, "A survivable WDM-PON with alternate-path switching," *IEEE/OSA Optical Fiber Communication Conference / National Fiber Optic Engineers Conference (OFC/NFOEC)*, Paper JThB71, Anaheim, CA, 2006.

[10] P. Fan, H. Chen, M. Chen, and S. Xie, "Self-protected Scheme for Wavelength Reusable WDM Passive Optical Networks," *IEEE/OSA Optical Fiber Communication Conference / National Fiber Optic Engineers Conference (OFC/NFOEC)*, paper JWA69, Los Angeles, CA, 2011.

[11] S. B. Park, D. K. Jung, D. J. Shin, H. S. Shin, S. Hwang, Y. J. Oh, "Bidirectional wavelength-division-multiplexing self-healing passive optical network," *IEEE/OSA Optical Fiber*

Communication Conference / National Fiber Optic Engineers Conference (OFC/NFOEC), Paper JWA57, Anaheim, CA, 2005.

[12] K. Lee, S.-G. Mun, C.-H. Lee, and S. B. Lee, "Reliable wavelength- division-multiplexed passive optical network using novel protection scheme," *IEEE Photon. Technol. Lett.*, vol. 20, pp. 679–681, May 2008.

[13] K. Lee, S. B. Lee, J. H. Lee, Y.-G. Han, S.-G. Mun, S.-M. Lee, and C.-H. Lee, "A self-restorable architecture for bidirectional wavelength-division-multiplexed passive optical network with colorless onus," *OSA Opt. Express*, vol. 15, no. 8, pp. 4863–4868, 2007.

[14] A. Chowdhury, M. F. Huang, H. –C. Chien, G. Ellinas, and G. K. Chang, "A Self-Survivable WDM-PON Architecture with Centralized Wavelength Monitoring, Protection and Restoration for both Upstream and Downstream Links," *IEEE/OSA Optical Fiber Communication Conference / National Fiber Optic Engineers Conference (OFC/NFOEC)*, San Diego, Paper JThA95, 2008.

[15] E. S. Son, K. H. Han, J. H. Lee, and Y. C. Chung, "Survivable network architectures for WDM PON", *IEEE/OSA Optical Fiber Communication Conference / National Fiber Optic Engineers Conference (OFC/NFOEC)*, Paper OFI4, Anaheim, California, USA, 2005.

[16] X. F. Cheng, Y. J. Wen, Z. W. Xu, Y. X. Wang, Y. K. Yeo, "Survivable WDM-PON with self-protection and in-service fault localization capabilities," *Optics Communications*, vol. 281, no. 18, pp. 4606-4611, 2008.

[17] K.H. Tse, W. Jia, and C.K. Chan, "A cost-effective pilot-tone- based monitoring technique for power-saving in RSOA-based WDM-PON," *Optical Fiber Communication Conference / National Fiber Optic Engineers Conference (OFC/NFOEC)*, Paper OThB6, California, USA, 2011.

[18] S. W. Wong, L. Valcarenghi, S-H. Yen, D. R. Campelo, S. Yamashita and L. Kazovsky, "Sleep Mode for Energy Saving PONs: Advantages and Drawbacks," *IEEE Global Communications Conference Workshops*, Dec. 2009.

[19] W. Lee, M. Y. Park, S. H. Cho, J. Lee, C. Kim, G. Jeong, and B. W. Kim, "Bidirectional WDM-PON Based on Gain-Saturated Reflective Semiconductor Optical Amplifier," *IEEE Photon. Technol. Lett.*, vol. 17, no. 11, pp. 2460-2462, Nov. 2005.

[20] J. Chen and L.Wosinska, "Analysis of protection schemes in PON compatible with smooth migration from TDM-PON to hybrid WDM/TDMPON," *IEEE/OSA J. Opt. Netw.*, vol. 6, no. 5, pp. 514–526, May 2007.

[21] J.-Y. Kim, S.-G. Mun, H.-K. Lee, and C.-H. Lee, "Self- Restorable WDM-PON with a Color-Free Optical Source," *IEEE J. Opt. Commun. Netw.*, vol. 1, no. 6, pp. 565-570, Nov. 2009.

[22] W. Lee, M. Y. Park, S. H. Cho, J. Lee, C. Kim, G. Jeong, and B. W. Kim, "Bidirectional WDM-PON Based on Gain-Saturated Reflective Semiconductor Optical Amplifier," *IEEE Photon. Technol. Lett.*, Vol. 17, no. 11, pp. 2460-2462, 2005.

[23] P. Chanclou, F. Payoux, T. Soret, N. Genay, R. Brenot, F. Blache, M. Goix, J. Landreau, O. Legouezigou, and F. Mallécot, "Demonstration of RSOA-Based Remote Modulation at 2.5 and 5 Gbit/s for WDM PON," *Optical Fiber Communication Conference / National Fiber Optic Engineers Conference (OFC/NFOEC)*, paper OWD1, Anaheim, CA, USA 2007.

[24] H. Takesue, T. Sugie, "Wavelength channel data rewrite using saturated SOA modulator for WDM networks with centralized light sources," *IEEE J. Lightw. Technol.*, vol. 21, no. 11, pp. 2546-2556, Nov. 2003.

Chapter 4. Upstream Multi-Wavelength Shared PON

In this chapter, we proposed an Upstream Multi-Wavelength Shared (UMWS) PON architecture based on a tunable self-seeding Fabry-Perot laser diode (FP-LD) at ONU. The performances of the wavelength and power stability, side-mode suppression ratio (SMSR), tuning range for the proposed tunable self-seeding laser module at ONU are experimentally investigated. The BER is measured with direct modulation on FP-LD of 1.25Gbit/s upstream data. The extensive simulations not only evaluate the enhanced performance from the upstream wavelength-sharing, but also for the first time investigate the impact of channel Switch Latency (SL) on the network performance.

4.1 Introduction

The passive optical networks (PONs) are a promising solution in overcoming the last mile bottleneck in access networks [1-3]. Time-division-multiplexing (TDM)-based PON systems such as Ethernet PON (EPON) and gigabit PON (GPON) are already standardized [4-5] and currently operating at line rates of 1.25Gbit/s for EPON and 2.5Gbits/s for GPON [6-7]. In these networks, the total available bandwidth is shared among multiple active users, resulting in a low average data rate per user [8]. The introduction of bandwidth-intensive applications such as IPTV, HDTV, and video-on-demand (VoD) will drive the per-user bandwidth requirement beyond the capability of

these conventional TDM-based PON networks in the near future [9]. Providing cost-effective, smooth capacity upgrades while maintaining compatibility with existing PON standards will be of great concern for network operators.

Hence, 10Gbits/s TDM-PONs [10-12] are investigated in order to satisfy higher capacity requirements. The 10Gbits/s downstream transmitter can be deployed easily using distributed feedback laser diode (DFB-LD) with external modulation. But 10Gbits/s upstream burst mode transceivers is expensive and not practical in the near future, since the cost of the optical network unit (ONU) is paid solely by each user. In the other hand, upgrading the network to a WDM-PON involves major changes in the outside plant infrastructure of the existing TDM PON, leading to unproved huge investment and delays in upgrade [13]. Hybrid TDM-WDM-PON architectures have captured the research interest over the past few years [8, 13-14]. If multiple wavelengths can be overlaid on the existing TDM-PON with minimum changes to its architecture, it provides an ideal interim solution for smooth and on-demand capacity upgrade of the existing networks. Such solutions where all ONUs are allowed to effectively share multiple upstream wavelengths based on their traffic requests have been investigated [15-17].

4.2 Related Works

Fig. 4.1 shows the Multi-Wavelength PON (MWPON) architecture with a feeding light source (FLS) at the OLT sending un-modulated light (λ_1 - λ_m) to the respective ONUs for the upstream communication [18]. The ONU consists of a coarse WDM (CWDM), a

receiver (RX), a reflective semiconductor optical amplifier (RSOA) transmitter, and two tunable filters. To avoid performance degradation caused by Rayleigh backscattering (RBS) noise, the dual feeder fiber configuration with a 2×N power splitter at remote node (RN) is used: one for carrying feeding light toward ONUs and the other for modulated upstream and downstream carriers.

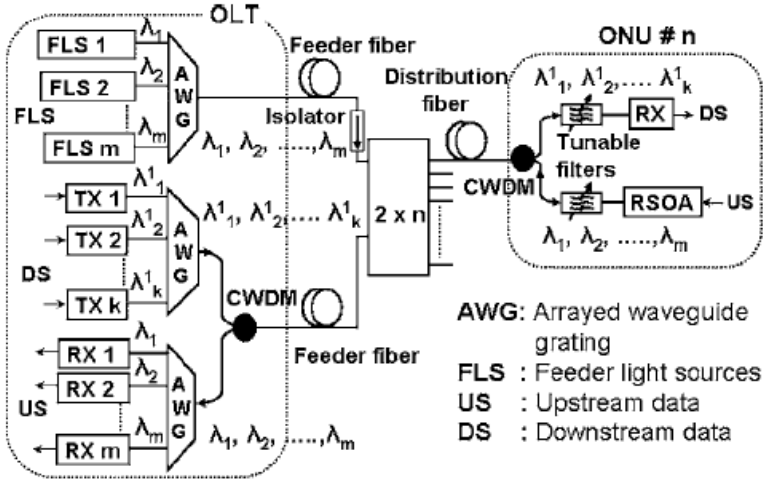

Fig. 4.1 Multi-Wavelength PON architecture with RSOA-based upstream transmitter [18]

Once the wavelengths for downstream and feeding light are assigned for an ONU by the bandwidth allocation scheme at the CO, this information is sent to the ONU via downstream messages. The ONU generates an input signals for filter controller circuits to tune its associated tunable filters for upstream and downstream links, respectively. Compared to 10G-EPON, the MWPON architecture has no compatibility issues in simultaneously supporting next-generation ONUs with higher data rates (10Gbit/s) and existing ONUs with low data rates (1Gbit/s). It is capable of allocating a dedicated pair of wavelengths to a user with high bandwidth demand while using the existing technology.

Thus the user enjoys a service level similar to that of a WDM-PON in a cost-effective way. But the scheme requires seeding lights sent from a FLS at the OLT, which increase investment cost and system complexity compared with the self-seeding technology at local ONU.

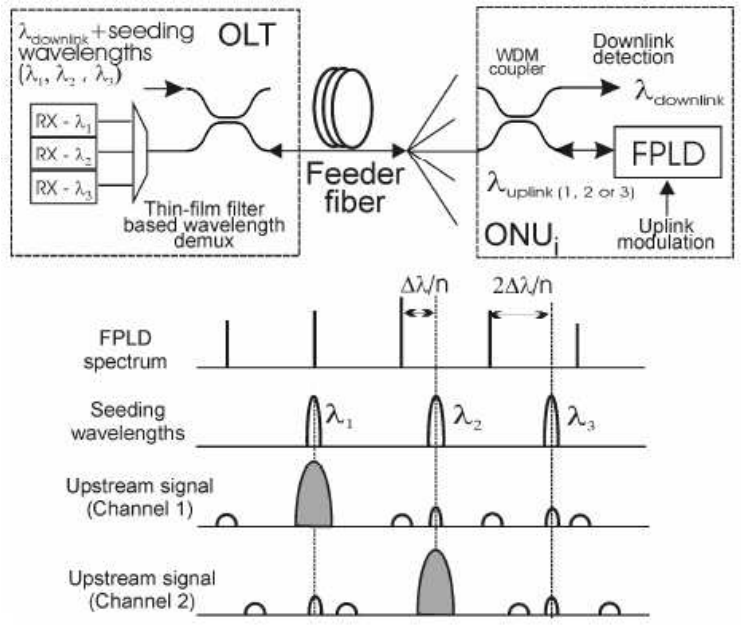

Fig. 4.2 Schematic for multi-wavelength upstream transmission employing FP-LD [19]

M. Attygalle et al. presented a single Fabry-Perot Laser Diode (FP-LD) as the channel selector and burst mode transmitter for upstream transmission by strategically tuning the temperature of FP-LD as shown in Fig. 4.2 [19]. Multiple seeding wavelengths (together with downstream channel) are transmitted at a channel separation of $\Delta\lambda(1+1/n)$, where '$\Delta\lambda$' is the mode spacing of the FP-LD [20-21] used at the ONUs and 'n' the number of seeding wavelengths. Initially, all FP-LDs will be wavelength-seeded at a single wavelength (λ1). When the upstream transmission capacity is pushed to the limit in this

channel or when some customers require higher upstream capacity, the OLT can send a request to those ONUs to tune their FP-LD transmitters to another seeding wavelength and join another separate upstream virtual channel (λ2 or λ3). The temperature tuning of the FP-LD can be achieved in a fraction of second. The temperature range to tune the FP-LD across a full FSR (140 GHz) up to 9 channels was observed to be only 9.1°C. The FP-LD transmitters at the ONUs should include a look up table to achieve the fast wavelength shift and this can be done at the manufacturing stage. But the realization of the accurate temperature tuning is very difficult and hence is very expensive.

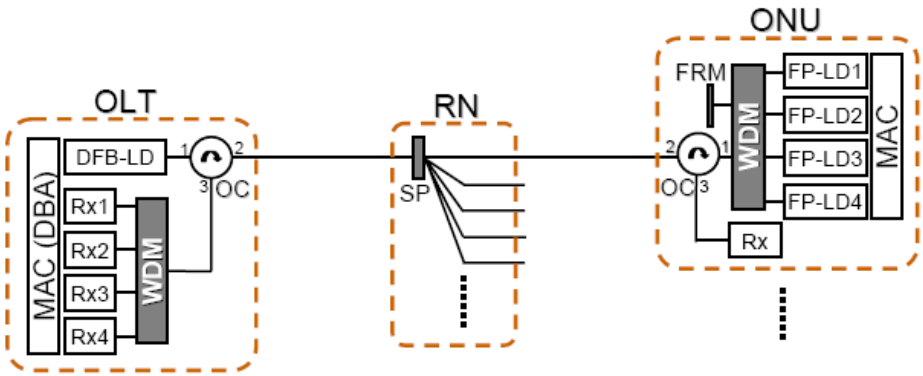

Fig. 4.3 10Gbit/s TDM-PON architecture using self-injected FP-LDs on each ONU [22]

Fig. 4.3 presents a 10-Gbps TDM-PON architecture [22]. In the OLT, the downstream signal uses a DFB-LD for broadcasting and sharing of information to each ONUs. In the RN, a 1×N passive optical splitter (SP) is used for distributing the whole traffic to each ONU. In each ONU, we use four FP-LDs, a 2×4 WDM and a fiber reflected mirror (FRM) to generate the four wavelength-multiplexed 2.5Gbit/s signals (λ1 to λ4) acting as the upstream signal transmitter to increase upstream bandwidth. The four filtered longitudinal modes will be reflected by the FRM and injected into the FP-LD. Based on the

seed-seeding operation, four wavelengths λ1 to λ4 on ONU will lase simultaneously. Thus, 10Gbit/s upstream signal can be obtained by directly modulating the four wavelength-multiplexed FP-LDs with electrically de-multiplexed 2.5Gbit/s data.

The proposed scheme provides an advantage of upgrading the present GPON which is TDM in nature to the 10Gbit/s PON by only modifying the equipments at the OLT and ONU while the fiber link between the OLT and ONU remain intact. However, the simple scheme is lack of flexibility in scheduling wavelengths and has lower resource utilization especially for those light-load ONUs. Besides, temperature control inside each ONU is required in order to ensure the four wavelengths sent to the OLT can be wavelength de-multiplexed and received properly.

4.3 Upstream Multi-Wavelength Shared PON

In this section, we presented a novel Upstream Multi-Wavelength Shared (UMWS) PON, based on some novel configurations of wavelength-tunable self-seeding FP-LD without fiber amplifiers inside the gain cavity at ONUs. The single-longitudinal-mode (SLM) output of the proposed tunable laser module at ONUs is implemented via the optical injection and feedback scheme of the FP-LD. Hence, it does not require external light injection sending from the OLT and dynamically locks onto anyone of many longitudinal modes of FP-LD by using a simple Sagnac fiber loop or a circulator-based fiber loop as a light reflector, instead of fiber reflective mirror (FRM) [23].

The proposed UMWS PON is believed to be a promising candidate for the next

generation access network thanks to the following reasons. First, the PON provides an advantage of simply upgrading the present TDM-PON in the upstream capacity by introducing multiple wavelengths (to avoid higher burst mode data speed at ONUs) and keeping the fiber transmission link intact. Moreover, all ONUs share the all upstream wavelengths to transfer upstream data with a wavelength or finer sub-wavelength granularity, which improves significantly bandwidth utilization by using inter-channel statistical multiplexing (via wavelength channel switch). Last but not least, the UMWS PON also presents a cautious upgrade path in that wavelength channels can be added on the user demand. More precisely, only ONUs with higher traffic demands may be upgraded by deploying proposed self-seeding laser module, while ONUs with lower traffic demands remain unaffected. Thus, a single-channel TDM-PON can be upgraded alternatively into a heterogeneous WDM/TDM PON in which the ONUs differ in upstream capabilities.

4.3.1 Architecture Design and Operation Principle

The UMWS PON architecture based on a tunable self-seeding FP-LD at ONU is shown in Fig. 4.4, where three ONU transmitter structures are displayed. In the OLT, a DFB-LD and a Mach-Zehnder modulator (MZM) are used to generate downstream broadcasting signal (λ_d) to each ONU. A $1\times m$ wavelength de-multiplexer/multiplexer (WDM) and a bank of Photo-Detectors (PDs) are used to simultaneously receive signals in multiple upstream wavelengths. An Erbium-doped fiber amplifier (EDFA) is installed before WDM to compensate the upstream transmission loss and to improve the power

budget. In RN, a 1×*n* optical splitter is applied to split downstream carrier (λ_d) power to each ONU and to combine multiple upstream wavelengths (λ_{1u} to λ_{mu}) sent back to OLT, respectively.

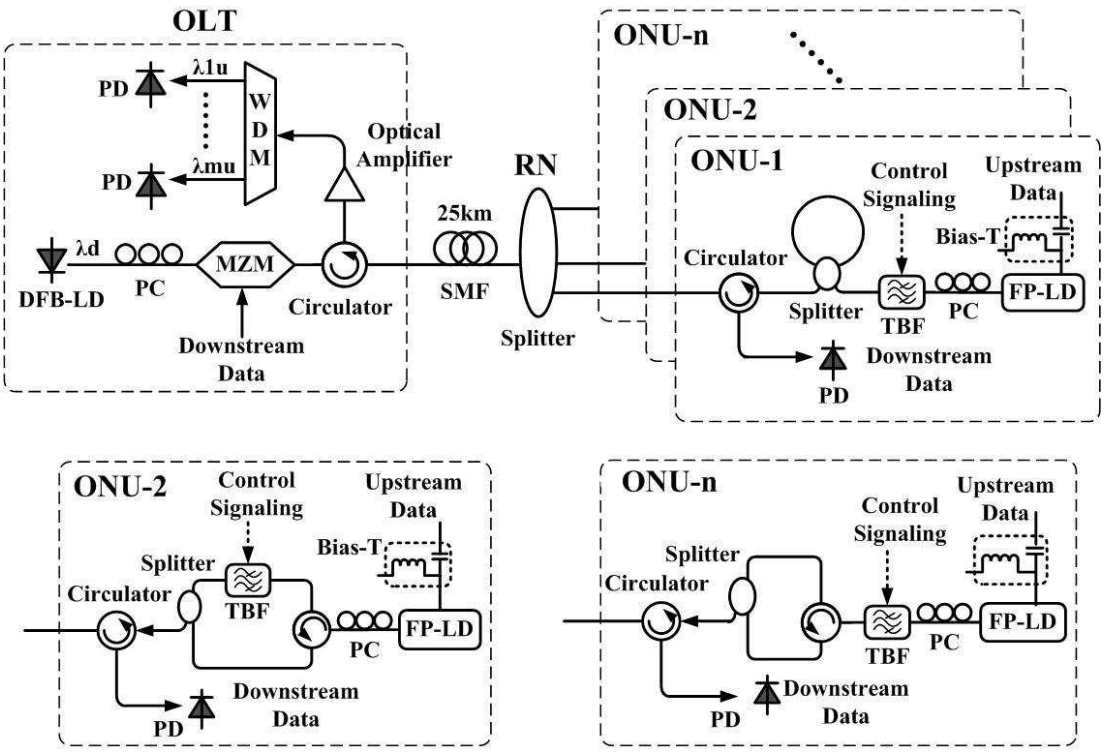

Fig. 4.4 Proposed UMWS-PON based on a tunable self-seeding FP-LD at ONUs. Three ONU transmitter structures are displayed in the inset ONU-1, ONU-2, ONU-n, respectively.

In ONU, we use an optical circulator to connect an upstream transmitter and a PD as a downstream receiver. Here, we proposed three different structures of upstream transmitter at ONU. The three structures have same function components: 1) a FP-LD as an original light source with multi-longitudinal-mode (MLM) output, 2) a tunable band-pass filter (TBF) used to dynamically filter a designated single longitudinal mode (SLM), and 3) a feedback device for self-seeding FP-LD to produce a power-constant SLM output. The

main difference of the three transmitter structures lies in the realization of the feedback device. In the inset ONU-1, we utilize a 2×2 optical coupler to construct a Sagnac fiber loop reflector as a feedback device for self-seeding FP-LD. In the inset ONU-2 and ONU-*n*, an optical circulator is linked to a 1×2 optical coupler to form a fiber loop reflector, and another port of the 1×2 optical coupler serves as an output of the fiber laser module. The TBF can be positioned either inside the fiber loop (eg. in ONU-2), or before the fiber loop (eg. in ONU-*n*).

The FP-LD has MLM output with ~45% front-facet reflectivity. The TBF is required to be capable of precisely changing their center wavelength according to a voltage signal. For example, micro-machined vertical cavity filters using multiple distributed Bragg reflectors (DBR) can be used for these tunable filters, which have fast tuning responses and wide wavelength tuning range with low tuning voltages [24-25]. Once the ONU receives the downstream control signal from the OLT on the assigned wavelength channel, the control circuits on the ONU are triggered for the TBF calibration. Thus, the MLM FP-LD is aligned to the certain filter mode of the TBF. The filtered longitudinal mode will be reflected by the feedback device and injected back into the FP-LD. Therefore, the feedback light is selected by the TBF and transmits through the following fiber path: FP-LD → TBF → feedback device → TBF → FP-LD → TBF → feedback device → Output. Hence, an optical SLM output is amplified by self-seeding operation of FP-LD.

Based on the self-seeding operation, upstream signal can be obtained by directly modulating the FP-LD in arbitrary wavelength by dynamically adjusting the TBF. The

polarization controller (PC) is placed inside the gain cavity to control the polarization state of the feedback light into the FP-LD properly, obtain maximum output power, and maintain wavelength stabilization. The injected light at the state of the TE mode of FP-LD will result in the maximum injection locking efficiency [26]. Some control schemes such as temperature and wavelength control are also required so to ensure nearly the same set of wavelengths can be produced by different ONUs. Furthermore, a dynamic bandwidth allocation (DBA) scheduler with two-dimension schedule functions for time and wavelength resources can be equipped at the OLT to allow efficient sharing of upstream wavelength resources with all ONUs. Due to the fact that only a small number (m = 3 or 4) of extended wavelengths can be deployed for incremental upgrades [27], the number m of extended wavelengths is usually smaller than the number of ONUs. The transmission is totally 25km single mode fiber (SMF) without dispersion compensation.

4.3.2 Experimental Results

Because the three different structures of ONU upstream transmitter have same operation principle and similar experiment results, we just illustrate the experimental results of the ONU-1 structure in Fig. 4.5 for the paper conciseness. In the proof-of-principle experiment, we use 1.5μm FP-LD with 1.25GHz modulation bandwidth to simulate the unavailable 1.3μm FP-LD in our lab.

Fig. 4.5 (a) shows the free-running output spectrum of the MLM FP-LD without self-seeding when the bias current and temperature are 30mA and 25^{o}C. The TBF has a 3dB bandwidth of 0.4nm and a ~3.5dB insertion loss. Thus, the MLM FP-LD is aligned

to a certain filter mode of the TBF. The filtered SLM will be reflected by the Sagnac fiber loop and injected back into the FP-LD. It is worth noting that the Sagnac fiber loop is composed of an optical coupler with the maximum splitter ratio (90:10), which provides 90% power for the output and 10% for the feedback to the FP-LD, to enhance output power of the self-seeding FP-LD module. It is because that a 50:50, 30:70 or 20:80 optical coupler will lead to the lower output power via experimental investigations. While the TBF is set at 1555.3nm, the stable SLM output is shown in Fig. 4.5 (b). Fig. 4.5 (c) presents the complex output power spectra of the proposed laser module in the tuning range of 1544.69nm to 1563.39nm with the tuning step of ~1.34nm.

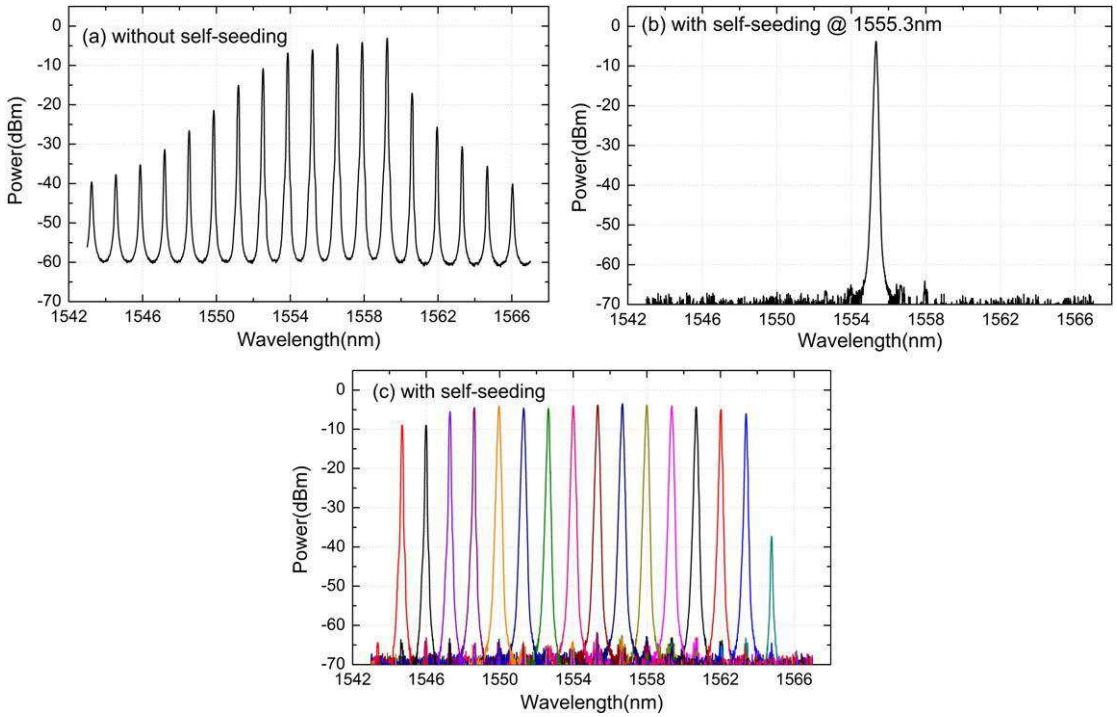

Fig. 4.5 (a) Original output spectrum of MLM FP-LD. (b) SLM output is obtained while the TBF is set at 1555.3nm. (c) Complex output spectra of proposed laser module.

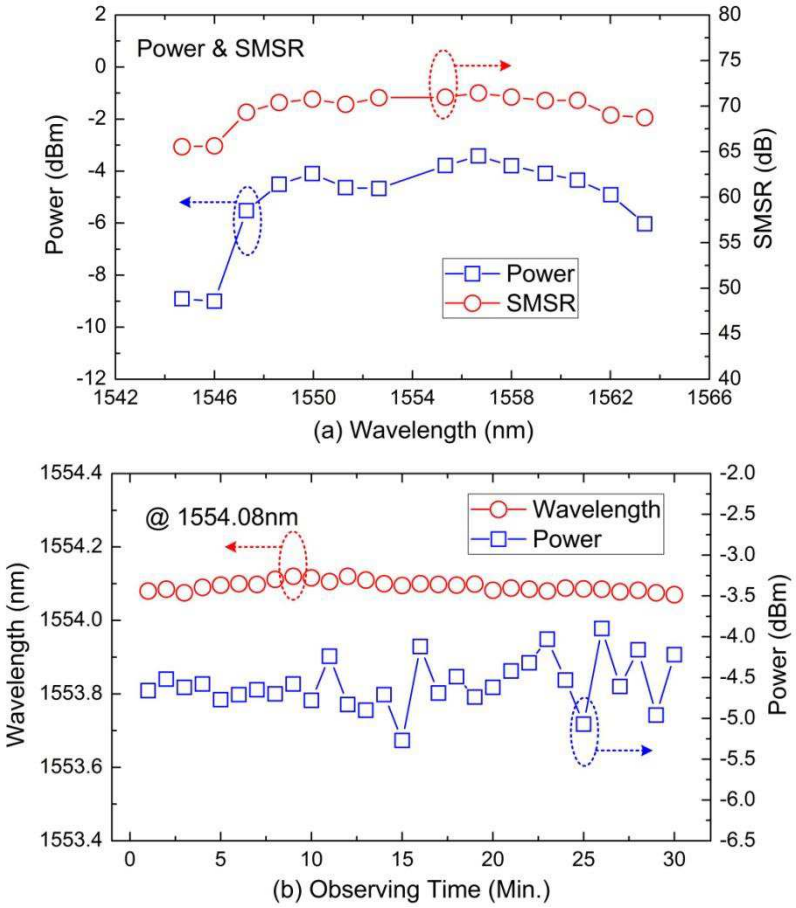

Fig. 4.6 (a) Output power and SMSR spectra in the wavelength range of 1544.69nm–1563.39 nm with a 1.34nm tuning step. (b) Output variations of central wavelength and power at 1554.08 nm over 30 min.

Fig. 4.6 (a) shows the output power and SMSR versus the different lasing wavelengths with a 1.34nm tuning step. The maximum output power of -3.4dBm is at the wavelength of 1546.0nm. The minimum output power is -9.0dBm at 1556.69 nm. The maximal output power difference ΔP_{max} is about 5.6dB. When the lasing wavelength is 1556.69nm,

the SMSR can reach 71.4dB. The minimum of SMSR is 65.5dB at 1544.96nm ($\Delta SMSR_{max}$ = 5.9dB). The output power of the laser is determined by the gain profile of the FP-LD, hence it is lower at both ends of the spectrum.

To investigate the output performances of power and wavelength stabilities, a short-term stability of ONU-1 is measured. Initially, the lasing wavelength is 1554.08nm and the observing time is over 30min. In Fig. 4.6 (b), the wavelength variation and the power fluctuation are 0.05nm and 1.37dB, respectively. After two-hour observing, the stabilized output is still maintained. As a result, the proposed wavelength-tunable fiber laser at ONUs has the advantage of simple configuration, high output efficiency, and wide wavelength tuning range.

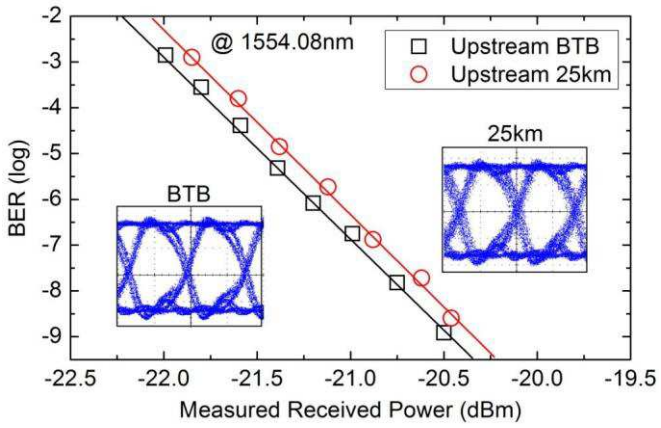

Fig. 4.7 BER and eye diagrams for the upstream traffic with BTB and 25km transmission

Fig. 4.7 presents the BER curves and eye diagram of the 1.25Gbit/s upstream signals at the lasing wavelength of 1554.08nm in the case of back-to-back (BTB) and after 25-km transmission without dispersion compensation. The power penalty is less than 0.2 dB.

To verify the feasibility in the upstream link using the proposed tunable self-seeding

laser with different split ratios at the RN, a power budget analysis for the upstream data was carried out using the minimum output power of around -9dBm at ONU (refer to Fig. 4.6 (a)). The EDFA gain reached about 30dB in OLT to compensate the upstream transmission loss and to improve the power budget. The receiver sensitivity of the upstream data was considered to be -20.4dBm according to the experimental data (refer to Fig. 4.7). In this analysis, the total loss except for the optical coupler at RN consist of a 0.8dB insert loss for the optical circulator at ONU, a 0.2dB/km transmission loss for a 25km optical fiber, a 5dB insert loss for WDM and a 0.8dB optical circulator loss at OLT. When the split ratio is 8, 16, 32, 64, the optical coupler loss at RN is 11, 14, 17, 21dB, respectively, where the insertion loss of the coupler is 2dB and a 3dB loss for each 1×2 power-split. The power margins shown in Table 4.1 indicate the feasibility of the larger split ratio and transmission scope in the proposed UMWS PON.

Table. 4.1 Power Margin Calculation for Upstream Data with Different Split Ratios

Split Ratio	**8**	**16**	**32**	**64**	**128**
Minimum output power at ONU (dBm)	-9	-9	-9	-9	-9
EDFA amplifier gain (dB)	30	30	30	30	30
Receiver sensitivity (dBm)	−20.4	−20.4	−20.4	−20.4	-20.4
Other insertion losses (dB)	11.6	11.6	11.6	11.6	11.6
Optical coupler loss at RN (dB)	11	14	17	21	24
Power Margin (dB)	**18.8**	**15.8**	**12.8**	**9.8**	**6.8**

4.4 Performance Analysis and Simulation Results

In the UMWS-PON, we assume that all ONUs can have full access to all upstream wavelengths by being equipped with the proposed tunable self-seeding FP-LD module.

Thus each ONU can generate any designed wavelength by using self-seeding operation according to the OLT scheduling information. We note that the inter-channel switch is realized via a tunable filter, which has tuning times in the scale of microseconds [24]. Hence, the filter tuning time cannot be neglected compared with the transmission time of a data packet with the packet length ranging from 64 to 1518 bytes on a 1Gbit/s link. Therefore, in the following simulations we not only evaluate the performance merit gained from the flexible sharing of the multiple upstream wavelength resources, but also for the first time investigate the impact of channel Switch Latency (SL) on the network performance.

Table. 4.2 Reference System Simulation Parameters

Parameters	Reference value
ONU number *n**	64 or 32 or (from 16 to 64)
Number *m* of upstream wavelength in a PON*	4 or 3
Link data rate from users to an ONU	100Mbps
Upstream rate of each wavelength channel	1Gbit/s
ONU buffer size	10Mbytes
Distance between the OLT and ONUs	from 5km to 20km
Upper bound limitation of transmission window	15000 Bytes

*Different values are taken in different simulation scenarios

In the upstream bandwidth allocation, decisions both on when and for how long (Timeslot) and on which Wavelength channel to grant an ONU upstream transmission are required to make efficient use of the upstream bandwidth. To solve the joint Wavelength and Timeslot Scheduling (WATS) problem, we consider an online scheduling strategy in the paper based on the multi-wavelength Interleaved Polling with Adaptive Cycle Time

(IPACT) [28] scheme. The OLT online scheduler schedules ONUs one-by-one without considering the bandwidth requirements of other ONUs. It schedules an ONU to transmit on the first available wavelength channel (FAWC) supported by that ONU, within a designed timeslot with window size purely according to the reported size in the previous Request message, as long as it has not exceeded the maximum window limit. In other words, we adopt the FAWC scheme in choosing wavelength channel, and the Limited assignment scheme [28] is used to prevent the upstream channel monopolization by one ONU with high data volume.

In this simulation, an UMWS PON is consisting of an OLT and N ONUs with m upstream wavelength channels. The Round Trip Time (RTT) delay for each ONU is assumed to be randomly (uniformly) over the interval [25μs, 100μs], which corresponds to the distance between OLT and ONUs ranging from 5 to 20 km. The access link data rate from users to an ONU is 100Mbit/s. The upstream rate of each wavelength channel is 1Gbit/s. The ONU buffer size is 10Mbytes. The upper bound limitation of transmission window length is 15000 Bytes when the Limited assignment scheme is adopt. The ONU traffic load follows the self-similar traffic source model [29], which is simulated by alternating Pareto-distributed ON/OFF source model. In our implementation, the shape parameter α is 1.4 and the Hurst parameter can be calculated by $H = (3-\alpha)/2 = 0.8$. The above simulation parameters are concluded in Table 4.2. For each simulation case, each scheduling result is the average over 10 simulations.

4.4.1 Performance Gain of the Upstream Wavelength Sharing

In the first simulation, we just evaluate the enhanced performance of the proposed UMWS PON compared with the prevailing TDM-over-WDM PON [30-31] without taking the channel Switch Latency (SL) into consideration. In UMWS PON, 64 ONUs share 4 upstream wavelengths by using the tunable self-seeding FP-LD module at each ONU. In the conventional TDM-over-WDM PON, all ONUs are grouped to 4 TDM-sub-PONs, each containing 16 ONUs and a fixed upstream wavelength. Let $load_i^{ave}$ be the average traffic load from ONU-*i*; $load_i^{\max}$ be the maximum admitted traffic load of ONU-*i*. We define the traffic Load Heterogeneity of ONU-*i* as follows:

$$Load\_Heterogeneity_i = load_i^{\max} / load_i^{ave} \tag{4.1}$$

We consider five types of traffic load profile for each ONU: each type has the identical average traffic load ($load_i^{ave}$ = 0.5) and different load heterogeneities ($Load\_Heterogeneity_i$ = 1, 1.2, 1.4, 1.6, and 1.8), respectively.

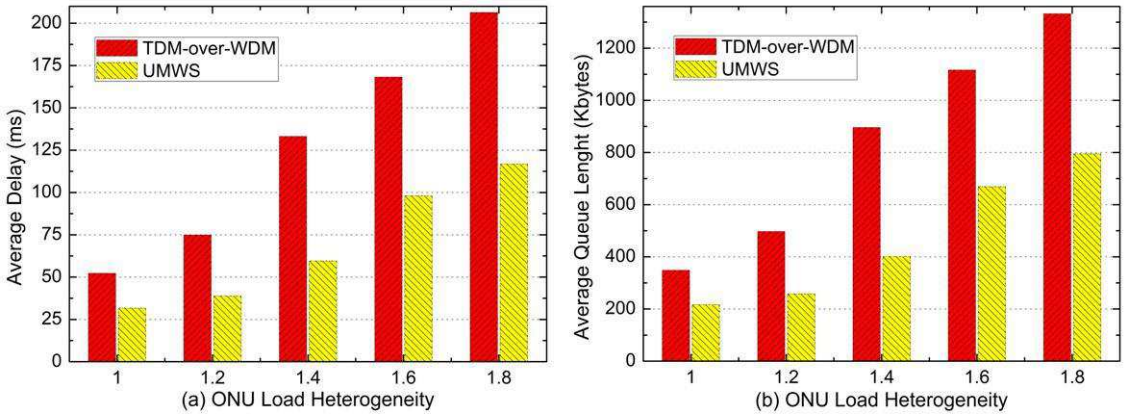

Fig. 4.8 Performance gain of UMWS PON in the (a) Average Delay and (b) Average Queue length compared with the conventional TDM-over-WDM PON.

Fig. 4.8 shows that the proposed UMWS PON significantly outperforms the

conventional TDM-over-WDM PON in the Average Delay and Average Queue length, which is primarily due to the sharing and flexible scheduling of upstream wavelength resource among all ONUs. We also note that as the heterogeneity of ONU traffic load becomes larger, the performance gain is increasing obvious. This signifies the UMWS PON can provide better performances in a more practical network scenario having heterogeneous traffic load.

4.4.2 Impact of Switch Latency under Different ONU Traffic Loads

In the simulation, the impact of the channel SL on the network performance is investigated under different ONU traffic load ranging from 0.1 to 0.9. We assume that all 32 ONUs have identical traffic load and 3 upstream wavelengths are available in a PON. We define the Channel Switch Ratio (CSR) as the number of channel switch times divided by the total number of GATE messages sent in a simulation lasting 20s running time, as shown in Eq. (2). We first illustrate the CSR performances to facilitate to explain other network performance parameters such as average delay and packet loss ratio.

$$CSR = \frac{Number\ of\ channel\ switch\ times}{Number\ of\ GATE\ messages}\ (\text{during 20s simulation time}) \qquad (4.2)$$

Fig. 4.9 depicts the CSR versus ONU load with different SL values. We take the SL=0 case as performance baseline, which corresponds to an ideal wavelength-sharing PON without channel SL consideration. For the SL=130 case, the CSR is always very low. The SL value is so large that it is equivalent to the largest transmission window length on a 1Gbit/s upstream link (that is 15000Bytes * 8 / 1Gbit/s = 120μs). This situation reduces significantly the channel switch time nearly to zero, which is similar to a static

wavelength-allocation PON without any channel switch action.

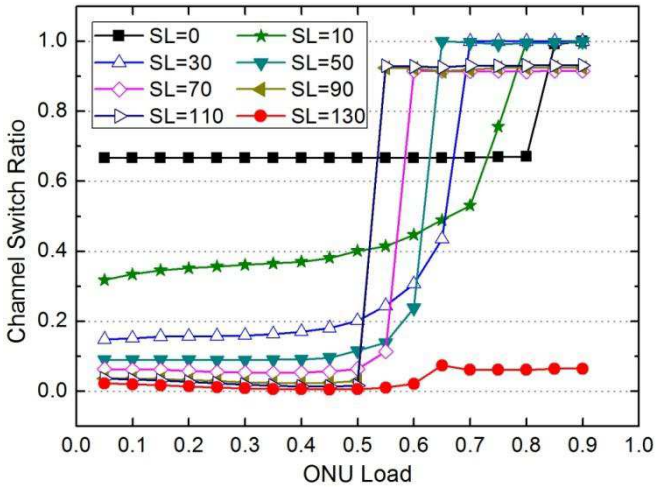

Fig. 4.9 Channel Switch Ratio (CSR) with different SL values under the ONU load variations.

For other SL cases, we observe that the CSR remains almost constant at the light loads and abruptly reaches the highest value at the heavy loads. The reason is that the lower load makes the earliest available time of different wavelength channels closer to each other and hence the channel switch is not necessary. At the heavier load, the earliest available times of each wavelength channel become quite different, which makes the channel switch turn to be more frequent. We also find that as the SL value increases, the CSR become smaller at light load but reaches the highest value earlier at heavy loads. It is due to the fact that the higher SL tends to reduce channel switch times at lighter load, but as the ONU load increases, the higher SL introduces more delay, which leads to more frequently switch the upstream channel.

Fig. 4.10 (a) and (b) show the average packet delay and packet loss ratio with the ONU load variation respectively. We observe that at the light load less than 0.5, the average

packet delay preserves a very low value for all SL cases, which leads to the nearly zero packet loss ratio. But when the ONU load is larger than 0.5, different SL curves separate each other. The higher the SL is, the lager average delay becomes and the earlier average delay reaches the maximal value. It results from the fact that CSR also reaches the highest value earlier as shown in Fig. 4.9. Because the larger packet delay will give rise to higher packet loss ratio, Fig. 4.10 (b) displays the same trend as Fig. 4.10 (a). It is noted that the SL = 130 performance is better than SL = 30 case. This result indicates the larger SL seriously spoils the upstream performances. Just when the SL is small enough (less than 30μs), the performance gain mentioned above can appear compared with a static wavelength-allocation PON, which is corresponding to the SL = 130 case.

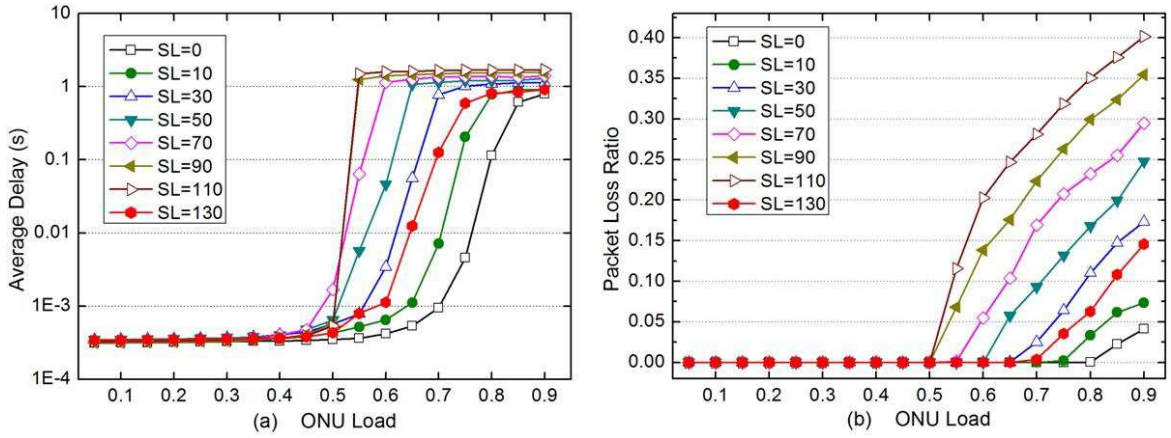

Fig. 4.10 (a) Average delay and (b) packet loss ratio versus the ONU load with different SLs.

4.4.3 Impact of Switch Latency under Varied On-Line ONU Numbers

In the simulation, we vary the on-line ONU numbers from 16 to 64, and randomly set each ONU load chosen from the interval [0.1, 0.9]. There are 3 upstream wavelength channels to be used in a PON. In the same way, we first illustrate the CSR performances

to study the impact of the channel SL on the network performance.

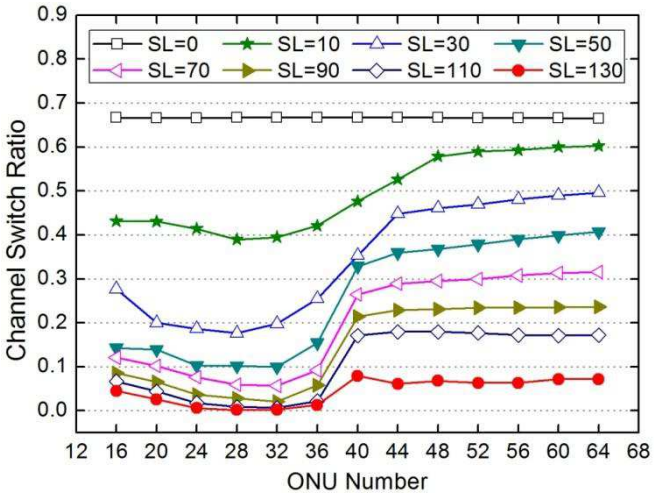

Fig. 4.11 Channel Switch Ratio (CSR) versus on-line ONU number with different SLs.

Fig. 4.11 shows the CSR of different SL values under the random traffic load and varied on-line ONU number. We find that the CSR decreases as SL increase. When SL = 0, the CSR has almost no difference at about 0.67 and while the SL = 130 the CSR is very small below 0.1. It is because the larger SL tends to prevent channel switch at certain degree. We also observe that the increase in the on-line ONU number represents the heavier network traffic load, which consequently leads to a slow rise of the CSR curve.

From Fig. 4.12, we observe that when the on-line ONU number is smaller, the average packet delay is also a very low value, and the packet loss ratio is nearly zero for all SL cases. But for the larger on-line ONU number, different SL curves separate each other. The higher the SL is, the lager average delay and the higher packet loss ratio become. We also note that the performance for SL = 130 case is slightly better than that for the SL values of more than 50μs. We know that the SL = 130 curve represents the performance

of a static wavelength-allocation PON. So we have same conclusion as in Fig. 4.10 that the performance gained from dynamic wavelength allocation scheme is obtain only when the SL is small enough (about 30μs), which is the 25% of the maximal admitted transmission window.

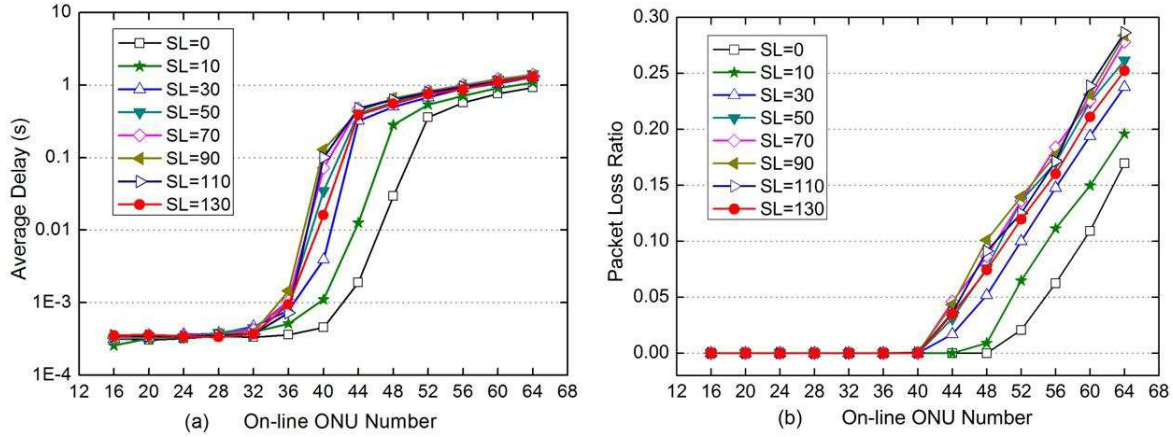

Fig. 4.12 (a) Average delay and (b) Packet loss ratio versus the on-line ONU number with different SLs

4.5 Conclusions

We propose a novel UMWS-PON based on the tunable self-seeding FP-LD module at ONU. The PON not only upgrades easily upstream capacity by introducing multiple wavelengths (to avoid higher burst mode data speed at ONUs), but also improves significantly bandwidth utilization with inter-channel statistical multiplexing. The outputs of the self-seeding FP-LD module have a good performance of output power, optical SMSR and stabilities in the wavelength tuning range of 1547.18nm to 1561.92nm with tuning step of 1.34nm via experimental investigation. The BER measurement is performed for 1.25Gbit/s upstream data. With the proposed PON infrastructure, we not

only evaluate the performance gained from the flexible sharing of the multiple upstream wavelength resources, but also for the first time investigate the impact of channel SL on the network performance. The extensive simulations show that the enhanced performance is obtained when the condition that the channel SL is relative small. Therefore we believe that the UMWS-PON would be a promising solution for next generation access networks.

References

[1] F.-T. An, D. Gutierrez, K. S. Kim, J. W. Lee, and L. G. Kazovsky, "SUCCESS-HPON: A next-generation optical access architecture for smooth migration from TDM-PON to WDM-PON," *IEEE Commun. Mag.*, vol. 43, no. 11, pp. S40–S47, Nov. 2005.

[2] G. Kramer and G. Pesavento, "Ethernet passive optical network (EPON): building a next-generation optical access network," *IEEE Commun. Mag.*, vol. 40, no. 2, pp. 66–73, Feb. 2002.

[3] L. G. Kazovsky, W.-T. Shaw, D. Gutierrez, N. Cheng, and S.-W. Wong, "Next-Generation Optical Access Networks," *IEEE J. Lightwave Technol.*, vol. 25, no. 11, pp. 3428-3442, 2007.

[4] IEEE Standard for Information Technology, IEEE Std 802.3ah-2004 (IEEE, 2004).

[5] ITU-T Recommendation G.984.2-2003, "Gigabit-capable passive optical networks (GPON): physical media dependent (PMD) layer specification," (ITU, 2003).

[6] M. Abrams, P. C. Becker, Y. Fujimoto, V. O'Byrne, and D. Piehler, "FTTP deployments in the United States and Japan-equipment choices and service provider imperatives," *IEEE J. Lightwave Technol.*, vol. 23, no. 1, pp. 236–246, 2005.

[7] K. Ohara, A. Tagami, H. Tanaka, M. Suzuki, T. Miyaoka, T. Kodate, T. Aoki, K. Tanaka, H. Uchinao, S. Aruga, H. Ohnishi, H. Akita, Y. Taniguchi, and K. Arai, "Traffic analysis of Ethernet-PON in FTTH trial service," *IEEE/OSA Optical Fiber Communication Conference / National Fiber Optic Engineers Conference (OFC/NFOEC)*, Paper ThA.A2, Atlanta, 2003.

[8] D. J. Shin, D. K. Jung, H. S. Shin, J. W. Kwon, S. Hwang, Y. Oh, and C. Shim, "Hybrid WDM/ TDM-PON with wavelength-selection-free transmitters," *IEEE J. Lightwave Technol.*, vol. 23, no. 1, pp. 187–195, 2005.

[9] S.-J. Park, C.-H. Lee, K.-T. Jeong, H.-J. Park, J.-G. Ahn, and K.-H. Song, "Fiber-to-the-home services based on wavelength-division-multiplexing passive optical network," *IEEE J. Lightwave Technol.*, vol. 22, no. 11, pp. 2582–2591, 2004.

[10] B. McDonald, "EPON deployment challenges – now and the future," *IEEE/OSA Optical Fiber Communication Conference / National Fiber Optic Engineers Conference (OFC/NFOEC)*, Paper JWA96, Anaheim, CA, 2007.

[11] K. McCammon and S. W. Wong, "Experimental validation of an access evolution strategy: smooth FTTP service migration path," *IEEE/OSA Optical Fiber Communication Conference / National Fiber Optic Engineers Conference (OFC/NFOEC)*, Paper NThB3, Anaheim, CA, 2007.

[12] 10G EPON study group public articles, http://www.ieee802.org/3/av.

[13] Y.-L. Hsueh, M. S. Rogge, S. Yamamoto, and L. G. Kazovsky, "A highly flexible and efficient passive optical network employing dynamic wavelength allocation," *IEEE J. Lightwave Technol.*, vol. 23, no. 1, pp. 277–286, Jan. 2005.

[14] G. Talli and P. D. Townsend, "Hybrid DWDM-TDM long-reach PON for next-generation optical access," *IEEE J. Lightwave Technol.*, vol. 24, no. 7, pp. 2827–2834, 2006.

[15] C.-J. Chae and T. Jayasinghe, "Bandwidth-efficient capacity upgrade of Ethernet passive optical network systems," *IEE Electron. Lett.*, vol. 42, no. 16, pp. 938–939, Aug. 2006.

[16] J.-J. Yoo, H.-H. Yun, T.-Y. Kim, K.-B. Lee, M.-Y. Park, B.-W. Kim, and B.-T. Kim, "A WDM-Ethernet hybrid passive optical network architecture," *International Conference on Advanced Communication Technology (ICACT)*, 2006.

[17] T. Jayasinghe, C.-J. Chae, and R. S. Tucker, "Multi-wavelength Ethernet PON with RSOA based upstream modulators," *Opto-Elecronics and Communications Conference (OECC)*, paper 5E3-4, Taiwan, July 2006.

[18] T. Jayasinghe, C.-J. Chae, and R. S. Tucker, "Scalability of RSOA-based multi-wavelength Ethernet PON architecture with dual feeder fiber," *OSA J. Opt. Netw.*, vol. 6, no. 8, pp. 1025-1040, 2007.

[19] M. Attygalle, Y. J. Wen, J. Shankar, "Increasing upstream capacity in TDM-PON with multiple-wavelength transmission using Fabry-Perot laser diodes," *OSA Opt. Express*, vol. 15, no. 16, pp. 10247-10252, Aug. 2007.

[20] Z. Xu, Y. J. Wen, W.D. Zhong, C.-J. Chae, Y. Wang, C. Lu, and J. Shankar, "High speed WDM-PON using Fabry-Pérot laser diodes wavelength-locked by CW seed light," *OSA Opt. Express*, vol. 15, no. 6, pp. 2953-2962, Mar. 2007.

[21] N. Kashima, "Dynamic properties of FP-LD transmitters using side-mode injection locking for LANs and WDM-PONs," *IEEE J. Lightwave Technol.*, vol. 24, no. 8, pp. 3045-3058, 2006.

[22] C.-H. Yeh, C.-W. Chow, C.-H. Wang, F.-Y. Shih, Y.-F. Wu, and S. Chi, "Using four wavelength-multiplexed self-seeding Fabry-Perot lasers for 10 Gbps upstream traffic in TDM-PON," *OSA Opt. Express*, vol. 16, no. 23, pp. 18857-18862, 2008.

[23] C. H. Yeh, F. Y. Shih, C. H. Wang, C. W. Chow, and S. Chi, "Cost-effective wavelength-tunable fiber laser using self-seeding Fabry-Perot laser diode," *OSA Opt. Express*, vol. 16, no. 1, pp. 435-439, 2008.

[24] T. Amano, F. Koyama, T. Hino, M. Arai, and A. Mastutani, "Design and fabrication of

GaAs-GaAlAs micromachined tunable filter with thermal strain control," *IEEE J. Lightwave Technol.*, vol. 21, no. 3, pp. 596–601, 2003.

[25] C. Sciancalepore, B. B. Bakir, X. Letartre, J.-M. Fedeli, N. Olivier, D. Bordel, C. Seassal, P. R.-Romeo, P. Regreny, and P. Viktorovitch, "Quasi-3D Light Confinement in Double Photonic Crystal Reflectors VCSELs for CMOS-Compatible Integration," *IEEE J. Lightwave Technol.*, vol. 29, no. 13, pp. 2015-2024, 2011.

[26] M. Schell, D. Huhse, W. Utz, J. Kaessner, D. Bimberg, and I. S. Tarasov, "Jitter and dynamics of self-seeded Fabry–Perot laser diodes," *IEEE J. Sel. Top. Quantum Electron.*, vol. 1, no. 2, pp. 528–534, 1995.

[27] M. P. McGarry, M. Reisslein, and M. Maier, "WDM Ethernet passive optical networks," *IEEE Commun. Mag.*, vol. 44, no. 2, pp. 15–22, 2006.

[28] D. J. Shin, D. K. Jung, H. S. Shin, J. W. Kwon, S. Hwang, Y. Oh, and C. Shim, "Hybrid WDM/TDM-PON with wavelength-selection-free transmitters," *IEEE J. Lightwave Technol.*, vol. 23, no. 1, pp. 187–195, 2005.

[29] K. Park and W. Willinger, "Self-similar network traffic: an overview," Self-Similar Network Traffic and Performance Evaluation, K. Park and W. Willinger, eds. (Wiley Interscience, 2000).

[30] G. Talli and P. D. Townsend, "Hybrid DWDM-TDM long-reach PON for next-generation optical access," *IEEE J. Lightwave Technol.*, vol. 24, no. 7, pp. 2827–2834, 2006.

[31] G. Kramer, B. Mukherjee, and G. Pesavento, "Interleaved polling with adaptive cycle time (IPACT): a dynamic bandwidth distribution scheme in an optical access network," *Photonic Netw. Commun.*, vol. 4, no. 1, pp. 89–107, 2002.

Chapter 5. Fault-Tolerant Scheduling in Optical Grid

Optical grid systems have been viewed as a promising virtual computing environment to support large-scale distributed computing applications. For such a system involving many heterogeneous Grid and network resources, the faults of these resources seem to be inevitable. In this chapter, we first provide a survey of allocation and scheduling problem in optical Grid systems, including the problem background, and potential research problems and challenges. Then we proposed two fault-tolerant scheduling schemes for optical Grid applications: 1) the first one focus on optical link failures with application deadline requirement, the proposed Availability-Driven Scheduling (ADS) scheme can provide better performances in terms of availability and network resource utilization, while satisfying given deadline; 2) the second one studies issue of handling grid resource failures in optical Grids by using a primary-backup approach to allocate simultaneously two copies of each computation task to two different Grid resources for data process. It improves greatly application availability and induces less the overhead in scheduling length when the more network resources are available.

5.1 Introduction

In this work, we focus on the problem of Grid resource allocation and scheduling on optical networks, which is the core function of the Grid scheduler. The problem is the

spatial and temporal assignment of Grid tasks to shared resources distributed over the optical network [1]. The main of goal of this problem is to minimize the completion time or the schedule length of Grid requests, which may contain multiple dependent tasks. To achieve the best performance in an optical Grid, it may be necessary to consider the allocation of optical network resources and the allocation of Grid computing resources in a joint manner. We first provide a survey of allocation and scheduling problem in optical Grid, including the problem background, and potential research problems and challenges.

5.1.1 Computationally Intensive vs. Data Intensive

Grid request can be divided into two categories: 1) computation intensive Grid requests, and 2) data-intensive Grid requests. For a computation-intensive Grid request, the Grid tasks require only a limited amount of data transfer among different data storage locations. Grid resource reservation and task scheduling problems for this type of request usually assume that network resources are always available, and that advance reservation of the resources is not required. There are number of research studies [2-5] that address the problem of Grid task scheduling and allocation for computation intensive Grid requests. In data-intensive Grid requests, most of the Grid tasks require and process huge amounts of data, which may require the transfer of data from different data storage locations. Most existing approaches applied for computation intensive Grid requests perform poorly on data-intensive requests where the bulk of the execution time is spent on retrieving and transferring data. Data-intensive applications, such as simulations for weather, geological, astrophysics and human genome computation, access and process huge amounts of data

and sometimes may require little computation. In this case, the efficient distribution of computation resources has an insignificant impact on the overall execution time of the application. To process efficiently such Grid requests, Grid resources and optical network resources need to be reserved and scheduled in advance. The problem of Grid task scheduling and allocation for data-intensive Grid requests has been addressed in [6-9].

5.1.2 Resource Centric vs. Application Centric

There are two major parties when considering Grid computing service communities: 1) Grid resource users who send Grid application requests, and 2) Grid resource providers who provide and share their resources. These two parties usually have different goals and objectives. Grid users are concerned with the performance of Grid services or the performance of their applications, such as speed and response time of the application when it runs on the Grid. On the other hand, Grid resource providers are usually concerned about the cost and the performance of their resources. Therefore, the objectives of Grid resource allocation and scheduling can be divided into two groups: application-centric and resource-centric [10]. Application-centric objectives focus on the performance of each individual Grid application, and are mostly time related, such as the minimizing the schedule length of a Grid application, which is total period of time that the application spends on the Grid. Resource-centric objectives aim to optimize the performance of the shared resources, and are mostly related to resource utilization, such as maximizing Grid throughput, minimizing Grid resource utilization, and minimizing blocking probability of a Grid application request.

For application-centric objective, most of the previous studies focus on minimizing the completion time of Grid requests. The general scheduling problem of minimizing task completion time is NP-hard [11]. Heuristic approaches [1, 8, 12-14] have been proposed to address this problem. The work in [1] proposed Extended List Scheduling (ELS) to schedule Grid resources and network resources in a joint manner to minimize the completion time of a Grid request. ELS sorts all Grid task based on the priority of each task in the list, where the priority of each task is assigned based on task ordering techniques. Then, ELS reserves and schedules resources for each task one-by-one based on the sorted list. The work in [12] further improves the performance of ELS by modifying the scheduling order to search for better solutions. The work in [13] modifies ELS to reserve and schedule resources for a Grid request with pipelined tasks. In [8], the authors propose an ELS algorithm with a hop bytes metric based Grid resource selection scheme to reduce optical link resource contention in order to improve the static Grid request completion time.

For resource-centric objective, most works focus on minimizing Grid request blocking probability. The work in [13] proposed heuristic approaches to improve the algorithm scalability over an ILP. In [14], the authors proposed a heuristic based on the adaptive penalty function to minimize resource cost for a single static Grid request. The works in [14-15] proposed heuristic algorithms to reduce resource reservation time conflict.

5.1.3 Real-time Performance vs. Availability

A Grid task may have tight real-time requirements that the computation should be

finished before a given deadline. Running real-time Grid tasks in an optical Grid system, which is a heterogeneous and complex optical network, is susceptible to a wide range of failures as revealed by a recent survey [16]. If an unexpected fault happens, the task will be interrupted and re-executed until the fault disappears. The completion time may then become very large and the task may fail to finish on time. Therefore, using an effective fault-tolerant scheduling in the optical Grid is essential for real-time Grid tasks.

Using a fault-tolerant scheme (e.g., a protection scheme), however, generally consumes more optical network resources for backup lightpaths and induces longer completion time, which might violate the task deadline. The conflicting requirements of good real-time performance imposed by the Grid tasks and of high QoS in a reliable optical network, introduce a new challenge for joint task scheduling schemes. Note that in this work, the terms application and job are used interchangeably.

5.2 Availability-Driven Scheduling with Lightpath Protection

In the section, a fault-tolerant scheduling problem for Grid applications with deadline requirement is considered in optical Grids. This problem is NP-complete because the conventional Grid scheduling without any fault tolerance is a well-known NP-complete problem [1, 12, 17]. Hence, we design and evaluate a heuristic Availability-Driven Scheduling (ADS) scheme for real-time Grid applications. We focus only on optical link failures since network nodes (e.g., Optical Cross-Connect (OXC) or amplifier) are usually much more reliable than links [18-19]. We assume that a 1+1 dedicated path

protection (DPP) is available for communication tasks in Grid applications. For a real-time Grid application, the proposed ADS scheme first verifies whether the deadline can be met without any availability improvement. If so, the ADS scheme iteratively enhances the application availability level in a cost-effective way under the condition that the availability enhancement does not result in the deadline violation; otherwise, the Grid application is dropped, because its execution is infeasible. The simulation results show that compared with other Grid scheduling schemes, the proposed ADS scheme can provide better performances in terms of availability and network resource utilization, while satisfying given deadline.

5.2.1 DAG Application Model

A Grid application generally consists of tens, hundreds, or even thousands of inter-dependent computation tasks and communication tasks, which are modeled by directed acyclic graphs (DAGs). Each DAG application is formulated as $J=(V,E,d)$, where $V=\{v_1,v_2,...,v_n\}$ represents a set of inter-dependent real-time computation tasks, E is a set of weighted and directed edges used to represent communication tasks among computation tasks, and d is the DAG application's deadline. Each computation task v_i is characterized by a parameter $c(v_i)$, which denotes the amount of data to be processed. The weight on each edge e denotes the volume of data to be transmitted, which is also called as the communication task cost $c(e)$. Each computation task can be scheduled to an available Grid computing resource for data process. Each communication task can be

scheduled to a lightpath for data transfer. Thus joint (computation and communication) task scheduling is an important issue in making cost-effective utilization of optical network and Grid resources.

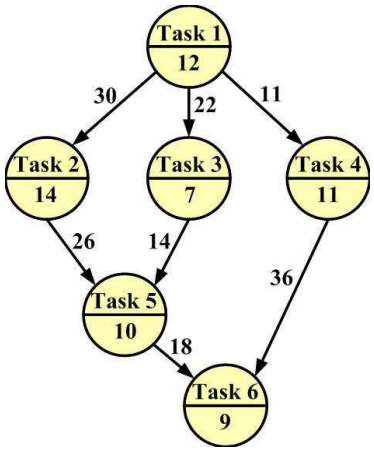

Fig. 5.1 Illustration of a DAG application

Fig. 5.1 shows an example DAG where each node is assigned an average execution cost, and each edge is assigned a weight. In the DAG, all executed tasks must satisfy task precedence constraints: 1) each computation task can be processed only after all its predecessors have finished and all the data needed have been transferred; 2) each communication task can start only after that the predecessor computation task is completely finished.

5.2.2 Optical Grid System Model

The optical Grid system shown in Fig. 5.2 includes some Grid computing resources, such as supercomputers, clusters, storages and visualization devices, which are connected by an optical network with OXC nodes and optical links. Each optical link contains several wavelength channels. Each Grid resource is attached to one OXC node via a

dedicated access link. We model the optical Grid system as a graph $G_{ON} = (S, L, w, G)$, where S is a set of optical switch nodes (i.e. OXC), L is a set of optical links, w is the number of available wavelengths in each optical link, and G is the set of all Grid computing resources connected by the optical network. We assume that each optical switch is equipped with all-wavelength converters, and thus there is not any wavelength continuity constraint with the lightpath routing.

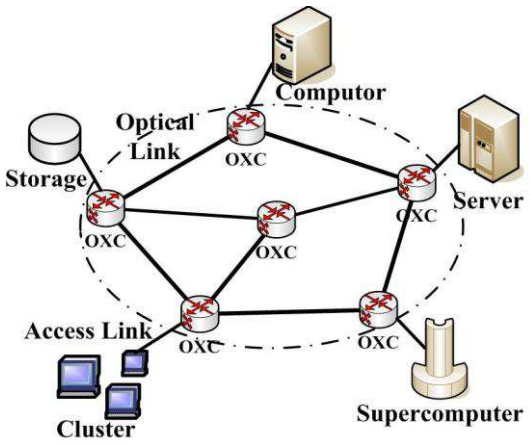

Fig. 5.2 Optical Grid system model

5.2.3 DAG Scheduling and Constraints

The DAG scheduling algorithm must satisfy the following constraints:

1) Grid computing resource constraint, which ensures that the computation tasks assigned to the same Grid computing node should not be processed at the same time;
2) Network resource constraint, which ensures that communication tasks with a same wavelength on a common physical link should not be transferred at the same time.

The objective of the DAG scheduling considered is to maximize the application availability level without violating the real-time requirement and precedence constraint of

the DAG applications. For purpose of simplicity, we only employ the "end" technique [1] in scheduling, which means that the scheduler can only schedule a task starting from time t on the corresponding (network or Grid) resources which are free in $[t,\infty]$.

To improve the DAG application availability, a 1+1 Dedicated Path Protection (DPP) scheme is available and some communication tasks may have two copies, called primary copy e^P and backup copy e^B, transferred simultaneously on two link-disjoint lightpaths in optical networks. There are two important parameters to be derived:

1) $t_{ea}(v)$ is the earliest available time for the computation task v; this indicates the time when all data from v's predecessors have arrived;

2) $t_{es}(v)$ is the earliest start time for the computation task v; this additionally signifies that the Grid computing resource node $g(v)$ is available to start the task execution.

Thus, $t_{es}(v) \geq t_{ea}(v)$. And at time $t_{ea}(v)$, the Grid computing node $g(v)$ may not be ready to execute task v.

In what follows, we derive the expressions of those time parameters for the DAG scheduling. We first consider a scheduling computation task v_i with one direct predecessor task v_j. Let $f(v_j)$ be the finish time of v_j, $t_{es}(e_{ji})$ the earliest start time of communication task e_{ji}, $c(e_{ji})$ the transmitted data volume, BW the lightpath bandwidth, and $c(e_{ji})/BW$ is the transmission time for communication task e_{ji}. The

earliest available time $t_{ea}^{k,v_j}(v_i)$ of the computation task v_i on the k^{th} Grid computing resource node of the same type as the computation task is given by the following expression:

$$t_{ea}^{k,v_j}(v_i)=\begin{cases} f(v_j), & \text{if } g(v_i)=g(v_j) \\ t_{es}(e_{ji})+c(e_{ji})/BW, & \text{otherwise} \end{cases} \tag{5.1}$$

where $g(v_i)$ is the computing node of task v_i, $t_{es}(e_{ji})$ depends on how the communication task e_{ji} is scheduled on the paths. If the communication task e_{ji} is just assigned to one lightpath without any protection measure, which is referred as Case1, the earliest start time of communication task e_{ji} is given by:

$$\text{Case1: } t_{es}(e_{ji})=\max\left\{t_{ea}\left(lp(e_{ji})\right), f(v_j)\right\} \tag{5.2}$$

$t_{ea}\left(lp(e_{ji})\right)$ is the earliest available time of the lightpath $lp(e_{ji})$ from $g(v_j)$ to $g(v_i)$. However, the communication task e_{ji} cannot be executed when a link failure occurs in the lightpath $lp(e_{ji})$.

With the 1+1 DPP scheme, a communication task e_{ji} is provisioned by a primary lightpath $lp(e_{ji}^P)$ and a link-disjoint backup lightpath $lp(e_{ji}^B)$. According to the task precedence constraints, the computation task v_i then must also wait for the data transmission on the backup lightpath to complete. This case is referred as Case2 and one has the following expression:

$$\text{Case2: } t_{es}(e_{ji})=\max\left\{t_{ea}\left(lp(e_{ji}^P)\right), t_{ea}\left(lp(e_{ji}^B)\right), f(v_j)\right\} \tag{5.3}$$

In this case, no further operations are required when a link fails (assuming link failures are rare events such that there can be at most one failure during one communication).

We now consider the case of scheduling task v_i with all its direct predecessors. Task v_i must wait until the last data needed from all its predecessors has arrived. Hence, the earliest available time of v_i on the k^{th} Grid computing resource node is the maximum of $t_{ea}^{k,v_j}(v_i)$ over all its predecessors:

$$t_{ea}^{k}(v_i) = \max_{e_{ji} \in E} \left\{ t_{ea}^{k,v_j}(v_i) \right\} \tag{5.4}$$

With Eq. 5.4, we can obtain the earliest start time $t_{es}^{k}(v_i)$ on the k^{th} Grid computing resource node $g_k^r \in G$ of type r by checking if the node is idle since from time $t_{ea}^{k}(v_i)$. The value $t_{es}^{k}(v_i)$ is in turn used to derive $t_{es}(v_i)$, which is the earliest start time for the task on any computing resource node of type r. The $t_{es}(v_i)$ is given as follows:

$$t_{es}(v_i) = \min_{g_k^r \in G} \left\{ t_{es}^{k}(v_i) \right\} \tag{5.5}$$

Consequently, the finish time of the computation task v_i is obtained as follows:

$$f(v_i) = t_{es}(v_i) + c(v_i)/p \tag{5.6}$$

where $c(v_i)$ is the amount of processed data of the computation task v_i, p is the data processing capability of the Grid computing resource node assigned for the computation task v_i. We assume that each Grid computing resource node has (the same) one unit data processing capability $(p = 1)$.

5.2.4 Availability Model and Scheduling Objective

We only focus on link failure scenarios and adopt the 1+1 DPP scheme to improve the availability of real-time DAG applications. We assume that different network links fail independently; for any single link, the normal operating times and repair times are independent processes with known mean values (Mean Time to Failure (MTTF) and Mean Time to Repair (MTTR)). The link availability is calculated as follows [19]:

$$a_j = \frac{MTTF}{MTTF + MTTR} \tag{5.7}$$

In the case of no path protection (NPP), the overall lightpath availability is the product of all the availabilities of the links along lightpath P. For the 1+1 dedicate path protection (DPP), the availability of a communication task e is computed as:

$$A_e = \begin{cases} \prod_{j \in P} a_j, & \text{NPP} \\ A_p + \left(1 - A_p\right) \times A_b, & \text{DPP} \end{cases} \tag{5.8}$$

where A_p is the primary lightpath availability and A_b is the backup lightpath availability.

Our scheduling algorithm aims at maximizing the entire DAG application availability without violating the DAG's deadline. The proposed ADS scheme has to measure the availability benefit gained by an application. We model the availability benefit as an availability-level function denoted by $AL\left(DAG\right): A_e \to \Re$, where $\Re$ is the summation of the following set of real numbers:

$$AL\left(DAG\right) = \sum_{e \in E} w_e A_e \tag{5.9}$$

In Eq. 5.9, w_e is the weight of a communication task $e \in E$ and one has $\sum_{e \in E} w_e = 1$.

w_e is chosen as the ratio of the communication task cost $c(e)$ of the edge e over the sum of all communication task costs of a DAG application. Thus, we define an optimization formulation to maximize an availability benefit of a real-time DAG application, while assuring that the scheduling length SL (also called as completion time) satisfies a deadline d constraint:

$$\text{Maximize } AL(DAG) = \sum_{e \in E} w_e A_e \tag{5.10}$$

$$\text{Subject to}: SL(DAG) \le d \tag{5.11}$$

5.2.5 Availability-Driven Scheduling scheme

The ADS algorithm outlined in Fig. 5.3 aims at achieving a higher availability under the two following constraints: 1) increase the availability level without any deadline violation and 2) satisfy the task precedence constraints. In other words, this algorithm tries to iteratively enhance the DAG availability in a cost-effective way under some given real-time requirements.

Initially, the ADS algorithm sorts all the computation tasks in a list according to some priority schemes at step 1. For example, a bottom-level priority is adopted to calculate the bottom level $BL(v_m)$ of each computation task v_m, which is the length of the longest path from node v_m to a sink task v_s, including the communication cost $c(e_{mn})$. The sink node has no any successor (i.e. $\boldsymbol{SUC}(v_s) = \varnothing$) in the DAG. The set of all direct successors of node v_m is denoted by $\boldsymbol{SUC}(v_m)$. It can be calculated recursively by [20]:

$$BL(v_m) = c(v_m) + \underset{v_n \in \mathbf{SUC}(v_m)}{Max} \left[BL(v_n) + c(e_{mn}) \right] \tag{5.12}$$

Input : A Real-Time DAG, Deadline = d, an Optical Grid G_{ON}
Output : Schedule Length SL and Availability Level AL
01. Sort the computing tasks $v \in V$ in a list by one sorting policy
02. Calculate a tentative finish time F_{NPP} without any availability improvement considerations
03. **If** $(d \geq F_{NPP})$
04. Calculate a tentative finish time F_{DPP} with each communication task $e \in E$ to be protected
05. **Else Return** $(FAIL)$
06. **If** $(d < F_{DPP})$
07. Initiation finish time $F_{ADS} \leftarrow F_{NPP}$
08. **While** ($F_{ADS} < d$ **and** $\exists e \in E$ not protected) **do**
09. **For** ($e \in E$ **and** e not protected)
10. Compute $\theta_e = \dfrac{w_e * \left(A_e^{DPP} - A_e^{NPP} \right)}{\left(H\left(p_e^{DPP} \right) + H\left(b_e^{DPP} \right) - H\left(p_e^{NPP} \right) \right)}$
11. **End For**
12. Selecte e subject to $\text{Max}(\theta_e)$ and add e to $E^{ADS} \subseteq E$
13. Update the finish time F_{ADS} with set E^{ADS}
14. **End While**
15. Schedule DAG in optical grids with set E^{ADS}
16. **Else** Schedule DAG in optical grids with each communication task $e \in E$ to be protected
17. **Return**$(SL$ and $AL)$

Fig. 5.3 Availability-Driven Scheduling (ADS) algorithm

Before maximizing the availability level of a job, the ADS scheme first verifies whether the feasible schedule is available, just satisfying the deadline and precedence constraints; this can be accomplished by calculating a tentative finish time F_{NPP} without any availability enhancement at step 2. The finish time F_{NPP} is obtained from the conventional DAG scheduling with no path protection (NPP) consideration [1, 12, 17],

which is coherent with Case 1 of the DAG scheduling model. More specifically, an unscheduled task with the highest bottom level value is selected from the above priority list and is allocated to a type-compatible Grid resource node so that it can complete as soon as possible. The optimal resource node on which the task has is allocated with the earliest start time can be found using an exhaustive search among all the resource nodes. Until all tasks are scheduled in optical Grid, the schedule length is given out as the result of tentative finish time F_{NPP}.

If the deadline requirement is met (step 3), that is, the finish time F_{NPP} is within the deadline, we further obtain another tentative finish time F_{DPP} with each communication task $e \in E$ to be protected (step 4); otherwise, the DAG job is rejected because of its infeasible schedule (step 5).

It is noted that the tentative finish time F_{DPP} is calculated in a similar way the F_{NPP} is computed. The main difference lies in that with 1+1 DPP scheme, all communication tasks are protected by a primary lightpath and a link-disjoint backup lightpath. The two primary-backup lightpaths are established simultaneously in optical Grid and are all available in the same duration. Therefore, the Grid resource node which has the earliest finish time of data transmission on both primary and backup lightpaths will be chosen to execute the successor computation task. The earliest start time $t_{es}\left(e_{ji}\right)$ of communication task is expressed just as Eq. (5.3) in the Case 2 of the DAG scheduling model.

The relation between the tentative finish time F_{DPP} and the DAG deadline d is the key for invocating or not the iterative optimization process. If the finish time F_{DPP} is

also smaller than the deadline d, step 16 executes the DAG scheduling with each communication task $e \in E$ to be protected; otherwise, one will improve the DAG application availability level in an iterative way (from step 7 to 13).

To improve the DAG availability in a cost-effective way, the ADS scheme chooses the most appropriate communication task e to be protected during each while-iteration starting at step 8. Specifically, it gives a higher priority to a communication task e with a higher weight that brings a larger availability gain and consumes lower network link resources. Hence, we define the following benefit-cost ratio function θ_e, which measures the increase of availability level with the increase of occupied link resources:

$$\theta_e = \frac{w_e \Delta A_e}{\Delta H(p)} = \frac{w_e * \left(A_e^{DPP} - A_e^{NPP}\right)}{\left(H\left(p_e^{DPP}\right) + H\left(b_e^{DPP}\right) - H\left(p_e^{NPP}\right)\right)} \tag{5.13}$$

In Eq. 5.13, the numerator represents the weighted enhancement of the availability level, A_e^{DPP} and A_e^{NPP} denote the availability of communication task e in the respective case of DPP and NPP, whereas the denominator indicates the consumed link resources, $H\left(p_e^{DPP}\right)$ and $H\left(b_e^{DPP}\right)$ being the hop count along the primary path and the backup path for the communication task e in the case of DPP scheme.

At step 7, the finish time F_{ADS} is initiated to be F_{NPP}. Under the condition that the finish time F_{ADS} does not violate the DAG deadline, for each unprotected communication task $e \in E$, the ADS scheme identifies the best candidate that has the highest benefit-cost ratio $Max(\theta_e)$, and adds it into the set $E^{ADS} \subseteq E$ (steps 9 to 12). Step 13 updates the finish time F_{ADS} with the set E^{ADS}. Thus, the DAG application

availability is enhanced by additionally protecting a communication task e with the highest benefit-cost ratio. The while-iteration process continues until that the finish time F_{ADS} is larger than the deadline d or that all communication tasks are protected. In practice, step 15 executes the DAG schedule in optical Grids with the final communication-task-protection set E^{ADS}. Finally, we obtain the schedule length SL and the application availability level AL of the submitted DAG job.

5.2.6 Simulation Results and Analyses

To examine the performance of the ADS algorithm, we developed a Java-based simulator and compared our scheme with two other heuristic algorithms: ELS_NPP and ELS_DPP. The former uses an Extending List Scheduling (ELS) scheme [1] with No Path Protection (NPP) consideration; ELS is a greedy algorithm used for the conventional DAG scheduling without any availability improvement. The latter provides primary and backup paths for each communication task e to improve the DAG application availability. We believe that comparing the ADS scheme with these two scheduling algorithms is meaningful; the superiority of our scheme will be clearly noticed.

Table. 5.1 Reference System Parameters

Parameters	Reference value
CCR (Communication Computation Ratio)	6,7,8,9
Number of computing tasks in a DAG	100
Mean value of computation task cost	10, (from 6 to 14)
Mean number of edges per node	4
MTTR (Mean Time To Repair)	24h
1/MTTF (Mean Time To Failure)	300 FIT/km

The communication computation ratio (CCR) of a randomly generated DAG is defined as the sum of all the communication task costs divided by the sum of all the computation task costs in a DAG. Table 5.1 summarizes the key system parameters in our simulations. The CCR value in the simulations is chosen as one integer ranging from 6 to 9 and the number of computation tasks is set to 100. The computation task costs per node in a DAG are selected uniformly from 6 to 14 around the mean value 10. The communication task costs are also taken from a uniform distribution, whose mean value depends on the CCR value and on the mean value of computation task cost. The mean number of edge per node is assumed to be 4.

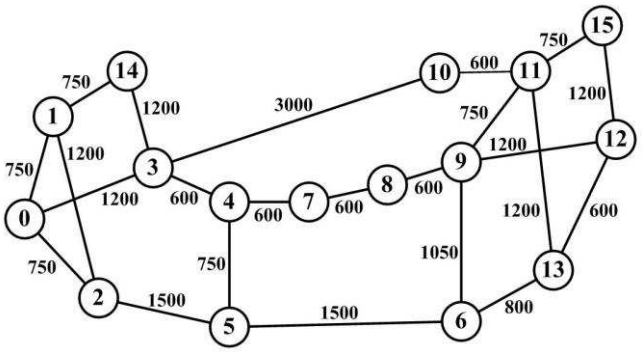

Fig. 5.4 16-node NSFNET topology

The 16-node NSFNET used in the simulations is shown in Fig. 5.4. The labels on the links are the lengths of the links in kilometers. Another used network topology is a 16-node ring network and the link length between two adjacent nodes is set to be 100 kilometers. In this simulation, the MTTR is assumed to be 24 hours and 1/MTTF is 300 FIT/km for the above networks (1 FIT = 1 failure in 10^9 hours) [19]. We assume that each optical switch is equipped with all-wavelength converters and has only one Grid

computing resource connected, which has one unit data processing capability. It is assumed that all the computation tasks and Grid computing resources are of three different types. For each case, each scheduling result is the average over 10 simulations.

The performance metrics to evaluate the system performance in our simulations include the following:

1) Availability. It is the primary optimal objective (see Eq. 5.10 and Eq. 5.11).
2) Communication Task Protection Ratio (CTPR). This is the ratio of the number of protected communication tasks $\left|E^{ADS}\right|$ ($E^{ADS} \subseteq E$) over the number of all the communication task number $\left|E\right|$ in a DAG. Thus, the CTPR for an application DAG is calculated as follows:

$$CTPR\left(DAG\right) = \frac{\left|E^{ADS}\right|}{\left|E\right|} \tag{5.14}$$

3) Network Resource Utilization (NRU). It is defined as the ratio of the total occupied bandwidths over the total supplied bandwidths of all the involved wavelengths and optical link resources during the whole scheduling period.

$$NRU = \frac{\sum_{e_i \in E} \sum_{l \in P(e_i)} BW\left(\lambda_l\left(e_i\right)\right) \times \left[ET\left(e_i\right) - ST\left(e_i\right)\right]}{\sum_{all\ invovled\ l\ \text{and}\ \lambda} BW\left(\lambda_l\right) \times SL} \tag{5.15}$$

In Eq. 5.15, $P\left(e_i\right)$ represents one or two (primary and backup) path(s) provisioned for the communication task e_i. $BW\left(\lambda_l\left(e_i\right)\right)$ is the bandwidth of the occupied wavelength λ_l on optical link l for the communication task e_i; the end time and

start time of communication task e_i are denoted as $ET(e_i)$ and $ST(e_i)$, respectively. SL is the total scheduling length of the whole DAG application.

4) Job Complete Time. This is the job completion time for all the tasks in a DAG. It is also called as scheduling length SL of a DAG application.

5.2.6.1. Impacts of Different Network Resource Scenarios

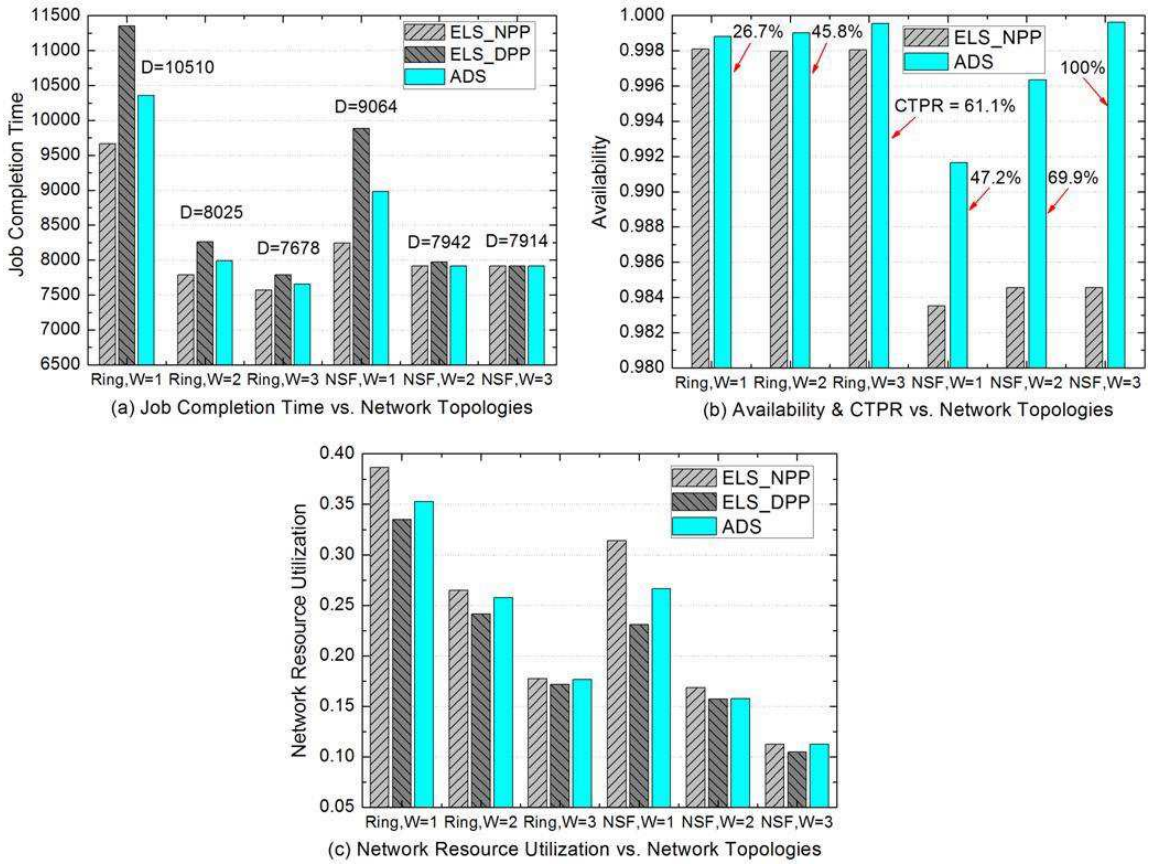

Fig. 5.5 Performance impacts of network topologies and available wavelength resources

We choose two different network topologies: the 16-node Ring network and the 16-node NSFNET with three possible wavelength numbers ($W = 1, 2$ *or* 3). The CCR is set to be equal to 8. For each network scenario, the deadline value for the ADS scheme is

denoted as the character D in Fig. 5.5 (a) and is the average of the job completion time of the ELS_NPP and the ELS_DPP schemes: $D = \frac{(F_{NPP} + F_{DPP})}{2}$.

Fig. 5.5 (a) depicts the Job Completion Time of a DAG application versus network topologies under the three different DAG scheduling schemes. The different network topologies and different available wavelength values represent different amount of available network resources. We observe that the DAG completion time becomes shorter as the available wavelength resource increases from 1 to 3 for both the ELS_NPP and the ELS_DPP schemes. That is because more independent tasks in a DAG application can be executed concurrently when more network resources are available. When the available wavelength number is larger than 3, the two scheduling schemes (ELS_NPP and ELS_DPP) have almost the same job completion time. This is due to the fact that more network resources are available for backup lightpaths and the DAG applications' precedence constraints become dominant when the available network resources are sufficient. We also observe that the completion time with the ADS scheme is smaller than the protected ELS_DPP scheme (but larger than the non-protected ELS_NPP scheme), and that it remains within the deadline constraints, leading to a feasible scheme.

Fig. 5.5 (b) only shows the availability performance for the ELS_NPP and ADS schemes. The ELS_DPP scheme usually has higher application availability (10^{-5} unavailability for the ring network and 10^{-3} unavailability for the NSFNET). It is noted that the ADS scheme significantly enhances the DAG availability at the cost of longer job completion time compared with the ELS_NPP scheme (see Fig. 5.5 (a)) and this is

especially prominent with the NSFNET. This is because the ELS_NPP scheme simply shows the baseline performance due to its conservative nature without trying to improve the DAG availability. For the ELS_NPP scheme, we find that a DAG application can obtain a higher availability with the Ring network scenario than with the NSFNET scenario. This is mainly attributed to the shorter optical link length (100km for each link) and the higher optical link availability of the Ring network. The percentage values indicated with red arrows in Fig. 5.5 (b) are the CTPR. We find that the larger the CTPR value, the more remarkable the availability performance improvement. The higher CTPR values usually occur when the ELS_NPP and ELS_DPP schemes have similar completion time. It indicates that more communication tasks are protected in DAG scheduling.

From Fig. 5.5 (c), we observe that the network resource utilization has the same diminishing trend as the job completion time when the number of available wavelengths per optical link increases. More available network resources alleviate the network link resource contentions and shorten the completion time; on the other hand, the inherent precedence constraints of the DAG application become increasingly a dominant feature, which keeps more involved network resources idle during most of the execution period of a DAG application. For each network scenario, the ELS_NPP scheme achieves the highest network resource utilization and the ELS_DPP scheme has the lowest utilization. This also indicates that more protected communication tasks implies lower network resource utilization. The reason is that ELS_DPP scheme consumes double network resources for each communication task compared to the ELS_NPP scheme, which in turn

reduces the number of independent tasks to be executed concurrently and results in more spare time of involved network resources.

5.2.6.2. Impact of the Communication-Computation Ratio (CCR)

The simulations are carried out over the NSFNET with one available wavelength, but similar conclusions can be made with other network topologies.

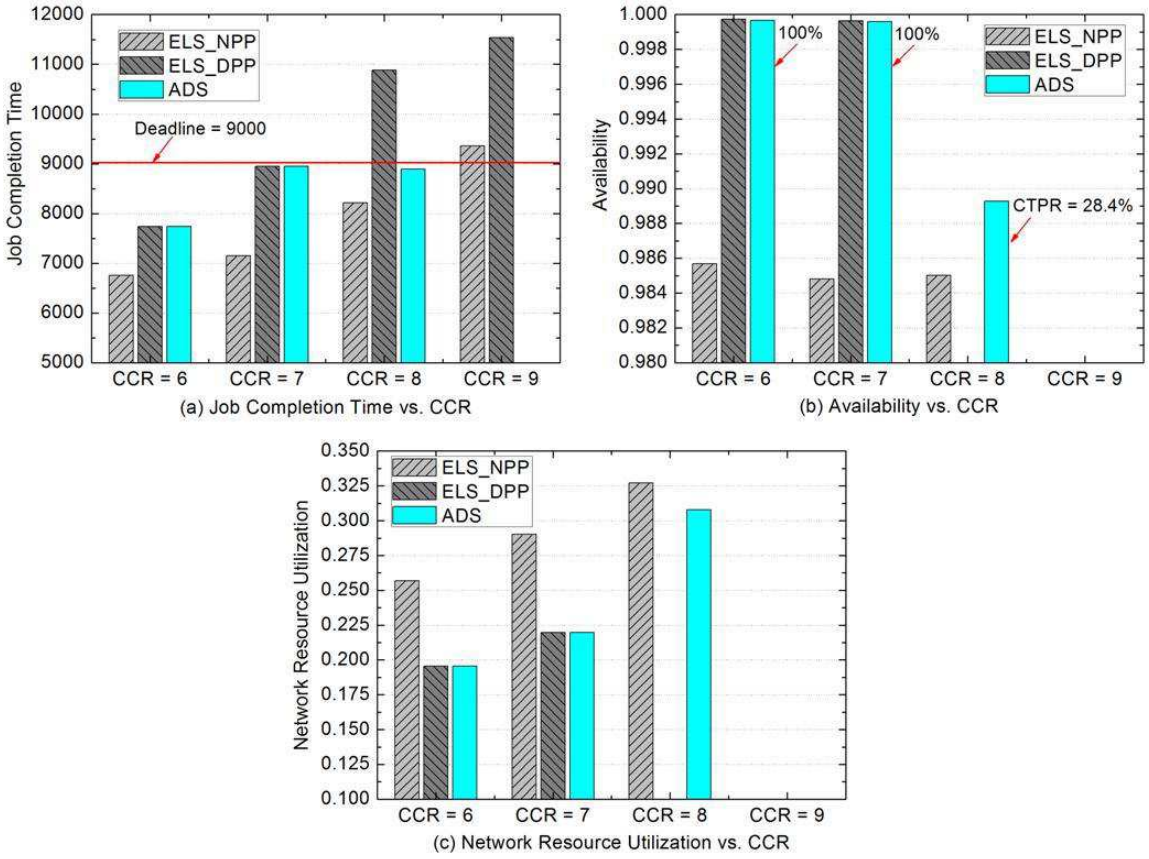

Fig. 5.6 Performance impact of the CCR

The DAG application deadline is set to 9000 as shown in Fig. 5.6 (a). As the CCR is increasing from 6 to 9, the job completion time for both the ELS_NPP and ELS_DPP schemes becomes larger, because the communication task sizes of a DAG application are also increasing. The ADS scheme always generates feasible scheduling results within the

deadline as long as the ELS_NPP scheme is also feasible. When the CCR is equal to 9, the job completion time of both the ELS_NPP and the ELS_DPP schemes exceed the deadline. Hence the ADS scheme could not generate a feasible schedule and the corresponding position is left blank. Similarly, when any of the three scheduling schemes was not able to generate feasible scheduling results satisfying the DAG deadline requirement, the space is left blank in Fig. 5.6 (b) and Fig. 5.6 (c).

In Fig. 5.6 (b), the percentage values indicate the CTPR. We observe that the ADS scheme obtains the best availability performance, and even a 100% CTPR, like the ELS_DPP scheme, in the case of a CCR equal to 6 or 7. This is because the deadline constraint is relatively loose and there is enough time used to protect all communication tasks in a DAG. When the CCR is set to 8, the ADS scheme partly protects 28.4% of the communication tasks in a DAG and enhances the availability under the deadline constraints, contrarily to the ELS_NPP scheme.

Fig. 5.6 (c) plots the network resource utilization of the different scheduling schemes for various CCR values. We can see that the ELS_NPP scheme has the best performance among the three scheduling schemes in each situation. The reason for this is exactly the same as already observed in Fig. 5.5 (c). We can also notice that the network resource utilization of each scheme increases as the CCR value increases. This can be explained as follows: as the load of communication task is heavier when the CCR value increases, consequently, the occupied duration of network (link) resources and the whole DAG's scheduling length (job completion time) are similarly increased by the same amount of

time. According to the definition of the network resource utilization (see Eq. 5.15), the utilization ratio becomes higher and higher as the CCR increases.

5.2.6.3. Impact of the Application Deadline

The simulations are carried out over the NSFNET with one available wavelength. The CCR is equal to 8. In this context, the value of the deadline is between that of the job completion times of the ELS_NPP scheme and of the ELS_DPP scheme, and this facilitates the study the deadline variation impact on the ADS scheme. For a tested DAG application with 100 computation tasks, the job complete time is respectively equal to 8228 for the ELS_NPP scheme, and equal to 10023 for the ELS_DPP scheme. The DAG application deadline for the ADS scheme varies from 8000 to 10400.

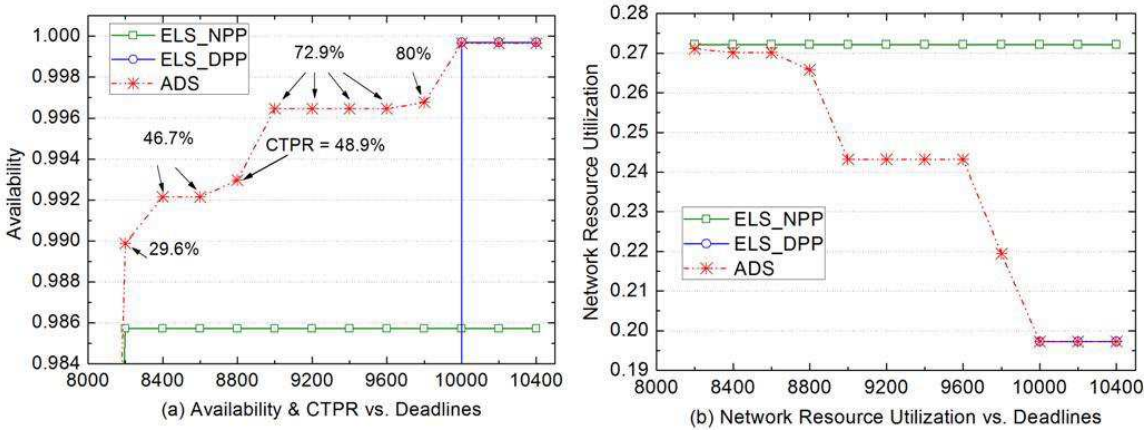

Fig. 5.7 Performance impact of the DAG application deadline

The ADS scheme fully exhibits its better performance over the ELS_NPP scheme, and the ELS_DPP scheme is not even able to produce feasible schedule results when the application has a relatively tight deadline in Fig. 5.7 (a). As the deadline becomes looser, the availability and CTPR of the ADS scheme is rising, because more communication

tasks in a DAG can be protected within the looser deadline. When the deadline is larger than 10023, the ELS_DPP scheme can produce feasible schedule results, and even the ADS scheme achieves the same best availability performance as the ELS_DPP scheme.

In Fig. 5.7 (b), when the deadline is about 8200, both the ADS scheme and the ELS_NPP scheme have high network resource utilization (about 27.2%). As the deadline becomes looser, the network resource utilization of the ADS scheme is lower than that of the ELS_NPP scheme and becomes smaller and smaller. When the deadline is larger than 10023, the ADS scheme still achieves with the ELS_DPP scheme the lowest network resource utilization (about 19.8%). This means that the communication task protection consumes more network resources, which in turn reduces the number of independent tasks to be executed concurrently, thus resulting in lower network resource utilization.

These simulation results clearly demonstrate that the optical Grid system can even gain more performance benefits with our ADS scheme when the real-time DAG applications have relatively tight deadline requirements. This is because the ADS scheme is self-adaptive compared to the ELS_NPP and ELS_DPP schemes which have no flexibility on the job deadline requirements.

5.3 Fault-Tolerant Scheduling with Grid Resource Protection

In the above section, we focus only on optical link failures for the DAG scheduling and assume that Grid resource nodes are usually very reliable. Actually, DAG applications running in optical Grid system are also fragile as a wide range of grid resource failures,

which include hardware failures (e.g., host crash), software errors (e.g., immature middleware), and other failure sources (e.g., machine removed by the owner) [21]. However, the issue of handling grid resource failures in optical grids has not been studied although they are very critical.

In the section, we propose a Grid Resource Protection (GRP) scheme for scheduling DAG application, in which a primary-backup approach is used to allocate simultaneously two copies of each computation task to two different Grid resources for data process. The DAG's availability model is constructed to measure availability benefit gained by the proposed GRP scheme. The simulation results show that the ELS_GRP algorithm improves greatly DAG availability and induces less the overhead in scheduling length when the more network resources are available.

5.3.1 GRP Scheme

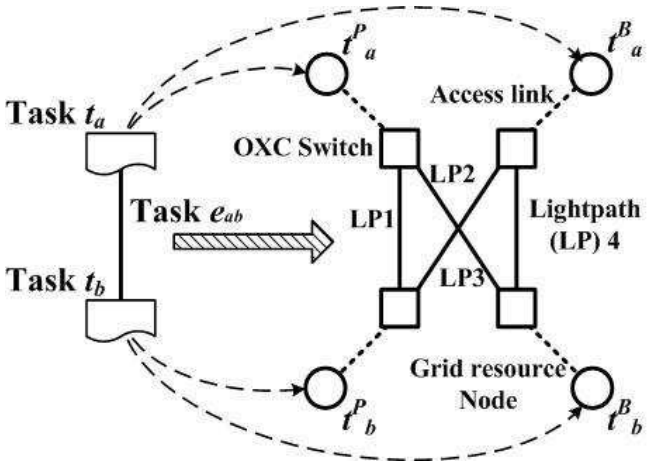

Fig. 5.8 Primary-backup approach applied for each computing task

To improve DAG application availability, a primary-backup approach is illustrated in

Fig. 5.8 and each computing task t has two copies, t^P and t^B, executed simultaneously on two different Grid resource nodes ($g\left(t^P\right) \neq g\left(t^B\right)$), so that the communication task as a successor of the computing task may be protected by four lightpaths (LP1 ~ LP4). There are two important parameters: 1) $eat(t)$, which is the earliest available time for task t, and 2) $est(t)$, which is the earliest start time for task t. The former indicates a time when all data from t's predecessors have arrived; the latter additionally signifies that Grid resource node $g(t)$ is available to start execution.

Thus, $est(t) \geq eat(t)$. At time $eat(t)$, node $g(t)$ may not be ready for t to execute.

In what follows, we derive the two value's expressions for DAG scheduling. We first consider scheduling task t_i with one direct predecessor task t_j. The earliest available time $eat_k\left(t_j, t_i\right)$ on the kth Grid resource node is given by the following Eq. 5.16:

$$eat_k\left(t_j, t_i\right) = \begin{cases} f\left(t_j\right), & \text{if both } g\left(t_i^P\right) \text{and } g\left(t_i^B\right) \in \left\{g\left(t_j^P\right), g\left(t_j^B\right)\right\} \\ est\left(e_{ji}\right) + d_{ji}/BW, & \text{otherwise} \end{cases} \tag{5.16}$$

where $f\left(t_j\right)$ is the finish time of t_j, d_{ji} is the transferred data volume of e_{ji}, BW is the network bandwidth, and $\frac{d_{ji}}{BW}$ is the transmission time for e_{ji}.

$est\left(e_{ji}\right)$ depends on how the communication task e_{ji} is scheduled on the links. There are two cases: 1) just one of two Grid resource nodes ($g\left(t_i^P\right)$ and $g\left(t_i^B\right)$) belongs to the set $\left\{g\left(t_j^P\right), g\left(t_j^B\right)\right\}$, which are allocated to predecessor communication task t_j; 2)

both the two Grid resource nodes ($g\left(t_i^P\right)$ and $g\left(t_i^B\right)$) do not belong to the set $\left\{g\left(t_j^P\right), g\left(t_j^B\right)\right\}$. The expression $est\left(e_{ji}\right)$ is given in Eq. 5.17:

$$est\left(e_{ji}\right)=\begin{cases}\max\left\{eat\left(R_{PTi}\right), eat\left(R_{BTi}\right), f\left(t_j\right)\right\}, \\ \qquad\qquad \text{Case-1: if either } g\left(t_i^P\right) \text{or } g\left(t_i^B\right) \in \left\{g\left(t_j^P\right), g\left(t_j^B\right)\right\} \\ \max\left\{eat\left(R_{PTP}\right), eat\left(R_{BTP}\right), eat\left(R_{PTB}\right), eat\left(R_{BTB}\right), f\left(t_j\right)\right\}, \\ \qquad\qquad \text{Case-2: if both } g\left(t_i^P\right) \text{and } g\left(t_i^B\right) \notin \left\{g\left(t_j^P\right), g\left(t_j^B\right)\right\}\end{cases} \tag{5.17}$$

$eat\left(R_{PTi}\right)$, $eat\left(R_{BTi}\right)$ are the earliest available time of the route R_{PTi} from $g\left(t_j^P\right)$ to $g\left(t_i\right)$ and of the R_{BTi} from $g\left(t_j^B\right)$ to $g\left(t_i\right)$, respectively. Similarly, R_{PTP}, R_{BTP}, R_{PTB}, R_{BTB} as shown in Fig. 5.8 are four lightpath routes for communication task e_{ji} when both $g\left(t_i^P\right)$ and $g\left(t_i^B\right)$ are totally not overlaid with $g\left(t_j^P\right)$ and $g\left(t_j^B\right)$.

We now consider the case of scheduling primary and backup of task t_i with all its predecessors. Task t_i must wait until the last data needed from all its predecessors has arrived. Hence, the $eat_k\left(t_i\right)$ is the maximum of $eat_k\left(t_j, t_i\right)$ over all its predecessors:

$$eat_k\left(t_i\right)=\max_{\left(t_j,t_i\right)\in E}\left\{eat_k\left(t_j, t_i\right)\right\} \tag{5.18}$$

With Eq. 5.18 in place, we can obtain the $est_k\left(t_i\right)$ on the kth node by using the end technique [1], which means the scheduler can only schedule a task form time t on the Grid resources that are free in $\left[t, \infty\right]$. $est_k\left(t_i\right)$ is in turn used to derive $est\left(t_i\right)$. The expression for $est\left(t_i\right)$ is given as follows:

$$est(t_i) = \min_{G_k \in G} \{est_k(t_i)\} \tag{5.19}$$

5.3.2 Availability Model and Scheduling Objective

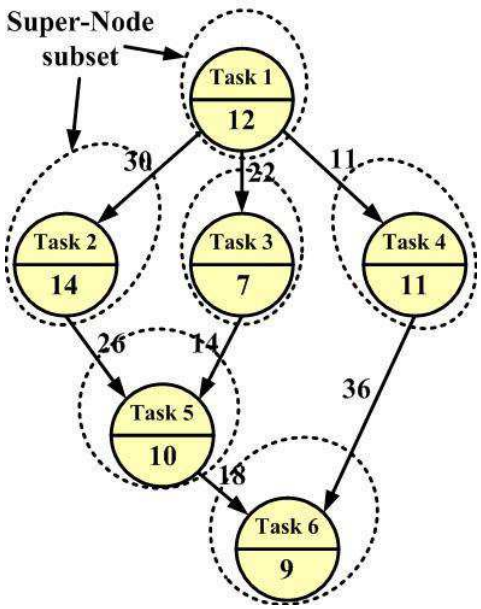

Fig. 5.9 Example for super-node subsets in a DAG application

The GRP scheduling scheme aims at improving the application availability using a primary-backup approach for each computing task. To quantify the availability benefit gained by a DAG application, we partition a DAG into many super-node subsets. Each subset contains both one computing task node and its incoming communication links. The availability of each super-node SuN_i is given by the following expression:

$$AL(SuN_i) = AL(SuN_i^P) + (1 - AL(SuN_i^P)) \times AL(SuN_i^B) \tag{5.20}$$

where $AL(SuN_i^P)$ and $AL(SuN_i^B)$ are the availability level of primary copy and backup copy for each super-node SuN_i, respectively, which are determined by the Eq.

5.21. The superscript * represents either primary copy or backup copy.

$$AL\left(SuN_i^*\right)=\begin{cases} AL\left(t_i^*\right), & \text{if } g\left(t_i^*\right)\in\left\{g\left(t_j^P\right),g\left(t_j^B\right)\right\} \\ AL\left(t_i^*\right)\times\prod AL\left(R_{ji}^*\right), & \text{otherwise} \end{cases} \tag{5.21}$$

In Eq. 5.21, $AL\left(t_i^*\right)$ is the availability of computing task t_i, and the availability of route R_{ji}^* from predecessor node j to node i is computed as the Eq. 5.22, when $g\left(t_i^*\right)\notin\left\{g\left(t_j^P\right),g\left(t_j^B\right)\right\}$ is satisfied.

$$AL\left(R_{ji}^*\right)=AL\left(R_{ji}^{PT*}\right)+\left(1-AL\left(R_{ji}^{PT*}\right)\right)\times AL\left(R_{ji}^{BT*}\right) \tag{5.22}$$

Now, we can define an availability-level function to compute the availability benefit gained by a DAG application, as shown in the Eq. 5.23:

$$AL\left(DAG\right)=\sum_{i=1}^{|E|}\left[w\left(SuN_i\right)\times AL\left(SuN_i\right)\right] \tag{5.23}$$

Note that $w\left(SuN_i\right)$ is the weight of ith super-node, which is chosen as the ratio of the computing cost in task t_i and communication costs in its all ingress links over the total sum of all communication and computing costs in DAG, thus one has $\sum_{i=1}^{|E|}w\left(SuN_i\right)=1$.

5.3.3 Simulation Results and Analysis

In this section, we evaluate the performance of the Extended List Scheduling with Grid Resource Protection (ELS_GRP) scheme for randomly generated DAG applications for different network topologies: 2-node network, 16-node NSFNET (shown in Fig. 5.4) and Mesh Tours (shown in Fig. 5.8). The MTTR is assumed to be 12 hours and 1/MTTF is 300 FIT/km. We assume that each optical switch is equipped with all-wavelength

converters and has only one Grid resource connected, which has one unit data processing capability. The availability of Grid resource at a node level randomly varies from 0.32 up to 0.98 with the larger standard deviation [22]. We assume that the availabilities of two Grid resources in 2-node network are 0.74 and 0.86, respectively.

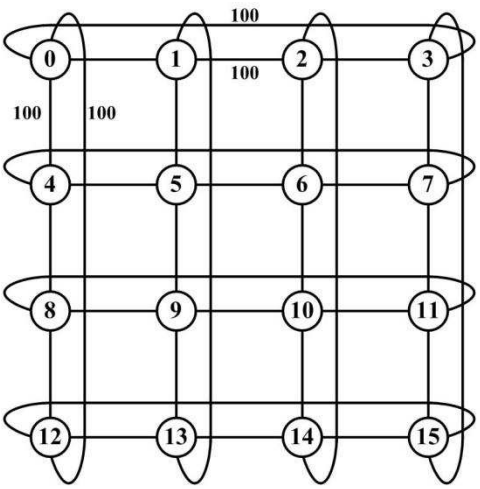

Fig. 5.10 16-node Mesh Tours topology

The CCR value in the simulations is chosen as one integer ranging from 1 to 4 and the number of computation tasks is set to 50, 100, 150 or 200. The computation task costs per node in a DAG are selected uniformly from 6 to 14 centered on 10. The average out degree per node is assumed to be 4.

As we can see in Fig. 5.11 (a) when CCR is 1, the scheduling length (SL) is rising in proportion to DAG size for two scheduling schemes. The SL difference between ELS and ELS_GRP in 2-node network is larger than in 16-node NSFNET as DAG size increases. That is because that more Grid resources are available for allocating two copies of each computing task in NSFNET. We hence conclude that the proposed ELS_GRP scheme

greatly improves the availability of the DAG application at the small price of a larger scheduling time which becomes ignorable when the network resources are sufficient.

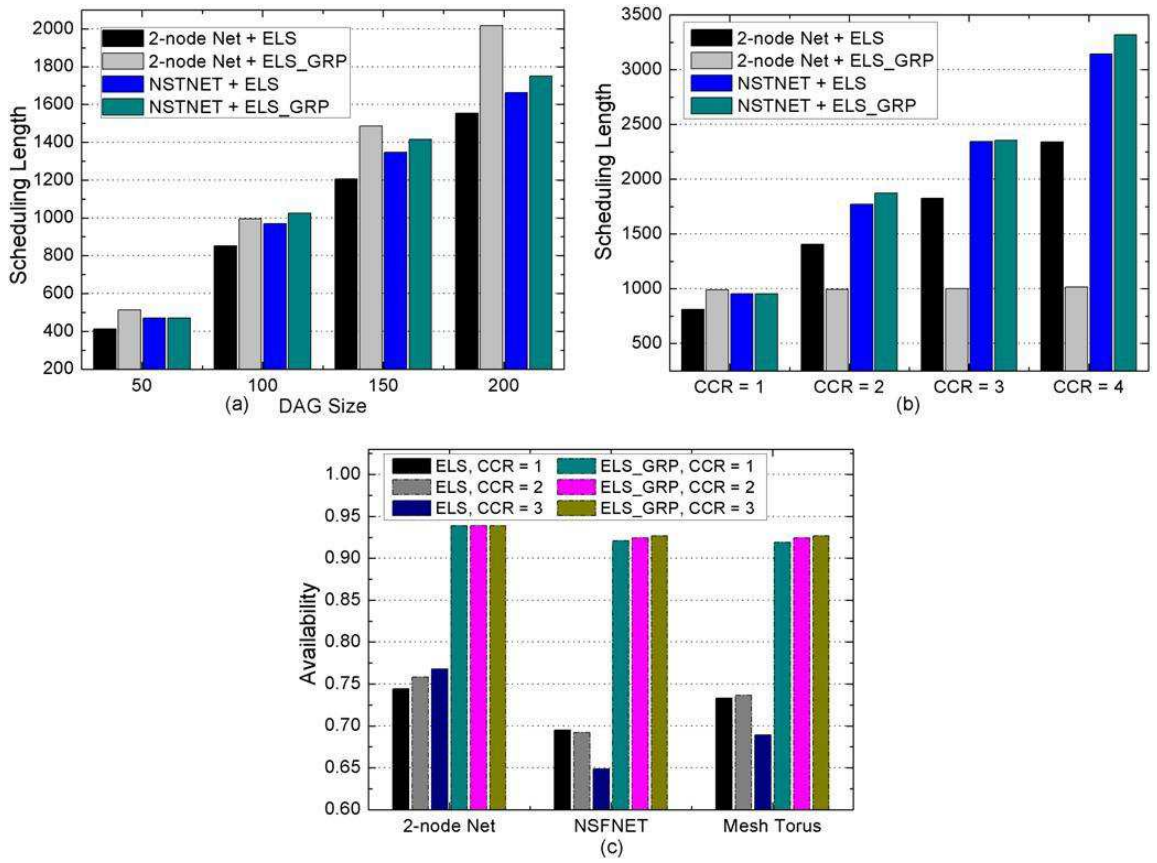

Fig. 5.11 Performances of (a) Scheduling length (SL) versus DAG size, (b) SL versus CCR value, and (c) availability versus different network topologies

Fig. 5.11 (b) depicts the SL with respect to different CCR value when the DAG size is set to 100. As CCR is increasing from 1 to 4, the communication load in a DAG is heavier. The SL increases proportionally for ELS scheme, but it remains identical for ELS_GRP scheme in 2-node network. The reason is that only two Grid resources are served for two copies of each computing task in the same time and there is no

communication task to be executed when the ELS_GRP scheme is applied. We also find that the two schemes have near performance in the scheduling length as CCR value increases in 16-node NSFNET topology. This is due to the fact that the two schemes have no difference in the occupied time for the communication tasks when the network resources are sufficient. Thus, the CCR variation has no impact on the SL of DAG application with the two scheduling schemes.

However, Fig. 5.11 (c) shows that the ELS_GRP scheme improves greatly DAG availability, because the two copies of each computing task are scheduled in two different Grid resources. For ELS scheme, we observe that the more the available network resources are, the lower the DAG availability becomes in different network topologies. This is due to the fact that the Grid resource's availability is lower generally and the more the Grid resources are involved for a DAG, the lower the availability of the whole DAG application becomes. Another observation is that the impact of CCR variation on the DAG availability for ELS_GRP scheme can be ignored. It is because that the DAG availability improvement comes mainly from the backup technique of the Grid resource rather than form lightpath protection. The lightpath availability for each communication task is higher about 0.95 on the average.

5.4 Conclusions

In this chapter, we presented two fault-tolerant scheduling schemes for optical Grid applications.

1) Fault-tolerant DAG scheduling scheme considering optical link failure scenarios. An extended DAG scheduling model incorporating the communication task protection is developed. The proposed ADS scheme iteratively improves the availability in a cost-effective way under the application deadline requirements. The performance of our ADS scheme is evaluated for different network scenarios and is compared with two other DAG scheduling schemes: ELS_NPP and ELS_DPP. We concluded that the ADS scheme is a good candidate to provide reliable real-time DAG applications over optical Grid systems.
2) Fault-tolerant DAG scheduling scheme solving grid resource failures in optical Grids by using primary-backup approaches. The simulation results show that the ELS_GRP algorithm improves significantly DAG availability and induces less the overhead in scheduling length when the more network resources are available.

References

[1] Y. Wang, Y. H. Jin, W. Guo, W. Q. Sun, W. S. Hu, and M. Y. Wu, "Joint scheduling for optical grid applications," *OSA J. Opt. Netw.*, vol. 6, no. 3, pp. 304–318, 2007.

[2] N.K. Roy, "Real time resource management and adaptive parallel programming for a cluster of computers: a comparison of different approaches in a computationally intensive environment," Proc. *IEEE International Symposium on Network Computing and Applications (NCA)*, pp. 216-226, Cambridge, MA, 2001.

[3] Y. Wang, L. Wang, G. Dai, "QGWEngine: A QoS-Aware Grid Workflow Engine," Proc. *IEEE Congress on Services 2008*, pp.561-566, 2008.

[4] V. Di Martino and M. Mililotti, "Scheduling in a grid computing environment using genetic algorithms," in *International Parallel and Distributed Processing Symposium (IPDPS)*, pp. 235-239, Aug. 2002.

[5] K.-M. Yu and C.-K. Chen, "An Adaptive Scheduling Algorithm for Scheduling Tasks in Computational Grid," in Proc. of *IEEE Grid and Cooperative Computing (GCC)*, pp. 185-189, Shenzhen, China, Oct. 2008.

[6] W. Guo, W. Sun, W. Hu, and Y. Jin, "Resource Allocation Strategies for Data-Intensive Workflow-Based Applications in Optical Grids," in *IEEE Singapore International Conference on Communication systems*, pp. 1-5, Singapore, Oct. 2006.

[7] V. Lakshmiraman and B. Ramamurthy, "Joint Computing and Network Resource Scheduling in a Lambda Grid Network," *IEEE International Conference on Communications (ICC)*, pp. 1-5, Dresden, June 2009.

[8] Y. Jin, Y. Wang, W. Guo, W. Sun, and W. Hu, "Joint Scheduling of Computation and Network Resource in Optical Grid," in Proc. of *International Conference on Information, Communications & Signal Processing (ICICS)*, pp. 1-5, Singapore, Dec. 2007.

[9] X. Liang, X. Lin, and M. Li, "Adaptive Task Scheduling on Optical Grid," in Proc. Of *IEEE Asia-Pacific Conference on Services Computing (APSCC)*, pp. 486-491, Guangzhou, China, Dec. 2006.

[10] F. Dong and S. G. Akl, "Scheduling Algorithms for Grid Computing: State of the Art and Open Problems," *School of Computing, Queen's University, Kingston, Ontario, Technical Report 2006-504*, 2006.

[11] Q. Tao, H. Chang, Y. Yi, C. Gu, and Y. Yu, "QoS Constrained Grid Workflow Scheduling Optimization Based on a Novel PSO Algorithm," Proc. *Grid and Cooperative Computing (GCC)*, pp. 153-159, Lanzhou, China, Aug. 2009.

[12] Z. Sun, W. Guo, Z. Wang, Y. Jin, W. Sun, W. Hu, and C. M. Qiao, "Scheduling Algorithm for Workflow-Based Applications in Optical Grid," *IEEE Journal of Lightwave Technology*, vol. 26, no. 17, pp. 3011-3020, 2008.

[13] X. Liu, C. Qiao, W. Wei, X. Yu, T. Wang, W. Hu, W. Guo, and M.-Y. Wu, "Task Scheduling and Lightpath Establishment in Optical Grids," *IEEE Journal of Lightwave Technology*, vol. 27, no. 12, pp. 1796 - 1805, 2009.

[14] H. Nguyen, M. Gurusamy, and L. Zhou, "Provisioning lightpaths and computing resources for location-transparent scheduled grid demands," Proc. of *International Conference on Optical Network Design and Modeling (ONDM)*, pp. 1-6, Mar. 2008.

[15] N. Jue, J.P. Kannasoot, "Resource-efficient task assignment and scheduling in optical grids," *IEEE/OSA Optical Fiber Communication Conference/National Fiber Optic Engineers Conference (OFC/NFOEC)*, Paper OWR7, San Diego, CA, 2010.

[16] R. Medeiros, W. Cirne, F. Brasileiro, and J. Sauvé, "Faults in grids: why are they so bad and what can be done about it?," Proc. *Int. Workshop on Grid Computing*, pp. 18–24, Tokyo, Japan, 2003.

[17] X. Liu, W. Wei, X. Yu, C. Qiao, and T. Wang, "Distributed computing task assignment and lightpath establishment (TALE)," *IEEE High Speed Networks Workshop*, Anchorage, AK, May 11, 2007.

[18] L. Song and B. Mukherjee, "Impacts of multiple backups and multi-link sharing among primary and backups for dynamic service provisioning in survivable mesh networks," *IEEE/OSA Optical Fiber Communication Conference/National Fiber Optic Engineers Conference (OFC/NFOEC)*, Paper OThJ3, Anaheim, CA, 2007.

[19] J. Zhang and B. Mukherjee, "A review of fault management in WDM mesh networks: basic concepts and research challenges," *IEEE Networking*, vol. 18, no. 2, pp. 41–48, 2004.

[20] O. Sinnen and L. Sousa, "Communication contention in task scheduling," *IEEE Trans. Parallel Distrib. Syst.*, vol. 16, no. 6, pp. 503–515, 2005.

[21] S. Hwang, C. Kesselman, "A Flexible Framework for Fault Tolerance in the Grid," *Journal of Grid Computing*, vol. 1, no. 3, pp. 251-272, 2003.

[22] A. Iosup, M. Jan, O. Sonmez, D. H. J. Epema, "On the Dynamic Resource Availability in Grids," *IEEE/ACM Grid Computing Conference*, pp. 26-33, Austin, Texas, 2007.

Chapter 6. Conclusions and Future Works

6.1 Summary of the Thesis

The first half (charpter-2 to Charpter-4) of this thesis addresses some challenges in a traditional WDM-PON, including optical multicast overlay scheme, network protection architecture and tunable FP-LD self-seeding scheme. The charpter-5 focuses on the issue of maximizing grid application availability in real-time optical Grid systems through fault-tolerant scheduling. More specifically, the following novel research contributions are presented in this thesis.

1. Multicast Overlay Scheme in WDM-PON

Multicast overlay scheme in a WDM-PON can be realized by establishing one-to-many light paths on the optical layer, and thus reduces the loading of the electronic network processors or routers on the network layer and achieves much higher processing speed. In this thesis, we have proposed our two feasible schemes to overlay multicast transmission onto the existing point-to-point traffic in a WDM-PON.

1) In the first approach, by using a dynamic wavelength reflector in each WDM channel, OLT selectively enable the multicast data imposed on the corresponding downstream unicast carrier. We have also provided several possible different configurations of the wavelength reflector. By employing re-modulation technique, no light source is needed in the ONUs, which effectively reduces the cost and complexity.

2) The second approach uses a dual-parallel MZM to generate the optical sidebands for multicast DPSK data modulation. The downstream unicast data is modulated in NRZ format carried on the optical baseband carrier, which will be re-modulated with the upstream NRZ data at the respective ONU. By simply switching the RF control signal on or off in each wavelength channel, the centralized multicast function can be reconfigured dynamically. As the downstream unicast signal and the upstream signal are carried on different fiber feeders, while the upstream signal and the multicast signal are carried on different subcarriers, though on the same fiber feeder, the possible Rayleigh backscattering effect is much alleviated.

2. Protection Switching Schemes in WDM-PONs

A survivable WDM-PON architecture which provides automatic protection switching (APS) capability can avoid enormous loss in data and business due to fiber cuts. We have proposed and demonstrated two novel automatic protection switching schemes:

1) Centrally-controlled intelligent protection scheme in a single WDM-PON: By monitoring the optical power of each channel on both the working and protection paths, the proposed scheme can tell the connection status of both the working and protection paths of each channel, and hence can perform an effective protection switching with the aid of the proposed logic decision unit in more practical operation scenarios. The scheme can deal with both the feeder fiber and the distribution fiber failures.

2) Cross-protection dual-PON-based architecture: It can provide 1+1 protection for

downstream traffic and 1:1 protection for upstream data against both feeder fiber and distribution fiber failures by using the fiber links and AWGs of the neighboring WDM-PON. It has the minimum number of extra protection fibers, much improved wavelength utilization and better transmission performance compared with the other existing protection schemes. No additional dedicated light source in ONUs is needed by using re-modulation technique.

3. Upstream Multi-Wavelength Shared PON

Providing cost-effective, smooth capacity upgrades while maintaining compatibility with existing PON standards will be of great concern for network operators. A novel UMWS-PON is proposed based on the tunable self-seeding FP-LD module at ONU. The PON not only upgrades easily upstream capacity by introducing multiple wavelengths, but also improves significantly bandwidth utilization by sharing wavelength resources. We also for the first time study the impact of channel SL on the network performance. The extensive simulations show that the enhanced performance is obtained when the condition that the channel SL is relative small.

4. DAG Applications in Optical Grids

Because optical grid systems involve many heterogeneous Grid and network resources, the faults of these resources seem to be inevitable. We have proposed two fault-tolerant scheduling schemes for optical Grid applications:

1) The first scheme focus only on optical link failures, the proposed Availability-Driven Scheduling (ADS) scheme iteratively improves the availability in a cost-effective

way under the application deadline requirements. Its performance is evaluated in different network scenarios and compared with two other DAG scheduling schemes.

2) The second one addresses issue of handling grid resource failures in optical Grids by using a primary-backup approach to allocate simultaneously two copies of each computation task to two different Grid resources for data process. It improves greatly application availability and induces less the overhead in scheduling length when the more network resources are available.

6.2 Future Works

As to the future works of this thesis, there are some issues are deserved to be studied:

1） A possible research work for the future is to design a more flexible architecture for WDM-PONs, which can not only support multicast data transmission but also provide self-protection. Meanwhile, a novel energy-saving scheme for WDM-PON could be also incorporated. Subcarrier modulation technique can be readily used for this purpose, by employing different subcarriers for different function. However, the problem lays in the system complexity and independent control realization. But it is believed an interesting research topic in a WDM-PON.

2） The enormous initial capital and operational expenditures have hindered the wide deployment of WDM-PONs. Hence, developing a potentially low-cost WDM-PON based on self-seeding reflective semiconductor optical amplifiers (RSOAs) will be much desired. However, several key technical issues should be some investigated

that could severely affect the transmission performance of self-seeding RSOAs. These issues include the fiber link characteristics of the round-trip path, the RSOA physical characteristics, the modulation extension ratio of up- and down-stream signals, the AWG filtering effect and its channel isolation, the polarization effect of the reflection module, the impact of chromatic dispersion.

3） Optical Grid applications with energy-saving and low-latency constraints have been emerging. However, our proposed availability-driven task allocation schemes only concentrate on availability improvements when making allocation decisions. Consequently, the energy consumption of the schedules could be very large, which is unfavorable or in some situations even not tolerated. We will address the issue of allocating DAG tasks with a joint objective of energy-saving, high-availability and short-latency on an optical Grid system. A novel task allocation strategy needs to be developed to find an optimal allocation that minimizes overall energy consumption and maximizes application availability while confining the length of schedule to an ideal range.

List of Publications

JOURNALS (SCI Index)

[1] **Min Zhu**, Wei Guo, Shilin Xiao, Yi Dong, Weiqiang Sun, Yaohui Jin, and Weisheng Hu, "Design and performance evaluation of dynamic wavelength scheduled hybrid WDM/TDM PON for distributed computing applications," ***OSA Optics Express***, vol. 17, no. 2, pp. 1023-1032, Jan. 2009.

[2] **Min Zhu**, Shilin Xiao, Zhao Zhou, Wei Guo, Lilin Yi, Meihua Bi, Weisheng Hu, and Benoit Geller, "An upstream multi-wavelength shared PON based on tunable self-seeding Fabry-Pérot laser diode for upstream capacity upgrade and wavelength multiplexing," ***OSA Optics Express***, vol. 19, no. 9, pp. 8000-8010, Apr. 2011.

[3] **Min Zhu**, Wei Guo, Shilin Xiao, Anne Wei, Yaohui Jin, Weisheng Hu, and Benoit Geller, "Availability-Driven Scheduling for Real-Time DAG Applications in Optical Grids," ***IEEE/OSA Journal of Optical Communications and Networking***, vol. 2, no. 7, pp. 469-480, July 2010.

[4] **Min Zhu**, Wen-De Zhong, Shilin Xiao, and Weisheng Hu, "A New Cross-Protection Dual-WDM-PON Architecture with Carrier-Reuse Colorless ONUs," ***Elsevier Optics Communications***, vol. 285, no. 15, pp. 3254-3258, July 2012.

[5] **Min Zhu**, Shilin Xiao, Zhao Zhou, Meihua Bi, "Tunable Self-Seeding Fabry-Perot Laser Diode for Upstream Multi-Wavelength Shared EPON," ***SPIE Optical Engineering***, vol. 50, no. 3, pp. 035003- 1-4, March 2011.

[6] **Min Zhu**, Wen-De Zhong, and Shilin Xiao, "Cost-effective Centralized Automatic Protection Switching Scheme for Reliable Wavelength-Division-Multiplexing Passive Optical Network," ***SPIE Optical Engineering***, vol. 51, no. 5, pp. 055005-1-7, May 2012.

[7] **Min Zhu**, Shilin Xiao, Wei Guo, Yaohui Jin, Weisheng Hu, and Benoit Geller,

"Novel WDM-PON architecture for simultaneous transmission of unicast data and multicast services," ***OSA Chinese Optics Letters***, vol. 8, no. 10, pp. 972-975, Oct. 2010.

[8] **Min Zhu**, Shilin Xiao, Meihua Bi, He Chen and Weisheng Hu, "Cost-effective Tunable Fiber Laser based on self-seeded Fabry-Perot Laser Diode using a Sagnac Loop Reflector," ***OSA Chinese Optics Letters***, vol. 8, no. 12, pp. 1150-1151, Dec. 2010.

[9] He Chen, Shilin Xiao, **Min Zhu**, Jie Shi, Meihua Bi, "A WDMA/OCDM system with the capability of encoding multiple wavelength channels by employing one encoder and one corresponding optical code," ***OSA Chinese Optics Letters***, vol. 8, no. 8, pp. 745-748, 2010.

[10] Zhao Zhou, Shilin Xiao, **Min Zhu**, and Meihua Bi, "Analysis of IPACT network performance considering channel switch latency for WDM-EPON," ***OSA Chinese Optics Letters***, vol. 9, no. 6, pp. 060602- 1-4, June 2011

[11] Lei Cai, Zhixin Liu, Shilin Xiao, **Min Zhu**, Rongyu Li, and Weisheng Hu "Video-service- overlaid wavelength-division-multiplexed passive optical network," ***IEEE Photonics Technology Letter***, vol. 21, no. 14, pp. 990-992, 2009.

[12] He Chen, Shilin Xiao, Lilin Yi, Zhao Zhou, **Min Zhu**, Jie Shi, Yi Dong, Weisheng Hu, "A tunable encoder/decoder based on polarization modulation for the SAC-OCDMA PON," ***IEEE Photonics Technology Letter***, vol. 23, no. 11, pp. 748-750, 2011.

CONFERENCES (EI Index)

[1] **Min Zhu**, Wei Guo, Shilin Xiao, Anne Wei, Benoit Geller, Weiqiang Sun, Yaohui Jin, and Weisheng Hu, "Availability-Aware Joint Task Scheduling for Real-Time Distributed Computing Applications over Optical Networks," in Proc. ***IEEE ICC 2010***, South Africa, May 2010.

[2] **Min Zhu**, Shilin Xiao, Zhao Zhou, Wei Guo, Lilin Yi, Weisheng Hu, "Upstream Multi-Wavelength Shared PON with Wavelength-Tunable Self-seeding Fabry-Perot Laser Diode," in Proc. ***IEEE/OSA OFC 2011***, California, March 2011, **OThK3**.

[3] **Min Zhu**, Wei Guo, Shilin Xiao, Benoit Geller, Weiqiang Sun, Yaohui Jin, and Weisheng Hu, "Demonstration of Time-Wavelength Co-Allocation (TWCA) Problem in Novel Dynamic Wavelength Scheduled WDM-PON for Distributed Computing Applications," in Proc. ***SPIE APOC 2008***, vol. 7137 **(Best Student Paper Nomination)**.

[4] **Min Zhu**, Shilin Xiao, Wei Guo, He Chen, Zhixin Liu, Lei Cai, "Overlay of Multicast Service in WDM-PON Based on Dynamic Wavelength Reflection Scheme," in Proc. ***SPIE ACP 2009***, vol. 7633 **(Best Student Paper Honorable Mention)**.

[5] **Min Zhu**, Shilin Xiao, Wei Guo, Anne Wei, Yaohui Jin, Weisheng Hu, Benoit Geller, "Fault-Tolerant Scheduling Using Primary-Backup Approach for Optical Grid Application," in Proc. ***SPIE ACP 2009***, vol. 7633.

[6] **Min Zhu**, Shilin Xiao, Wei Guo, Meihua Bi, He Chen and Weisheng Hu, "Joint Scheduling for Massive Data Aggregations over WDM Backbone-Access Networks," in Proc. ***IET ICOCN 2010***, pp. 168-172, Oct. 2010.

[7] **Min Zhu**, Shilin Xiao, Wei Guo, Meihua Bi, Zhao Zhou, Yaohui Jin and Weisheng Hu, "Using Wavelength-Tunable Self-seeding Fabry-Perot Laser for Upstream Transmission in Hybrid WDM/TDM PON," in Proc. ***SPIE ACP 2010***, pp. 405-406, Dec. 2010.

[8] **Min Zhu**, Wen-De Zhong, Shilin Xiao, "A Centrally-Controlled Self-Protected WDM-PON Using N×N Arrayed Waveguide Gratings," in Proc. ***IET ICOCN 2011***, pp. 1-2, Dec. 2011.

[9] **Min Zhu**, Wen-De Zhong, Shilin Xiao, "A Centrally-Controlled Intelligent Protection Switching Scheme for WDM-PONs," in Proc. ***IEEE ICCC 2012***, Aug. 2012.

[10] Cheng Yang, Shilin Xiao, **Min Zhu**, Weilin. Xie, Zhixin Liu, Linzhi Ge, Yi Xiang,

and Jianwen Wei, “A Novel Scheme of Unicast and Multicast in WDM-PON Using Reflective Semiconductor Optical Amplifier,” in Proc. ***SPIE ACP 2009***, **TuBB5**.

[11] Zhao Zhou, Shilin Xiao, **Min Zhu**, Meihua Bi, Yi Xiang, Cheng Yang and Jianwen Wei, “Effects of the Channel Switch Latency in Hybrid WDM/TDM PON,” in Proc. ***SPIE ACP 2010***, vol. 7989.

[12] Shilin Xiao, Zhao Zhou, Meihua Bi, **Min Zhu**, He Chen, “Evolution scenarios for passive optical access networks,” in Proc. ***ICICS 2011***, pp. 1-5, Dec. 2011.

[13] Jie Shi, Shilin Xiao, He Chen, **Min Zhu**, Meihua Bi, “Simultaneous Measurement of Strain and Temperature using a High-Birefringence Fiber Loop Mirror and an Erbium-Doped Fiber”, in Proc. ***SPIE ACP 2010***, pp. 473-474, Dec. 2010.

[14] Yi Xiang, Shilin Xiao, Zhixin Liu, **Min Zhu**, Daozi Ding, Cheng Yang, and Jianwen Wei, “A Novel WDM-PON Architecture Enabling Multicasting with Color-Free ONUs Based on WSS and Interleaver,” in Proc. ***SPIE ACP 2009***, **TuT3**.

[15] Linzhi Ge, Shilin Xiao, Zhixin Liu, **Min Zhu**, Lei Cai, Tao Xiao, and Daozi Ding, “A Scheme to Realize Multicast/Broadcast by Superimposing DPSK Signal onto Manchester/ NRZ Signal,” in Proc. ***SPIE ACP 2009***, **WL55**.

[16] Lei Cai, Shilin Xiao, Zhixin Liu, Rongyu Li, **Min Zhu**, and Weisheng Hu, “Cost-effective WDM-PON for simultaneously transmitting unicast and broadcast/ multicast data by superimposing IRZ signal onto NRZ signal,” in Proc. ***ECOC 2008***, **Th.1.F.4**.

PATENTS

[1] **Min Zhu**, Shilin Xiao, Lilin Yi, Wei Guo, He Chen, “Quick Dynamically Reconfigurable Optical Packet Buffer in All-Optical Networks,” ***Chinese patent*** (Chinese version), **Grant number: ZL 200810042493.X**;

[2] **Min Zhu**, Shilin Xiao, Wei Guo, He Chen, Yi Xiang, Jie Shi, “Subcarrier Multicast

Overlay System in Wavelength-Division-Multiplexing Passive Optical Network," ***Chinese patent*** (Chinese version), Application number: 200910310575.2;

[3] **Min Zhu**, Shilin Xiao, Wei Guo, He Chen, Jie Shi, "Self-seeding Multi-wavelength Dynamical Scheduling Optical Network Unit in Passive Optical Network," ***Chinese patent*** (Chinese version), Application number: 200910311682.7;

[4] **Min Zhu**, Shilin Xiao, Wei Guo, He Chen, Jie Shi, "Wavelength-Division-Multiplexing Passive Optical Network Supporting Reflection Routing Multicast Overlay Scheme," ***Chinese patent*** (Chinese version), Application number: 200910311715.8;

[5] **Min Zhu**, Shilin Xiao, Wei Guo, Meihua Bi, He Chen, "Mutually Injected Multi-wavelength Dynamical Scheduling Optical Network Unit in Passive Optical Network," ***Chinese patent*** (Chinese version), Application number: 201010165943.1;

[6] Wen-De Zhong, **Min Zhu**, "Novel and Intelligent Protection Approach for WDM-PONs," ***US patent***, Application number: 61/577,423;

[7] Wen-De Zhong, **Min Zhu**, "Novel Energy-saving and self-healing WDM-PON," ***US patent***, Application number: 61/607,294.